



Dissertations

Theses and Dissertations

1997

Multinuclear Magnetic Resonance Studies of Anion Binding to Copper, Zinc-Superoxide Dismutase, and of Lithium Transport and Binding in Cultured Neuroblastoma Cells

Cherian Zachariah
Loyola University Chicago

Follow this and additional works at: https://ecommons.luc.edu/luc_diss

 Part of the [Chemistry Commons](#)

Recommended Citation

Zachariah, Cherian, "Multinuclear Magnetic Resonance Studies of Anion Binding to Copper, Zinc-Superoxide Dismutase, and of Lithium Transport and Binding in Cultured Neuroblastoma Cells" (1997). *Dissertations*. 3662.

https://ecommons.luc.edu/luc_diss/3662

This Dissertation is brought to you for free and open access by the Theses and Dissertations at Loyola eCommons. It has been accepted for inclusion in Dissertations by an authorized administrator of Loyola eCommons. For more information, please contact ecommons@luc.edu.



This work is licensed under a [Creative Commons Attribution-NonCommercial-No Derivative Works 3.0 License](#).
Copyright © 1997 Cherian Zachariah

LOYOLA UNIVERSITY OF CHICAGO

**MULTINUCLEAR MAGNETIC RESONANCE STUDIES OF ANION BINDING TO
COPPER, ZINC-SUPEROXIDE DISMUTASE, AND OF LITHIUM TRANSPORT
AND BINDING IN CULTURED NEUROBLASTOMA CELLS**

A DISSERTATION SUBMITTED TO
THE FACULTY OF THE GRADUATE SCHOOL
IN CANDIDACY FOR THE DEGREE OF
DOCTOR OF PHILOSOPHY

DEPARTMENT OF CHEMISTRY

BY

CHERIAN ZACHARIAH

CHICAGO, ILLINOIS

JANUARY 1997

Copyright by Cherian Zachariah, 1996

All rights reserved.

ACKNOWLEDGEMENTS

I am grateful to my mentor Dr. Duarte Mota de Freitas for the excellent supervision during the course of this dissertation. I am also thankful to Dr. de Freitas for his patience, encouragement and financial support that he gracefully provided during this study. I would like to thank him for providing me with an opportunity to acquire cell culture techniques.

I am grateful to my committee members, Dr. David S. Crumrine, Dr. Kenneth W. Olsen, Dr. Mir Shamsuddin, and Dr. Howard Laten, for their time and suggestions during the course of this work. I would also like to thank Dr. Mehboob Peeran for introducing me to the Chemistry Department at Loyola.

My sincere "obrigado" to our collaborators Drs. Carlos Geraldos, Margarida Castro, Conceicao Lima and Catarina Oliveira for their time and help with cell cultures. I would like to thank them for their gracious hospitality during my three week stay in Portugal. Special thanks to Dr. Evan B. Stubbs, Jr., of the Department of Molecular and Cellular Biochemistry, Loyola University Medical Center, for providing us the neuroblastoma cells and assistance in cell culture. I would also like to thank Mr. Joseph N. Schleup, Dept. of Biology, Loyola University Chicago, for his help with electron microscopy, and Dr. A. Nappi for the assistance provided for photographing cells. I would also like to take this opportunity to thank the NMR lab managers Mr. Chris Clifford and Dr. David French for their technical support on the NMR spectrometer.

I sincerely thank Dr. Ravichandran Ramasamy (Dept. of Cardiovascular Medicine, U.C.

Davis) for his support during the latter part of this dissertation; and Elias Fernandez, my labmates, past and present, Qinfen Rong, Yuling Chi, Wanrong Lin, Chandra Srinivasan, Hanan Hasan, Louis Amari and Dr. Yang Nan for their encouragement and constructive criticisms. I would specially like to thank Joyce Nikolakopoulos for all her help with cell culture and perfusion.

I would like to take this opportunity to acknowledge the support of the faculty, staff and all the graduate students in the Chemistry Department. I would like to thank the Graduate School for the Dissertation Fellowship.

Special thanks go to my parents for their unfailing love and support all through this day, and to all my friends for their support during my stay at Loyola.

To my parents

TABLE OF CONTENTS

ACKNOWLEDGEMENTS	iii
LIST OF FIGURES	x
LIST OF TABLES	xii
LIST OF ABBREVIATIONS	xv
ABSTRACT	xviii
CHAPTER	
I. INTRODUCTION	1
1. Superoxide Dismutases.....	1
2. Structure and Function of Cu, Zn-SOD.....	2
3. Anion Binding Studies of Cu, Zn-SOD.....	7
4. Vanadium in Biological Systems.....	15
5. Interactions of Vanadate with Proteins.....	15
6. Lithium in Medicine	17
7. Lithium Transport in RBCs	19
8. Lithium Transport in Nerve Cells.....	21
9. Lithium Ionophores.....	23
10. Mechanisms of Lithium Action	24
11. Analytical Methods for Detection of Vanadate and Li ⁺ in Biological Samples	27
II. STATEMENT OF THE PROBLEMS	29
III. EXPERIMENTAL APPROACH	33

1. Materials	33
1. Reagents	33
2. Enzymes	34
3. Cell Culture	34
2. Sample Preparation	35
1. Preparation of Reduced, Zinc-only and Apoprotein Forms of Cu, Zn-SOD	35
2. Preparation of Arginine and Lysine Modified Cu, Zn-SOD.....	35
3. Cell Culture on Microcarrier Beads.....	36
4. Preparation of SH-SY5Y cells for Electron Microscopy	36
5. Preparation of SH-SY5Y Cell Membranes.....	39
6. Preparation of Shift Reagents.....	39
7. Determination of Protein Concentration.....	40
8. Activity Assay for Cu, Zn-SOD	40
9. Extraction of Phospholipids from SH-SY5Y Cell Membranes	40
3. Data Analysis	41
1. Determination of Binding Constants of Phosphates to Native Cu, Zn-SOD, and of Li ⁺ to SH-SY5Y Cell Membranes	41
2. Determination of Concentrations of Various Vanadate Species	42
3. Determination of Li ⁺ Transport Rates in SH- SY5Y Cells	43
4. Instrumentation	44

1. Nuclear Magnetic Resonance Spectrometer.....	44
2. Atomic Absorption Spectrophotometer.....	44
3. UV-Vis Spectrophotometer.....	44
4. Centrifuge.....	46
5. Scanning Electron Microscope.....	46
6. Vapor Pressure Osmometer.....	46
7. Lyophilizer.....	46
8. pH Meter.....	46
IV. RESULTS.....	47
1. Interactions of Native Bovine Cu, Zn-SOD with Biologically Relevant Phosphates and Synthetic Polyphosphates.....	48
1. Interactions of Adenine Nucleotides and 2,3-BPG with Native Cu, Zn-SOD.....	48
2. Interactions of Synthetic Polyphosphates with Native Cu, Zn-SOD.....	51
3. ³¹ P NMR Measurements of Biological Phosphates to Determine Their Binding Constants to Native Cu, Zn-SOD.....	51
4. ³¹ P NMR Measurements of Biological Phosphates and Synthetic Polyphosphates in the presence of Chemically Modified Cu, Zn-SOD.....	60
5. ¹³ C NMR Measurements of Biological Phosphates in the presence of Native Cu, Zn-SOD.....	64
6. Effect of Adenine Nucleotides and Synthetic Polyphosphates on the Activity of Native Cu, Zn- SOD.....	64
2. Interactions of Metal-Depleted and Reduced Forms of Cu, Zn-SOD with Vanadate.....	67

1. Interactions of Apo Cu, Zn-SOD with Vanadate.....	67
2. Interactions of Zinc-only Form of Cu, Zn-SOD with Vanadate	73
3. Interactions of Reduced Cu, Zn-SOD with Vanadate	73
4. Interactions of Native Cu, Zn-SOD with Vanadate.....	76
3. Li ⁺ Transport and Binding in Cultured Neuroblastoma Cells	85
1. Characterization of Microcarrier Beads to determine Suitability for Alkali Metal Ion Transport Using NMR	88
2. Viability of SH-SY5Y Cells in the Presence of Different Shift Reagents and LiCl.....	100
3. Li ⁺ Transport in SH-SY5Y Cells in Suspension.....	100
4. Li ⁺ Transport in SH-SY5Y Cells Anchored on Biosilon Beads	104
5. ⁷ Li NMR Relaxation Measurements in SH-SY5Y Cells	113
V. DISCUSSION	121
1. Interactions of Native Cu, Zn-SOD with Biologically- Relevant Phosphates.....	121
2. Biologically Relevant Phosphates and Activity of Native Cu, Zn-SOD	127
3. Interactions of Metal-Depleted and Reduced Forms of Cu, Zn-SOD with Vanadate	128
4. Characterization of Microcarrier Beads.....	133
5. Li ⁺ Transport and Binding In Neuroblastoma Cells	137
BIBLIOGRAPHY	144
VITA	158

LIST OF PUBLICATIONS	159
-----------------------------------	-----

LIST OF FIGURES

Figure	Page
1. Schematic drawing of the metal binding region of one subunit of Cu, Zn-SOD.....	4
2. Schematic representation of the solvent channel of Cu, Zn-SOD indicating the relative positions of positively charged amino acid residues	10
3. Schematic representation of the apparatus required for the perfusion of cells for NMR spectroscopy.....	37
4. ³¹ P NMR spectra of 5 mM ATP in the absence and presence of native and chemically modified Cu, Zn-SOD.....	61
5. ⁵¹ V NMR spectra of 2 mM vanadate in the presence of increasing concentrations of apo Cu, Zn-SOD.....	70
6. ⁵¹ V NMR spectra of 2 mM vanadate in the presence of increasing concentrations of reduced Cu, Zn-SOD	77
7. ⁵¹ V NMR spectra of 2 mM vanadate in the presence of the different derivatives of Cu, Zn-SOD at 0.2 mM.....	83
8. Plot of [V _x -Protein] vs relative charge	86
9. ⁷ Li and ²³ Na NMR spectra of buffer in the presence of different kinds of microcarrier beads	93
10. ¹³³ Cs NMR spectra of buffer in the presence of different microcarrier beads	96
11. ³⁵ Cl NMR spectra of buffer in the presence of Cytodex-1 beads with and without Mn ²⁺	98
12. Morphology of SH-SY5Y cells in the presence of LiCl and HTm(DOTP) ⁴⁺	102
13. ⁷ Li NMR spectra of SH-SY5Y cells in suspension showing Li ⁺ influx	105
14. Scanning electron micrograph of SH-SY5Y cells anchored on Biosilon beads.....	108

15. ^7Li NMR spectra of Li^+ influx into SH-SY5Y cells anchored on Biosilon beads.....	110
16. ^{31}P NMR spectrum of SH-SY5Y cells anchored on Biosilon beads	114
17. ^{31}P NMR spectrum of the phospholipid extract from SH-SY5Y cell membranes	119

LIST OF TABLES

1. NMR parameters of nuclei investigated at 7.0 T.....	45
2. ^{31}P NMR parameters of the biological phosphates in the presence of native Cu, Zn-SOD.....	49
3. ^{31}P NMR T_1 values for increasing concentrations of ATP in the presence of native Cu, Zn-SOD.....	52
4. ^{31}P NMR T_1 values for increasing concentrations of ADP in the presence of native Cu, Zn-SOD.....	54
5. ^{31}P NMR T_1 increasing concentrations of AMP in the presence of native Cu, Zn-SOD.....	55
6. ^{31}P NMR T_1 values for increasing concentrations of 2,3-BPG in the presence of native Cu, Zn-SOD.....	56
7. ^{31}P NMR T_1 values for increasing concentrations of diphosphate in the presence of native Cu, Zn-SOD.....	57
8. ^{31}P NMR T_1 values for increasing concentrations of inorganic phosphate of native Cu, Zn-SOD.....	58
9. Binding constants of biological phosphates to native Cu, Zn-SOD.....	59
10. ^{31}P NMR T_1 values of biological phosphates in the presence of native and chemically modified Cu, Zn-SOD.....	63
11. ^{13}C NMR chemical shifts and line widths of C atoms of ATP in the presence of native Cu, Zn-SOD.....	65
12. ^{13}C NMR chemical shifts and line widths of C atoms of AMP in the presence of native Cu, Zn-SOD.....	66
13. Activity of native Cu, Zn-SOD in the presence of the biological phosphates.....	68
14. ^{51}V NMR chemical shifts and line widths of different vanadate species with various concentrations of apo Cu, Zn-SOD.....	69

15. Concentrations of the different vanadate species with various concentrations of apo Cu, Zn-SOD.....	72
16. ⁵¹ V NMR chemical shifts and line widths of different vanadate species with various concentrations of zinc-only Cu, Zn-SOD.....	74
17. Concentrations of the different vanadate species with various concentrations of zinc-only Cu, Zn-SOD	75
18. ⁵¹ V NMR chemical shifts and line widths of different vanadate species with various concentrations of reduced Cu, Zn-SOD	79
19. Concentrations of the different vanadate species with various concentrations of reduced Cu, Zn-SOD.....	80
20. ⁵¹ V NMR chemical shifts and line widths of different vanadate species with various concentrations of native Cu, Zn-SOD.....	81
21. Concentrations of the different vanadate species with various concentrations of native Cu, Zn-SOD.....	82
22. Composition and physical properties of microcarrier beads used.....	89
23. NMR parameters of buffered solutions containing alkali metal ions in the presence of microcarrier beads	91
24. NMR parameters of buffered solutions containing alkali metal ions in the presence of Cytodex-1 beads with different concentrations of Dy(PPP) ₂ ⁷⁻	95
25. Viability of SH-SY5Y cells in the presence of shift reagents and LiCl	101
26. Li ⁺ influx into SH-SY5Y cells in suspension.....	107
27. Li ⁺ transport rates in SH-SY5Y cells anchored on Biosilon beads	112
28. ⁷ Li NMR relaxation measurements in SH-SY5Y cells	117

29. ^7Li NMR relaxation measurements with SH-SY5Y cell membranes.....	118
---	-----

LIST OF ABBREVIATIONS

AA	atomic absorption
ADP	adenosine diphosphate
ALS	amyotrophic lateral sclerosis
AMP	adenosine monophosphate
Arg	arginine
AT	acquisition time
ATP	adenosine triphosphate
Bicine	N,N-bis[2-hydroxyethyl]glycine
2,3 BPG	2,3 bisphosphoglycerate
¹³ C	carbon-13 isotope
³⁵ Cl	chlorine-35 isotope
CPMG	Carr-Purcell-Meiboom-Gill
¹³³ Cs	cesium-133 isotope
Cu,Zn-SOD	copper,zinc-superoxide dismutase
Cys	cysteine
δ	chemical shift in ppm
Δv _{1/2}	line width of NMR resonance at half height in Hz
1-D	one dimensional
DB14C4	dibenzyl-14-crown-4 or 6,6-dibenzyl-1,4,8,11-

	tetraoxacylotetradecane
DEAE	diethyl amino ethyl
DIDS	4,4'-diisothiocyanostilbene-2,2'-disulfonic acid
DME	Dulbecco's Modified Eagle
DPDE	diphosphodiester
Dy(PPP) ₂ ⁷⁻	dysprosium (III) triphosphate
Dy(TTHA) ³⁻	dysprosium (III) triethylenetetraminehexaacetate
EDTA	ethylenediamine tetraacetate
EPR	electron paramagnetic resonance
Fe-SOD	iron superoxide dismutase
HEPES	4-(2 hydroxyethyl)-1-piperazine-ethanesulfonic acid
His	histidine
H ₂ O ₂	hydrogen peroxide
HTm(DOTP) ⁴⁻	thulium [1,2,7,10-tetraazacyclododecane-N,N',N'',N'''- tetramethylene] phosphonate
Ile	isoleucine
⁷ Li	lithium-7 isotope
Leu	leucine
Lys	lysine
MIR	modified inversion recovery
Mn-SOD	manganese superoxide dismutase
²³ Na	sodium-23 isotope
NMR	nuclear magnetic resonance

O_2^-	superoxide
OH \cdot	hydroxyl radical
^{31}P	phosphorus-31 isotope
PC	phosphatidyl choline
PCr	phosphocreatine
PE	phosphatidyl ethanolamine
PE _p	PE plasmalogen
PI	phosphatidyl inositol
PME	phosphomonoesters
P _i	orthophosphate or inorganic phosphate
PP	diphosphate or pyrophosphate
PPP	triphosphate
PW	pulse width
PS	phosphatidyl serine
RBC	red blood cell
SOD	superoxide dismutase
Sph	sphingomyelin
SR	shift reagent
SW	spectral width
T ₁	spin-lattice relaxation time
T ₂	spin-spin relaxation time
Thr	threonine
^{51}V	vanadium-51 isotope

ABSTRACT

Copper, zinc-superoxide dismutase (Cu,Zn-SOD) is a metalloprotein and a suitable system for bioinorganic studies. The interaction of biologically relevant phosphates with native bovine Cu,Zn-SOD were followed by ^{31}P nuclear magnetic resonance (NMR) spin-lattice (T_1) relaxation measurements. Adenosine triphosphate (ATP) was shown to have the highest affinity constant followed by adenosine diphosphate and adenosine monophosphate. Using chemically modified Cu,Zn-SOD, the sites of interactions of these phosphates were determined to be arginine-141, lysine-120, and lysine-134 residues. ATP and inorganic phosphate were the only phosphates shown to inhibit the activity of the native enzyme.

The interactions of rapidly equilibrating vanadate monomeric, dimeric and tetrameric species with reduced and metal-depleted derivatives of bovine Cu,Zn-SOD was studied by ^{51}V NMR spectroscopy. Of the different derivatives studied, the vanadate tetramer interacted most strongly with reduced Cu,Zn-SOD, followed by the zinc-only derivative and the apo enzyme form, respectively. Much lower interactions were observed between the vanadate monomer and the dimer with the different derivatives.

Li^+ as lithium carbonate is the drug of choice in the treatment of bipolar disorder. Li^+ transport and binding were followed in the SH-SY5Y human neuroblastoma cell line using non-invasive NMR spectroscopy. The rates of Li^+ transport into SH-SY5Y cell suspensions in the presence of 5 mM HTm(DOTP) $^{4-}$ or 5 mM Dy(PPP) $_2^{7-}$ were within experimental error. Because the cell viability of a cell suspension decreased below 70% at the end of the NMR experiment,

these cells were anchored on non-permeable Biosilon microcarrier beads and perfused with a modified oxygenated medium to maintain the cell viability during the course of the NMR experiments.

Control studies using four different kinds of commercially available microcarrier beads demonstrated that Cytodex-1 and CultiSpher-G beads were permeable to both alkali metal ions and shift reagents; glass beads are not permeable to either alkali metal ions or shift reagents, but have been shown to have magnetic susceptibility effects. Biosilon beads were, however, non-permeable to ions.

Hence Li^+ transport was followed in SH-SY5Y cells anchored on Biosilon beads. Scanning electron microscopy revealed that these cells retain their morphology when anchored on beads. The rate of Li^+ influx was enhanced by a factor of 2 in the presence of the lithium-specific ionophore dibenzyl 14-crown-4. The rate of Li^+ efflux from Li^+ -loaded SH-SY5Y cells was also determined. The viability of the cells during the transport experiments was monitored by ^{31}P NMR spectroscopy. Li^+ was shown to interact with the cell membranes using NMR relaxation measurements.

CHAPTER I

INTRODUCTION

This chapter consists of two parts. Sections I.1 to I.5 deal with basic studies on the metalloprotein superoxide dismutase and Sections I.6 to I.11 with studies on lithium and its interactions in cells. In this dissertation, multinuclear NMR spectroscopy was used to probe interactions of anions with superoxide dismutase and of lithium in nerve cells.

I.1. Superoxide Dismutases

The appearance of oxygen and the subsequent proliferation of life in an oxygen-dependent environment led to the use of oxygen as the terminal electron acceptor providing greater energy and metabolic diversity. The benefits of oxygen to life are accompanied by its toxic and mutagenic properties (Fridovich, 1986; Moody and Hasan, 1982). The toxicity of oxygen is related to the generation of partially reduced, highly reactive intermediates such as superoxide radical (O_2^-), hydrogen peroxide (H_2O_2) and hydroxyl radical ($OH\cdot$), which are generated during normal oxygen metabolism and under unique circumstances like the "respiratory burst" of phagocytes. During the course of evolution, oxygen-tolerant organisms have developed defensive mechanisms to protect their cells from the deleterious effects of toxic oxygen intermediates. Superoxide dismutases (SODs) and hydrogen peroxidases are proteins which have evolved to provide such defensive mechanisms (Fridovich, 1995).

Superoxide dismutases are a group of proteins which contain different metal ions as

co-factors. The three distinct superoxide dismutases, the Cu,Zn-SOD, the Mn-SOD and the Fe-SOD are grouped under two families: the Cu,Zn-SOD and the Mn/Fe-SOD, which have evolved from different ancestral proteins, in different eras and have different properties. The Mn-SODs are found in prokaryotes and in the matrix of mitochondria, the related Fe-SODs are found in prokaryotes and in some plant families. Cu,Zn-SODs occur primarily in the cytosol of eukaryotic cells, in chloroplasts of plants, and in some bacteria (Steinman, 1982). The Cu,Zn-SOD isolated from bovine erythrocytes has been extensively characterized (Steinman et al., 1974; Tainer et al., 1982; Banci et al., 1994).

Superoxide dismutase activity appears to be highly essential for the survival of oxygen-metabolizing organisms. An early study of the distribution of the enzymes superoxide dismutase and catalase in various microorganisms (McCord et al., 1971), grouped under three categories based on their oxygen tolerance, namely aerobes, strict anaerobes and aerotolerant anaerobes, indicated that all aerobes contained both superoxide dismutase and catalase, while the strict anaerobes showed no superoxide dismutase and low, if any, catalase activity; the aerotolerant anaerobes contained superoxide dismutase while catalase activity was not significant. Further, all aerobes containing cytochrome-type systems were found to contain both superoxide dismutase and catalase. Aerotolerant anaerobes, which survive exposure to air and metabolize oxygen to a limited extent but do not contain cytochrome-type systems, were found to be devoid of catalase activity but did exhibit superoxide dismutase activity (McCord et al., 1971).

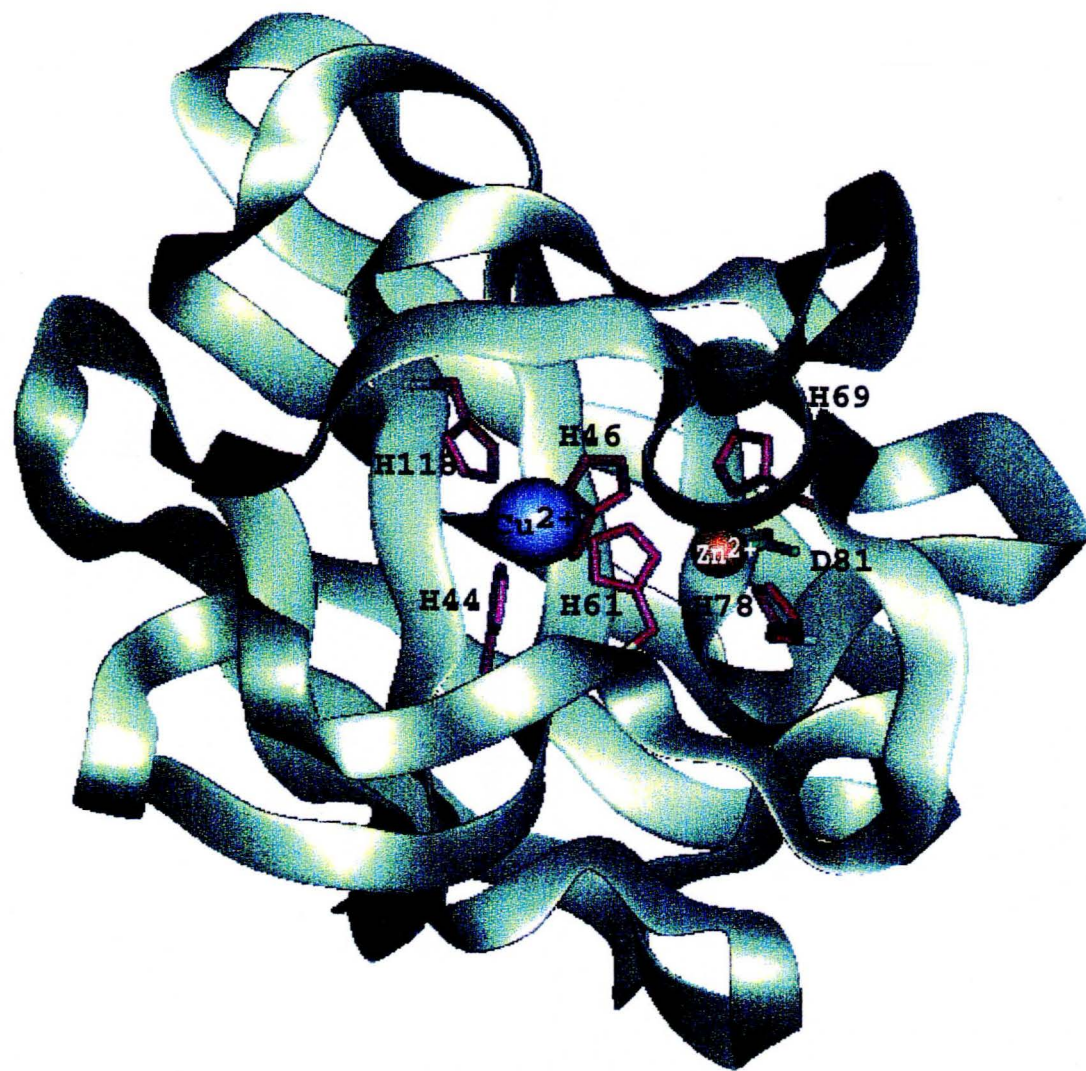
I.2. Structure and Function of Cu,Zn-SOD

Cu,Zn-SOD was first reported in 1938 by Mann and Keilin during fractionation of

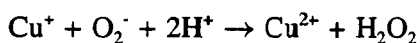
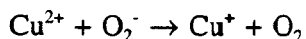
bovine red blood cell preparations (Mann and Keilin, 1938). The Cu,Zn-SOD proteins from different sources have been sequenced (Steinman et al., 1974; Johansen et al., 1979; Jabusch et al., 1980). The amino acid sequence of the native bovine erythrocyte Cu,Zn-SOD is known (Steinman et al., 1974), and its x-ray structure has been solved to a 2 Å resolution (Tainer et al., 1982). This metalloprotein is relatively easy to isolate and is suitable for bioinorganic studies in many respects (Valentine and Pantoliano, 1981; Valentine and Mota de Freitas, 1985). The protein is water soluble, thermally stable, and consists of two identical subunits, each subunit incorporating a Cu^{2+} ion and a Zn^{2+} ion. The molecular weight of each subunit is 16000, and is a flattened cylindrical barrel of β pleated sheets made up of eight antiparallel chains from which extend 3 loops of irregular structure; the two subunits are held together by weak hydrophobic interactions. The metal binding region is highly conserved between species, and contains a Cu^{2+} and a Zn^{2+} in close proximity to each other (Fig. 1). The Cu^{2+} is coordinated to four imidazole nitrogen atoms from His 44, 46, 61 and 118, and to a water molecule, giving Cu^{2+} a distorted square planar symmetry. The Zn^{2+} is coordinated to three imidazole nitrogen atoms from His 61, 69, 78, and a carboxylate group from Asp 81, giving Zn^{2+} an approximate tetrahedral geometry. His 61 forms a bridging ligand between the Cu^{2+} and the Zn^{2+} ions; the imidazole ring is in the form of a deprotonated imidazolate anion (Fig. 1). Upon reduction of Cu^{2+} to Cu^+ , the imidazole ring of His 61 is protonated, and no longer coordinates to the Cu^{2+} center (Valentine and Mota de Freitas, 1985).

The Zn^{2+} ion is believed to play a structural role in Cu,Zn-SOD with no coordination positions available. The Cu^{2+} ion, present at the bottom of the solvent channel, is responsible for the enzymatic activity of the protein, which is to catalyze the disproportionation of superoxide (O_2^-) (Fridovich, 1995). O_2^- can be formed in living systems during normal oxygen

Figure 1. Schematic drawing of the metal binding region of one subunit of Cu,Zn-SOD.



metabolism, and in other specific instances. The catalytic mechanism requires the alternate reduction and reoxidation of the Cu(II) during successive interactions of the Cu(II) with O_2^- .



Each of these half reactions proceed at nearly diffusion rates. Moreover, two protons are consumed for the dismutation of one O_2^- . H_2O_2 , one of the byproducts of dismutation, forms the substrate of another enzyme, namely peroxidase or catalase. Hence the protein requires both the oxidized and the reduced forms of copper for its activity. The x-ray structure of the reduced form of the bovine Cu,Zn-SOD is now known (Banci et al., 1994).

Cu,Zn-SOD exhibits a great degree of thermal stability (Roe et al. 1988). Using differential scanning calorimetry, it was observed that the apoprotein had a lower heat capacity maximum (T_m) of 57 °C compared to that of the native Cu,Zn-SOD, having two maxima at 89 and 96 °C, respectively. The addition of Zn^{2+} ions to the apoprotein lead to a change in T_m , the values being similar to those observed in the case of dithionite reduced Cu,Zn-SOD. The UV-visible and electron paramagnetic spectra (EPR) spectra and the activity of the bovine protein were not altered after heating a solution of the enzyme at pH 7.2 and 75 °C for 7 min (Simonyan and Nalbandyan, 1975). Furthermore, this property of the enzyme was demonstrated in the yeast protein using nuclear magnetic resonance (NMR) spectroscopy when the spectrum of the reduced Cu,Zn-SOD at 75 °C remained unchanged from that at 40 °C, indicating that the protein does not undergo any conformational change between 40 °C and 75 °C (Cass et al., 1978). The degree of stability was present only when metal ions were bound to the protein; the Zn^{2+} ion, rather than the Cu^{2+} ion, is more important in providing protein stability (Roe et al. 1988). These observations have led to the postulation of a structural role for Zn^{2+} in Cu,Zn-

SOD. Reduction of the conserved single disulfide bond between the Cys 55 and the Cys 144 residues caused a large loss of protein stability (Hill et al., 1974). More recent studies using differential scanning calorimetry indicated that the order of resistance to thermal inactivation of SODs is the same as the order of their ability to refold after unfolding (McRee et al., 1990; Lepock et al., 1990). Mutant human SOD and bovine SOD with buried Cys replaced with Ala and Ser were characterized by enzymic activity. Of the different mutants studied, removal of a free Cys residue led to mutants with increased thermostability (Hallewell et al., 1991).

Amyotrophic lateral sclerosis (ALS) is a degenerative disease affecting motor neurons in the cortex, brainstem and spinal cord (Tandon and Bradley, 1985). Familial ALS (FALS) is a form of ALS and forms about 10% of the cases of ALS; it has been shown that FALS occurs due to a defect in the gene **SOD1** that encodes a cytosolic Cu,Zn-SOD (Rosen et al., 1993).

Subsequent studies using yeast and neural cells (Rabizadeh et al., 1995) demonstrated that yeast mutants null for SOD1 but with yeast or human wild-type Cu,Zn-SOD, or of other FALS mutant Cu,Zn-SODs, did not exhibit paraquat sensitivity, though the SOD activity was moderately reduced. Overexpression of wild-type SOD1 in immortalized rat nigral neurons inhibited apoptosis, while expression of the FALS SOD1 mutants A4V and G37R enhanced apoptosis, though SOD activity was comparable to that of the wild-type. Hence SOD activity may not be the only criterion for FALS to set in.

1.3. Anion Binding Studies of Cu,Zn-SOD

O_2^- , the natural substrate of SOD, is negatively charged and highly reactive. The rate of O_2^- dismutation in the presence of the enzyme is $2 \times 10^9 \text{ M}^{-1} \text{ sec}^{-1}$ (Getzoff et al., 1992).

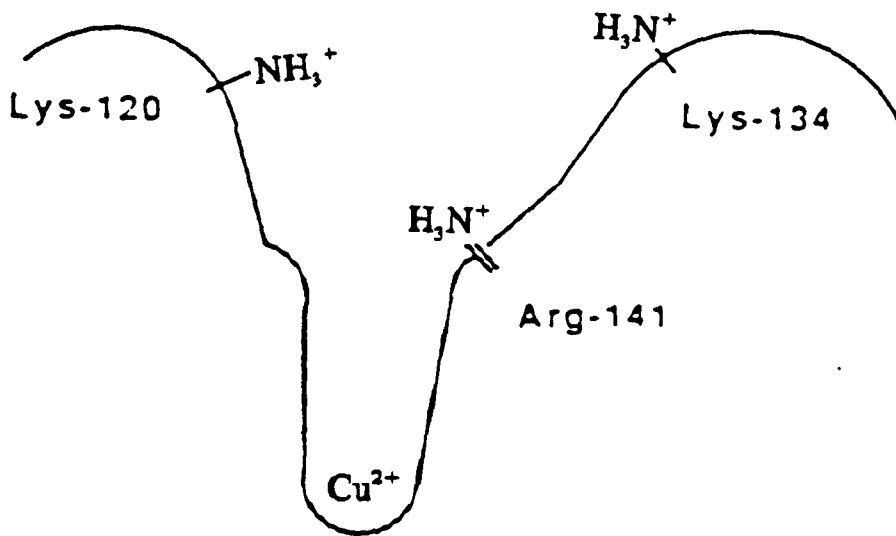
Anion binding studies have been conducted to provide information on the interactions of the substrate with the enzyme. Cu(II) is a d^9 transition metal ion, and thus it has a d-d transition band in the visible region of the spectrum. The electronic absorption spectrum of native Cu,Zn-SOD in the visible region has an absorption maximum at 680 nm. Small anions like CN^- , N_3^- , and halides have been shown to interact with Cu,Zn-SOD and are competitive inhibitors of the native Cu,Zn-SOD (Rigo et al., 1977). Generally very small changes are observed in the absorption spectrum upon anion binding. However, in the presence of cyanide, the d-d transition is blue-shifted to 550 nm, and in the case of azide, a new absorption band at 373 nm is obtained, which was assigned to an azide to Cu(II) charge-transfer band (Fee and Gaber, 1972; Valentine and Pantoliano, 1981).

The interactions of these anions with the enzyme have been investigated by NMR using the Cu,Co-derivative of SOD. This derivative contains Co(II) in place of Zn(II) and this metal ion replacement does not affect the catalytic and structural properties of the enzyme (McAdam et al., 1977; Djinović et al., 1992). The presence of high-spin Co(II) in place of Zn(II) can be used to detect isotropically shifted proton resonances of groups directly coordinated to the Co(II). Initial 1H NMR studies of the Cu,Co-SOD (Bertini et al., 1985) characterized the isotropically-shifted 1H NMR resonances in the protein by comparing the metal-proton distances obtained from the x-ray structure with the T_1 values of these signals and the field dependence of their line widths. The 1H NMR spectrum of the SOD- N_3^- complex indicated that there was a change in some of the isotropically-shifted resonances; these were assigned to the protons of His 44. The T_1 and the T_2 values of these resonances increased, indicating that there was a reduction in the effect of the paramagnetic Cu(II) on these protons. These protons were assigned to His 44 and interpreted in terms of the removal of His 44 from the coordination

sphere of Cu^{2+} , with simultaneous binding of azide to Cu^{2+} (Bertini et al., 1985; Banci et al., 1987). This result was further supported by extended x-ray absorption fine structure (EXAFS) studies on the azide-bound form of SOD (Blackburn et al., 1987). Other ^1H NMR studies using Cu,Co-SOD have proposed that ^1H NMR resonances assigned to His 46 move towards the diamagnetic position on binding both N_3^- and CN^- . The change is more pronounced in the case of CN^- than for N_3^- , which is consistent with the trend in which the larger affinity constant of the anion, the larger the change in the shifts of the resonances of the detaching histidine (Banci et al., 1989, 1990). The x-ray structure of the N_3^- -reacted Cu,Zn-SOD has been solved at 2.1 Å resolution (Carugo et al., 1994a). This study revealed that the N_3^- anion was coordinated directly to Cu(II) in both the subunits of the native Cu,Zn-SOD in place of the metal-bound water. The anion formed an ion pair with the conserved Arg-141 residue (vide infra). The EPR spectrum of the CN^- bound native Cu,Zn-SOD has an axial shape when compared to the rhombic spectrum of the native Cu,Zn-SOD. These two anions bind in an equatorial position after displacing an imidazole of a histidine residue (Rotilio et al., 1972).

X-ray analysis of the native bovine Cu,Zn-SOD indicate that the positively charged side chains of the residues Arg-141, Lys-120 and Lys-134 are present at 5, 12 and 13 Å away from the Cu(II), and aid in guiding the substrate towards the Cu(II) site in the enzyme (Tainer et al., 1982) (Fig.2). These residues (Arg-141, Lys-120 and Lys-134) can be chemically modified. Arg-141 is modified using phenylglyoxal (Malinowski and Fridovich, 1979), while Lys-120 and Lys-134 are modified using succinic anhydride (Marmochi et al., 1982). These modifications result in the shielding or the elimination of the positive charges present on these residues. These modified proteins exhibited residual activities of 15-20% of the native Cu,Zn-SOD. Interactions of anions such as phosphate, formate and chloride have also been reported

Figure 2. Schematic representation of the solvent channel of Cu,Zn-SOD indicating the relative positions of the positively charged amino acid residues.



(Mota de Freitas et al., 1987; Sette et al., 1992; Mota de Freitas et al., 1990b). The activity of native Cu,Zn-SOD decreased by 50% in the presence of phosphate when compared to HEPES at the same ionic strengths (Mota de Freitas and Valentine, 1984). The activity of arginine-modified Cu,Zn-SOD was not reduced significantly in the presence of phosphate. Association constants for N_3^- and CN^- binding to Cu,Zn-SOD decreased significantly in the presence of phosphate, but such large changes were not observed in the case of arginine-modified Cu,Zn-SOD (Mota de Freitas and Valentine, 1984). Interactions of native bovine Cu,Zn-SOD with inorganic phosphate was further studied using ^{31}P NMR T_1 and T_2 relaxation measurements (Mota de Freitas et al., 1987). Paramagnetic effects on the ^{31}P phosphate resonance, due to the Cu(II) present at the active site of native and chemically modified proteins, were used to characterize the interaction of phosphate with these proteins; these studies were conducted at the pH values of 6.3, 7.0 and 8.0. The concentrations of SOD and phosphate used were also varied. The relaxation rates, T_1^{-1} and T_2^{-1} , of the phosphate resonances increased in all cases in the presence of native Cu,Zn-SOD when compared to solutions containing no protein or reduced proteins. Hence the increased rates of relaxation of the phosphate resonances were attributed to the presence of the paramagnetic Cu(II) center in the native protein. The affinity constant of phosphate to native Cu,Zn-SOD was three times the value of that found for the arginine-modified Cu,Zn-SOD. The distance of the phosphate calculated from the relaxation rate of the bound phosphate indicated that phosphate was bound to the Arg-141 residue, which was known from the x-ray structure to be 5 Å away from the Cu(II) at the active site (Tainer et al., 1982).

Subsequent studies have characterized the interactions of different anions Cl^- , ClO_4^- , CH_3COO^- , borate and phosphate with native and arginine-modified Cu,Zn-SOD using ^1H and

^{31}P NMR (Desideri et al., 1988); a shift in the proton resonance from the NH of His 46 in the Cu,Co-SOD derivative indicated that these anions bind at the Arg-141 residue. This is due to the proximity of the NH_2 groups of Arg-141 to His-46. Formate was used as a probe in NMR studies of anion binding to Cu,Zn-SOD and Cu,Co-SOD (Sette et al., 1992). ^{31}P NMR was used to confirm this hypothesis. The ^{31}P line widths of the phosphate resonances were larger in the presence of native Cu,Zn-SOD when compared to the lysine- and arginine-modified Cu,Zn-SOD. With increasing concentrations of phosphate, the ^{31}P line widths decreased for both the native and lysine-modified SOD; there was no significant change in the line widths of Arg-141 modified Cu,Zn-SOD with increasing concentrations of phosphate, demonstrating that phosphate binding occurs at the Arg-141 residue (Desideri et al., 1988). ^{31}P NMR T_1 relaxation studies with recombinant human Cu,Zn-SOD with the Arg 143 replaced by isoleucine showed no differences in the T_1 values of the phosphate resonances in the presence of the mutant protein or in its absence (Bertini et al., 1991) confirming once again that the essential arginine is the main binding site for phosphate.

In the dismutation of O_2^- , Cu changes its oxidation state between +2 and +1. There have also been studies of anion binding to the reduced Cu,Zn-SOD. Initial ^{35}Cl NMR studies on reduced bovine Cu,Zn-SOD (Fee and Ward, 1976) used line width measurements to determine the site of interaction of Cl^- . The line width of the Cl^- resonance in the presence of the apoprotein (Cu,Zn-SOD with the Cu(II) and Zn(II) ions removed) was found to be less than observed in the presence of reduced Cu,Zn-SOD. Addition of CN^- to Cl^- in the presence of reduced Cu,Zn-SOD lowered the Cl^- line width to a value similar to that obtained in the case of apoprotein. This observation was interpreted as Cl^- binding to the Cu(I) present in the reduced Cu,Zn-SOD. Subsequent work by Mota de Freitas et al. (1990b) on Cl^- binding to

reduced Cu,Zn-SOD also used line width measurements of the Cl⁻ resonances. The Cl⁻ line widths of the Cl⁻ resonances were larger in the presence of reduced Cu,Zn-SOD when compared to those in the presence of reduced arginine-modified and reduced lysine-modified protein, indicating that Cl⁻ binds reduced Cu,Zn-SOD through the positively charged Arg-141, Lys-120 and Lys-134 residues.

Monomeric vanadate is a structural analog of phosphate. Solutions of vanadate contain, however, different species of vanadate depending on the concentration, pH and temperature. ⁵¹V NMR has been used to characterize the interaction of vanadate with bovine Cu,Zn-SOD (Wittenkeller et al., 1991); under the conditions studied, the vanadate solution contained the monomeric, dimeric and tetrameric forms of vanadate. This information is easily obtained from the ⁵¹V NMR spectrum. Upon addition of increasing amounts of native Cu,Zn-SOD, the intensities of the dimer and the tetramer ⁵¹V NMR resonances decreased, while smaller changes were observed in the case of the monomeric resonance. The line widths of the vanadate dimer and tetramer increased, with small changes seen in the case of the monomeric vanadate. The ⁵¹V T₁ and chemical shift values for the monomeric, dimeric and tetrameric species in solution were, however, similar in the presence and absence of Cu,Zn-SOD. The line width changes observed were the largest for the resonance of the vanadate tetramer, indicating that the vanadate tetramer binds most strongly to Cu,Zn-SOD. The line widths of the vanadate tetramer increased in the presence of arginine-modified Cu,Zn-SOD; smaller changes were observed in the case of the vanadate dimer. However, in the presence of lysine-modified SOD, the line widths and the intensities of the monomer, dimer and tetramer resonances did not change significantly, indicating that vanadate anions do not interact with the lysine modified protein. The absorbance spectra of native Cu,Zn-SOD showed no changes in the presence of vanadate;

hence, vanadate binds to the lysine residues and not to Cu(II). The vanadate tetramer was found to have the smallest dissociation constant thus far for anion binding studies of this protein, indicating strong binding to Cu,Zn-SOD. From the concentrations of the different vanadate species and of the enzyme, the number of vanadium atoms bound to a dimer of Cu,Zn-SOD was calculated to be 8. Hence each subunit of Cu,Zn-SOD binds one vanadate tetramer, and with an affinity constant even greater than that of O_2^- (Wittenkeller et al., 1991).

I.4. Vanadium in Biological Systems

Vanadium was discovered in 1802/1803 by A.M. Del Rio, a Spanish mineralogist (Rehder, 1995). The element was rediscovered in 1831 by a Swedish chemist and named it "vanadin" or vanadium (Hoppe et al., 1990). Vanadium is the most abundant transition metal in seawater, and occurs mostly in the form of $H_2VO_4^-$ up to a concentration of 20-35 nM. Vanadium is a trace metal, present in mammalian tissues at concentrations below 1 μ M (Nechay, 1984). However, ascidians are known to concentrate large amounts of vanadium in specialized vanadium-containing blood cells called vanadocytes (Webb, 1939).

I.5. Interaction of vanadate with proteins

Under physiological conditions, vanadium exists in the +4 and +5 oxidation states. V(IV) is present as VO^{2+} and V(V) is present as $H_2VO_4^-$. VO^{2+} has been substituted for Zn^{2+} in enzymes like carboxypeptidase A (DeKoch et al., 1974) and carbonic anhydrase (Fitzgerald and Chasteen, 1974). VO^{2+} is also reported to bind to albumins from different species (Sakurai et al., 1987) and calmodulin (Nieves et al., 1987). Vanadium (II) or vanadium (IV) is present in the vanadium nitrogenases found in nitrogen fixing bacteria; the chemical environment of

vanadium in this protein has been studied by x-ray absorption spectroscopy and extended x-ray absorption edge fine structure and vanadium was found to have a distorted octahedral coordination (Shah and Brill, 1977; George et al., 1988).

Vanadium (V) is present at the active center of vanadium haloperoxidases isolated from some brown and red algae, and was confirmed by using ^{51}V NMR spectroscopy. Vanadium (V) is surrounded by oxygen ligands, presumably by bidentate carboxylate groups (Rehder et al., 1991). X-ray absorption near-edge structure spectroscopy was used to study the coordination charge on vanadium in the native and reduced enzyme (Kusthardt et al., 1993), and confirmed the charge obtained from the ^{51}V NMR study. Reduced peroxidases have vanadium (IV) in the active center; they show axially symmetric vanadyl-type EPR spectra, and are similar irrespective of the source of the protein (Wever and Kustin, 1990).

The ability of vanadate to inhibit phosphate-dependent enzymes is due to the similarities of the shape and chemical properties of monomeric vanadate and phosphate. Low vanadate concentrations are usually used to study the interactions of vanadate with enzymes, so the major species involved in these studies is the monomeric vanadate. Na^+, K^+ -ATPase was shown to be inhibited by monomeric vanadate (Josephson and Cantley, 1977). Vanadate binds at two non-equivalent sites with different affinities, and was shown to bind at an aspartyl residue that is phosphorylated during the normal catalytic cycle (Chasteen, 1983). A detailed study by Goodno (1979) on the inhibition of myosin ATPase by monomeric vanadate showed that the presence of ATP slowed the onset of inhibition, which was faster in the presence of ADP. This was due the formation of the stable, inactive complex of protein-ADP-vanadate formed by the isomerization of the initial complex of similar composition. Other enzymes, such as acid phosphatases and alkaline phosphatases, are also inhibited by monomeric vanadate. Vanadate

forms a chelate at the active site which resembles the trigonal bipyramidal transition state occurring in the hydrolysis of the phosphate ester or the phosphoryl enzyme intermediate (VanEtten et al., 1974).

Oligomeric vanadates have been known to inhibit several enzymes. Using ^{51}V NMR and enzyme kinetics, glucose-6-phosphate dehydrogenase (G6PDH) was shown to be inhibited by vanadate dimer and tetramer (Crans and Schelble, 1990). Vanadate dimer and tetramer inhibit the enzyme by non-competitive inhibition with respect to G6PDH and by competitive inhibition with respect to NADP or NAD for G6PDH (Crans and Schelble, 1990). The tetramer also interacts with the enzymes 6-phosphogluconate dehydrogenase (Crans et al., 1990) and glycerol-3-phosphate dehydrogenase (Crans and Simone, 1991). Using ^{51}V NMR spectroscopy, the vanadate tetramer was found to be the species mediating the photocleavage of the myosin heavy chain at three specific sites (Cremona et al., 1990). The decamer has been found to inhibit hexokinase and phosphofructokinase (Boyd et al., 1985), and also bind to Ca^{2+} -ATPase (Csermely et al., 1985).

Vanadate has been shown to stimulate the oxidation of NAD(P)H in the presence of an O_2^- source including biological membranes. Vanadium (V) reacts with O_2^- to give the product peroxovanadyl, which is capable of oxidizing NAD(P)H rapidly by a free radical chain reaction. SOD has been shown to inhibit vanadate-stimulated NADH oxidation by xanthine oxidase (Liochev and Fridovich, 1990).

I.6. Lithium in Medicine

Lithium, in the form of lithium salts, is one of the few inorganic compounds used as a therapeutic agent today. The element was discovered in 1817. During the mid 19th century,

the lithium salt of uric acid was used to treat uric acid diathesis, a condition in humans related to mood, compounded with deposition of uric acid crystals in joints (Jefferson et al., 1985). In 1949, John Cade used lithium urate, the most soluble salt of uric acid, to determine uric acid toxicity in guinea pigs. He discovered that the compound had a calming effect when injected into the animals. He later administered lithium carbonate to psychiatric patients and found that it reduced psychotic excitement. This observation led to lithium being considered as an anti-manic medication (Cade, 1949). Lithium, in the form of carbonate and citrate salts, continues to be one of the most effective and selective drugs now available for the prophylactic treatment of both mania and depression in patients diagnosed with bipolar disorder (Lennox and Watson, 1994). Lithium salts have also been used in the treatment of other psychiatric illnesses like acute and recurrent major depression, schizophrenia, alcoholism; and non-psychiatric conditions such as low white blood cell count, hyperthyroidism and those associated with the Herpes simplex virus (Jefferson et al., 1985).

Lithium is commonly administered to patients as lithium carbonate, in doses between 500 and 1800 mg per day. The uptake of lithium into tissues is slow, leading to a delay of 5-10 days to reach the therapeutic level of 0.5-1.5 mM in plasma (Jefferson et al., 1985). Lithium has a narrow therapeutic range, and patients with plasma lithium concentrations 50% greater than the therapeutic range experience early signs of clinical toxicity such as tremor, fatigue, anorexia and nausea.

Lithium salts have been used in the treatment of bipolar disorder for over 40 years, and yet a clear understanding of the molecular mechanisms underlying the therapeutic action of lithium is unknown. The lithium ion (Li^+) is the active species which is responsible for the therapeutic action of lithium.

1.7. Lithium Transport in RBCs

In human red blood cells (RBCs), the transport of Li^+ and Na^+ ions across the cell membranes follows similar pathways. The uptake of Li^+ into human RBCs mainly occurs by passive diffusion across the pores present in the membrane. This pathway is known as the leak pathway, and at physiological conditions, contributes to both the influx and efflux of Li^+ across the RBC membrane; this diffusion of Li^+ is dependent upon the resting membrane potential and accounts for 70% of the Li^+ influx at therapeutic Li^+ levels (Ehrlich and Diamond, 1979; Mota de Freitas et al., 1991).

The second pathway through which Li^+ is transported into the RBC is through the anion exchange or the bicarbonate-sensitive pathway (Ehrlich and Diamond, 1979). Li^+ is transported as the anionic species LiCO_3^- through the membrane-spanning band 3 protein. This protein allows for the 1-1 exchange of Cl^- for Cl^- or Cl^- for HCO_3^- . Li^+ forms a complex with CO_3^{2-} giving LiCO_3^- . Li^+ influx into RBCs was increased when LiHCO_3 was used instead of LiCl in the incubation medium. This bicarbonate-dependent Li^+ influx is sensitive to the band 3 protein inhibitor 4,4'-diisothiocyanostilbene-2,2'-disulfonic acid (DIDS) (Cabantik and Rothstein, 1974).

The ouabain-sensitive sodium pump or Na^+, K^+ -ATPase transports Li^+ into RBCs only under conditions when intracellular Na^+ and K^+ are absent, and are replaced by choline (Ehrlich and Diamond, 1979). Li^+ ions may be transported through the chloride-dependent $\text{Na}^+ - \text{K}^+$ cotransport system. This pathway is inhibited by loop diuretics like furosemide (Canessa et al., 1982). Using different experimental conditions, it was demonstrated that Li^+ could replace Na^+ , but not K^+ , in the $\text{Na}^+ - \text{K}^+$ cotransport pathway.

Li^+ efflux occurs mainly through the $\text{Na}^+ - \text{Li}^+$ countertransport pathway (Duhm et al.,

1976). The intracellular Li^+ concentration is lower than that of the extracellular Li^+ concentration, and this distribution is maintained by the Na^+ - Li^+ countertransport system. This pathway does not require ATP; and is inhibited by phloretin, furosemide, quinine and quinidine (Duhm, 1981). At physiological conditions, Li^+ is transported out of the cell in exchange for Na^+ transported into the cell. The plasma concentration of Na^+ is 140 times that of Li^+ ; Li^+ is transported out of the cell against an electrochemical gradient, the energy for which is obtained from the Na^+ concentration gradient maintained across the cell membrane by the sodium pump. The Na^+ - Li^+ countertransport system accounts for about 75% of the Li^+ efflux in RBCs, while the remaining 25% occurs through the leak pathway.

Li^+ transport in human RBCs has been investigated by ^7Li NMR spectroscopy (Espanol and Mota de Freitas, 1987; Mota de Freitas et al., 1990a, 1990c). NMR spectroscopy along with the discovery of non-permeable shift reagents led to the development of non-invasive methods of studying Li^+ transport into intact cells. The presence of 3 mM $\text{Dy}(\text{PPP})_2^{7-}$ as the shift reagent was sufficient to discriminate between the Li^+ resonances arising from the intracellular milieu and from the suspension medium at therapeutic levels of Li^+ (Espanol and Mota de Freitas, 1987). Comparison of Li^+ transport in the presence of the shift reagents $\text{Dy}(\text{PPP})_2^{7-}$ and $\text{Dy}(\text{TTHA})^{3-}$ with the AA methods generally used in clinical studies revealed significant correlations between the transport rate obtained by AA and NMR using $\text{Dy}(\text{TTHA})^{3-}$ as the shift reagent; the presence in the suspension medium containing $\text{Dy}(\text{PPP})_2^{7-}$ as the shift reagent led, however, to higher rates of Li^+ efflux due to the greater charge on the shift reagent (Mota de Freitas et al. 1990a). An alternate NMR method utilizes a modified inversion recovery (MIR) pulse sequence, in the absence of shift reagents, to distinguish between intracellular Li^+ and that from the surrounding medium; this method provided lower rates of Li^+

efflux from Li^+ loaded cells when compared to the Li^+ transport in the presence of shift reagents other than $\text{Dy}(\text{TTHA})_3^{3-}$ (Mota de Freitas et al., 1990a).

I.8. Lithium Transport in Nerve Cells

RBCs have been used extensively by investigators to study Li^+ transport into cells. RBCs are easily obtained, and the electrolyte transport properties are similar to neurons. But due to the ability of the neuronal membranes to initiate and propagate action potentials, electrolyte transport across nerve membranes will be different from that of RBCs. Sodium channels present on the neuronal membranes control the passage of Na^+ across the membranes, and make the membrane electrically excitable. Earlier studies using the mouse neuroblastoma cell line N1E-115 (Richelson, 1977) demonstrated that, in the presence of the alkaloid veratridine (which selectively increases the permeability of electrically-excitabile membranes to Na^+), Li^+ uptake was stimulated. Tetrodotoxin, a known inhibitor of the Na^+ channel, inhibited the veratridine-stimulated entry of Li^+ , thus demonstrating that Li^+ entry into nerve cells occurs through the Na^+ channel in electrically excitable cells.

Li^+ influx into cells in a mixed population of chick glial and neuronal primary cell cultures was shown to be inhibited by the presence of phloretin and ouabain indicating that there is a Na^+ -dependent Li^+ uptake into these cells in culture (Szentistvanyi et al., 1979b).

A comprehensive study using the mouse neuroblastoma x rat glioma cell line 108CC15 delineated different pathways through which the Li^+ ion can be transported across neuronal cell membranes (Reiser and Duhm, 1982). The Na^+ - Li^+ countertransport system was shown to exist in this hybrid cell line wherein the cells exchange Na^+ on one side of the membrane for Li^+ on the other. The Na^+ - Li^+ countertransport system is insensitive to ouabain, similar to the

one reported in erythrocytes. The sodium pump is the second pathway through which Li^+ is transported across the cell membrane. The efflux of Li^+ from Li^+ loaded hybrid cells was not affected by ouabain, due to the lower affinity of the internal binding site for Li^+ than for Na^+ . However, Li^+ uptake by these hybrid cells was demonstrated to be ouabain-sensitive due to the inhibition of the sodium pump. Furthermore, Li^+ uptake was inhibited by external Na^+ and K^+ , in agreement with observations made with erythrocytes.

Li^+ is also transported through the action potential ionophore of hybrid cells. Veratridine, an activator of the voltage-dependent Na^+ channel, stimulated Li^+ uptake into cells; tetrodotoxin alone did not inhibit Li^+ uptake, indicating that Li^+ uptake into cells does occur via the voltage-sensitive Na^+ channels, and spontaneously opening of Na^+ channels does not appear to play a prominent role in Li^+ influx. The leak pathway similar to that found in human RBCs has not been reported for neuronal cells so far.

A recent study of Li^+ transport into human astrocytoma cells using NMR spectroscopy was reported (Bramham et al., 1996). Human 1321 N1 astrocytoma cells were anchored on Biosilon beads and suspended in a modified medium to monitor Li^+ transport. $\text{Dy}(\text{PPP})_2^{7-}$ at 5 mM was used to separate the intracellular ^7Li resonance from that of the surrounding medium. These cells are of glial origin, and the cells were not perfused; the NMR tube was periodically inverted to ensure that the cells were not depleted of oxygen or nutrients. The cell viability was monitored by ^{31}P NMR spectroscopy. A low intracellular Li^+ concentration was obtained which was attributed to an efflux mechanism present in astrocytomas (Bramham et al., 1996).

1.9. Lithium Ionophores

Ionophores belong to a group of compounds that selectively transport ions across membranes increasing their permeability to ions. Ionophores are classified under two categories a) channel-forming ionophores and b) carrier ionophores. The channel-forming ionophores create a channel within the membrane allowing the passage of ions across the membrane, e.g., gramicidin (Pressman, 1976; Hinton and Koeppe, 1985). The carrier ionophores diffuse within the membrane and can be anionic or neutral. Anionic ionophores possess a negative charge due to the presence of an ionizable group such as a carboxylic acid or hydroxyl group, and form an electrically neutral species when they complex with a metal ion, e.g., Monensin (Painter and Pressman, 1985). Neutral ionophores are electrically neutral and form a charged ionophore-metal ion complex e.g., Valinomycin (Pressman, 1976; Easwaran, 1985).

Numerous Li^+ ionophores have been reported in the literature (Pacey, 1985; Shinar et al., 1986). They include crown ethers, polyether open chain compounds, and cyclic compounds. The selectivity of the ionophore is determined by the size of the cavity of the ionophore and the diameter of the ion (Shinar et al., 1986). Crown ethers of the type 14-crown-4 (14C4) form 1:1 complexes with Li^+ (Kimura et al, 1986). The diameters of the Na^+ and K^+ ions exceed that of the cavity, thus a 2:1 complex (crown ether:cation) is formed with these ions. The presence of bulky substituents such as benzyl groups on the 14C4 ring improves the Li^+ selectivity by preventing the formation of the 2:1 complexes with Na^+ and K^+ . Increase in Li^+ transport rates in human RBCs in the presence of dibenzyl 14C4 (DB14C4) has been demonstrated (Abraha and Mota de Freitas, 1992).

I.10. Mechanisms of Lithium Action

Several hypotheses have been proposed to explain the mode of action of lithium at the molecular and cellular levels. Two interrelated hypotheses that we are currently investigating are competition between lithium and magnesium ions for the magnesium-binding sites in biomolecules (Frausto da Silva and Williams, 1976; Ramasamy and Mota de Freitas, 1989); the other is based on a cell membrane abnormality (Metzler, 1991).

Li^+ belongs to group 1A of the periodic table of elements. There exists a diagonal relationship between Li^+ and Mg^{2+} in the periodic table which is consistent with similar chemical properties for Li^+ and Mg^{2+} ; hence competition between these two ions for Mg^{2+} binding sites could occur. Mg^{2+} plays a crucial role in many biochemical processes occurring within the cell. Mg^{2+} is known to regulate the activity of many enzymes involved in metabolism and membrane transport processes.

Li^+ inhibits adrenergically-activated adenylate cyclase activity (Belmaker, 1981). It is proposed that this inhibitory action of Li^+ leads to its anti-manic effect. In contrast, the antidepressive effect of Li^+ may be due to the inhibition of the cholinergically-activated phosphatidylinositol system (Hallcher and Sherman, 1980). However, neither mechanism alone can explain both the anti-manic and antidepressive effects of Li^+ . G proteins play an important role in transducing messages across the cell membrane (Gilman, 1987; Hepler and Gilman, 1992). Avissar et al. (1988) have demonstrated that, at therapeutically efficacious concentrations, Li^+ blocked both adrenergic and cholinergic agonist-induced increases in GTP binding to cell membranes from rat cerebral cortex. Since increased GTP binding to G proteins is a characteristic of G protein stimulation, G proteins may be the site of action of Li^+ .

G proteins are membrane-bound heterotrimeric proteins that play an obligatory role in

the transduction of extracellular, receptor-mediated signals across cell membranes to various intracellular effectors. G proteins consist of three subunits, α , β and γ ; a large diversity exists in the α subunits and this modulates the activities of the different effectors. Binding of a specific membrane-bound receptor leads to the activation of a G protein. The activated G protein binds GTP, which leads to the release of the $\beta\gamma$ subunits from the heterotrimer. The activated G protein subsequently stimulates the membrane bound adenylate cyclase which regulates the synthesis of cyclic AMP (cAMP) from ATP (Gilman, 1987). Alternatively, the activation of G proteins may stimulate phospholipase C-mediated breakdown of phosphatidylinositol-4,5-bisphosphate, leading to the formation of the intracellular second messengers diacylglycerol (DAG) and inositol 1,4,5-triphosphate (IP_3). IP_3 then interacts with its receptor leading to the release of intracellular stores of Ca^{2+} (Berridge, 1987).

Certain agonist-mediated receptor stimulation leads to the inhibition of adenylate cyclase. This is due to the presence of two different kinds of G protein in membranes, one is the G_s , stimulation of which leads to increased cAMP synthesis, and the other is G_i , stimulation of which leads to the inhibition of adenylate cyclase (Hepler and Gilman, 1992). The two types of G proteins have distinct G_α subunits, $G_{s\alpha}$ and $G_{i\alpha}$, respectively. The activity of G proteins is at the center of receptor-effector communication, and forms a "molecular switch" that allows the cell to respond rapidly to external stimuli following a large amplification of the extracellular signal. The activation of G proteins, the formation of cAMP, and the dephosphorylation of inositol monophosphate are Mg^{2+} -dependent, and are inhibited by Li^+ (Avissar et al, 1988; Mørk, 1990; Pollack et al, 1994). Li^+ modulates the activity of various Mg^{2+} -dependent enzymes (Geisler and Mørk, 1990), and thus regulates certain cellular processes.

Previous studies have examined the levels and /or the activation of G proteins in patients

with bipolar disorder. Schreiber et al. (1991) have demonstrated enhanced agonist-stimulated binding of tritiated guanyl imidodiphosphate, a nonhydrolyzable analog of GTP, in leukocyte membranes of untreated bipolar patients. Such increases were not observed in the case of control subjects. Similar results were obtained by Young and coworkers, who in one study have reported increased levels of $G_{\alpha s}$ in postmortem brain tissue samples from the cerebral cortex of bipolar patients (Young et al., 1991). Another study by Young et al. (1994) demonstrated enhanced levels of $G_{\alpha s}$ in mononuclear leukocytes from depressed patients suffering from bipolar disorder, but not from depressed patients with unipolar depression.

Studies from our laboratory using multinuclear NMR spectroscopy provide evidence for competition between Li^+ and Mg^{2+} for various substrates of second messenger systems including ATP, ADP, GTP, GDP and IP_3 in aqueous solution (Abraha et al., 1991; Rong et al., 1992; Rong et al., 1994); for ATP in human erythrocyte suspensions (Ramasamy and Mota de Freitas, 1989) and for the phosphate head groups in the human RBC membrane (Mota de Freitas et al., 1994b). Evidence for the reversal of lithium inhibition of β -adrenergic and muscarinic receptor coupling to G proteins by Mg^{2+} has been demonstrated in membranes from rat cerebral cortex (Avissar et al., 1991).

Human RBCs have been used extensively in research to study biological processes because of their simple structure and easy availability. The cell membrane dysfunction hypothesis was postulated based on studies using human RBCs (Mendels and Frazer, 1974; Meltzer, 1991). One of the components of Li^+ transport in human RBCs is the Na^+ - Li^+ exchange pathway, which under physiological conditions is a Na^+ - Na^+ exchange protein, with a binding site for Li^+ . An initial clinical study of Na^+ - Li^+ exchange rates indicated a negative correlation between the exchange rates and RBC/plasma ratio of Li^+ (Pandey et al., 1977). The

rates of $\text{Na}^+\text{-Li}^+$ exchange were observed to be significantly lower in bipolar patients receiving lithium carbonate than in normal individuals (Pandey, et al., 1977; Ostrow et al., 1978; Szentistvanyi et al., 1979a). Studies using ^7Li NMR spectroscopy and atomic absorption (AA) also showed a lower rate of $\text{Na}^+\text{-Li}^+$ exchange rate in RBCs from bipolar patients when compared to that from normal individuals (Mota de Freitas et al., 1990c; Mota de Freitas et al., 1994a). The higher affinity of Li^+ to RBC membranes from bipolar patients may explain the observed lower $\text{Na}^+\text{-Li}^+$ exchange rates in RBCs when compared to that of normal individuals.

I.11. Analytical Methods for Detection of Vanadate and Li^+ in Biological Samples

Colorimetric methods have been used extensively in the past to determine vanadium concentrations in biological samples. Ligands such as N-cinnamoyl-N-(2,3-xylyl)hydroxylamine and N-phenylbenzohydroxamic acid in o-dichlorobenzene have been used for the analysis of vanadium in foods and in green vegetables like cauliflower and spinach respectively (Seiler, 1995). Atomic absorption spectrometry (AAS) has been employed to determine vanadium content in homogenous samples. Graphite furnace atomic absorption spectrometry is very sensitive and enables the determination of vanadium in the ppb range (Seiler, 1995). Inductively coupled-plasma emission spectrometry, inductively coupled-plasma mass spectrometry, and neutron activation analysis (NAA) are other methods which are used in determining vanadium concentrations in biological samples. NAA allows for the determination of vanadium in the pg vanadium per g of a sample (Seiler, 1995).

^{51}V NMR spectroscopy is used to determine the concentrations of vanadate in aqueous solutions. This method is non-invasive, non-destructive and allows for the simultaneous determination of different vanadium species in biological samples (Crans et al., 1990; Crans and

Simone, 1991; Wittenkeller et al., 1991).

Li^+ in biological samples can be determined by conventional methods such as flame emission photometry, atomic absorption spectrometry, fluorescence, ion-selective electrodes and neutron activation analysis (Mota de Freitas et al., 1991). AA is very selective to the element monitored and is highly sensitive. The development of highly selective Li^+ optical and fluorescent dyes, such as crownazophenol-5 and 1,8-dihydroxyanthraquinone, has led to the determination of Li^+ selectively in samples like blood plasma using optical and fluorescence spectroscopy (Kimura et al., 1985; Wheeling and Christian, 1984). Li^+ selective electrodes have been used to monitor Li^+ levels in serum from manic-depressive patients (Metzger et al., 1987). All these techniques require physical separation of cells from the plasma or surrounding medium and cell lysing. These methods are thus destructive in nature.

^7Li NMR spectroscopy has been developed to monitor Li^+ transport in human RBCs. It is possible to observe two different ^7Li NMR resonances, one from within the cells, and the other from the surrounding medium, by incorporating a membrane impermeable shift reagent in the medium (Espanol and Mota de Freitas, 1987). The advantage of this method is that it is non-invasive and non-destructive. An alternate ^7Li NMR method which does not require shift reagents in the suspension medium has also been used to monitor Li^+ transport in human RBCs. This method employs the MIR pulse sequence, which takes advantage of the large difference in spin-lattice relaxation times for the intra- and extracellular Li^+ ions (Mota de Freitas et al., 1990a). ^7Li NMR has also been employed to investigate Li^+ transport in manic-depressive patients (Mota de Freitas et al., 1990c, 1994a).

CHAPTER II

STATEMENT OF THE PROBLEMS

The purpose of this dissertation is two fold: 1) to determine the interactions between biologically relevant phosphates and vanadate with native Cu,Zn superoxide dismutase and metal-depleted derivatives of Cu,Zn-SOD respectively, using multinuclear NMR spectroscopy; and 2) to develop the methodology required to study Li^+ transport in nerve cells, and its interactions with intracellular components using ^7Li NMR spectroscopy.

Cu,Zn-SOD is a cytosolic metalloenzyme suitable for bioinorganic studies (Valentine and Mota de Freitas, 1985). Numerous anion binding studies have been conducted to determine the interactions between the protein and substrate molecules. Small anions like CN^- and N_3^- bind directly at the Cu^{2+} site (Rigo et al., 1977; Carugo et al., 1994a,b), while larger anions like phosphate and vanadate bind at the positively charged Arg and Lys residues respectively, which are located in the solvent channel of each of the monomers (Mota de Freitas et al., 1987; Wittenkeller et al., 1991). Tetrameric vanadate was the first large anion shown to bind Cu,Zn-SOD with a binding constant greater than that known for its natural substrate O_2^- . Since the vanadate tetramer was shown to interact strongly with native bovine Cu,Zn-SOD, it would be of interest to determine whether other large anions which are present in living cells interact with native Cu,Zn-SOD. AMP, ADP, ATP are metabolites found in living cells, and they possess increasing number of phosphate groups. The interactions of these compounds with native

Cu,Zn-SOD would provide information on whether this metalloprotein exhibits binding selectivity based on shape and charge on the anions. In addition, the interactions of the synthetic polyphosphates, triphosphate and diphosphate with native bovine Cu,Zn-SOD would indicate whether the adenosine group on the adenosine nucleotides specifically contribute to the binding of these compounds to the native protein. ^{31}P and ^{13}C NMR spectroscopy will be used to determine the interactions between native bovine Cu,Zn-SOD and different biological phosphates. The changes in chemical shifts, line widths and spin-lattice relaxation (T_1) values of the different phosphate groups in the presence of the native enzyme will be monitored to determine the interactions of these phosphate-containing compounds with native Cu,Zn-SOD.

The reduced Cu,Zn-SOD, the zinc-only derivative of Cu,Zn-SOD, and the apoprotein derivative of Cu,Zn-SOD represent progressive removal of charge/metal ions from the native protein with an increase in the overall negative charge on the protein molecule. Vanadium in vanadate (VO_4^{3-}) is present in the + 5 (d^0) state, where it is diamagnetic and cannot be characterized by optical spectroscopy. However the ^{51}V nucleus is 99.9 % abundant and is easily detectable by NMR, and different species of vanadate in solution give different ^{51}V NMR resonances. This is the only method which provides information on the speciation of vanadate in solutions. ^{51}V NMR spectroscopy will be applied to determine the interactions of the different derivatives of the protein with vanadate. The areas of the different ^{51}V NMR resonances can be used to calculate concentrations of the different vanadate species. The line widths at half-height intensity will provide information regarding the extent to which the different species of vanadate interact with the different protein derivatives. These investigations on anion binding to native and metal-depleted derivatives of Cu,Zn-SOD may assist in determining the effect of charge of the protein on anion binding and characterizing the types

of large anions which can be accommodated by the various binding sites of Cu,Zn-SOD.

Human RBCs have been used as a model system to study the transport and binding of Li^+ because of their simple structure, availability, and ease to maintain them viable over a long period of time. Conventional methods of analyzing Li^+ levels in biological samples involve centrifugation followed by cell lysis. NMR spectroscopy, a novel non-invasive technique, has been used in previous studies to provide information on both Li^+ transport and binding in human RBCs (Espanol and Mota de Freitas, 1987; Mota de Freitas et al., 1990a) and in vesicles. ^7Li spin-lattice (T_1) relaxation measurements provide a good method to monitor information on binding of Li^+ . It has been shown that the rates of Na^+ - Li^+ exchange in RBCs from bipolar patients were significantly lower than those from matched controls (Mota de Freitas et al., 1990c; Mota de Freitas et al., 1994a). Since manic-depression is a disorder of the nervous system, it would be appropriate to extend such studies by using nerve cells.

NMR spectroscopy is a relatively insensitive technique, and very high cell densities are required to perform NMR experiments with cells. RBCs can be obtained at very high cell densities, and can be maintained viable in suspensions containing nutrient-rich medium during the course of an NMR experiment (Mota de Freitas, 1993). However, the viability of most nucleated, respiring cells like nerve cells, cannot be maintained in suspension during the course of an NMR experiment (Egan, 1987; Kaplan et al., 1992; Swergold, 1992). In such cases, the cells need to be immobilized within the NMR sample, and continuously perfused with fresh modified growth medium to replenish oxygen and nutrients. The SH-SY5Y neuroblastoma cell line was chosen to investigate Li^+ transport and binding. SH-SY5Y cells are a clonal derivative of the SK-N-SH cell line and consist solely of the neuroblast phenotype (Biedler et al., 1973) and have been used in the past as a model system to investigate G protein function in the brain

(Carter and Medzihradsky, 1993; Laugwitz et al., 1993), and the effects of Li^+ on the phosphatidylinositol turnover (Stubbs and Agranoff, 1993). Also, this cell line has been used as a model system to investigate the regulation of ions such as Ca^{2+} (McDonald et al., 1994), Be^{2+} (Faraci et al., 1993), and Rb^+ (Spinedi et al., 1992), as well as for the study of alterations in membrane composition induced by lithium treatment (Liepkalns et al., 1993; Liepkalns et al., 1994). The cells will be anchored on impermeable microcarrier beads and the sample perfused continuously with a modified medium. Anchoring cells on microcarrier beads allows for perfusion of the cells without being washed away along with the perfusate, and for maintaining the total number of cells in the NMR window constant.

These studies will therefore provide additional information on both anion binding to Cu,Zn-SOD, and the application of NMR spectroscopy to study Li^+ interactions in neuroblastoma cells.

CHAPTER III

EXPERIMENTAL APPROACH

III.1. Materials

III. 1.1. Reagents

Ammonium metavanadate (NH_4VO_3) was purchased from Johnson Matthey, MA, the sodium salts of adenosine triphosphate (ATP), adenosine diphosphate (ADP), adenosine monophosphate (AMP), pyruvate, 2,3 bisphosphoglycerate (2,3 BPG), phenylglyoxal, succinic anhydride, sodium diphosphate (Na_4PP), 4-(2-hydroxyethyl)-1-piperazinesulfonic acid (HEPES), N,N-bis[2-hydroxyethyl]glycine (bicine), xanthine, xanthine oxidase (grade I), cytochrome-c (horse heart, type III), Dulbecco's Minimum Essential Medium Eagle (DMEM), fetal bovine serum, Trypan Blue and glass microcarrier beads were purchased from Sigma. Potassium phosphate monobasic (KH_2PO_4), potassium phosphate dibasic (K_2HPO_4), potassium chloride (KCl), choline chloride, calcium chloride (CaCl_2), magnesium chloride (MgCl_2), lithium chloride (LiCl), cesium chloride (CsCl), dysprosium nitrate [$\text{Dy}(\text{NO}_3)_3$], tetramethylammonium hydroxide (TMAH), triethylenetetraminehexacetic acid (H_6TTHA), sodium triphosphate (Na_3PPP), sodium chloride (NaCl), sodium dithionite ($\text{Na}_2\text{S}_2\text{O}_4$), ethylenediaminetetraacetic acid (EDTA) glucose and sucrose were from Aldrich, and deuterium oxide [D_2O] (99.8%) was from Cambridge Isotope Laboratories. Thulium [1,4,7,10-tetraazacyclododecane-N,N',N'',N'''-tetramethylene phosphonate] [$\text{Tm}(\text{DOTP})^{5-}$] as ($\text{H}_3\text{Na}_3\text{TmDOTP}.3\text{NaOAc}$) as a powder was

from Magnetic Resonance Solutions, Dallas, TX. The microcarrier beads used were Cytodex-1 from Pharmacia Biotech., Inc., Sweden, CultiSpher-G from HyClone Laboratories Inc., Utah and Biosilon from Nunc Inc., Denmark. The ionophore DB14C4 was purchased from Dojindo Laboratories (Japan).

III. 1.2. Enzymes

Bovine liver copper-zinc superoxide dismutase (Cu,Zn-SOD) was purchased as a lyophilized powder from Oxis International, Inc., CA.

III. 1.3. Cell Culture

The human neuroblastoma cell line SH-SY5Y was obtained from the laboratory of Professor Evan B. Stubbs Jr. at the Loyola University Medical Center and grown as a continuous cell line in our laboratory. Cells were grown at 37 °C in Dulbecco's Modified Eagle's Medium supplemented with 10% fetal bovine serum, 3.7 g/L bicarbonate in an incubator of humidified atmosphere with 5% (v/v) CO₂. Antibiotics were not used for regular cell culture. The cell line was propagated as follows. Cells were grown to confluency in T-75 cm² flasks and harvested using 10-15 mL Puck's D₁ solution (D-glucose 1g, sucrose 20g, NaCl 8g, KCl 0.5g, Na₂HPO₄·7H₂O 0.045g, KH₂PO₄ 0.03g per L of solution) by incubation at 37 °C for 15 min. The cell monolayer is gently displaced and transferred to a 50 mL centrifuge tube, centrifuged and gently resuspended in fresh medium. Aliquots of cells are transferred to T-75 cm² flasks containing about 18 mL fresh medium, mixed gently and placed in the incubator (Stubbs and Agranoff, 1993). All procedures associated with cell culture were carried out under sterile conditions.

III. 2. Sample Preparation

III. 2.1. Preparation of reduced, zinc-only and apoprotein forms of bovine Cu,Zn-SOD

The apoprotein form of the native bovine Cu,Zn-SOD was prepared by dialyzing the native enzyme against EDTA in 0.05 M acetate buffer at pH 3.9, followed by extensive dialysis against NaCl to remove the excess EDTA (McCord and Fridovich, 1969). The zinc-only derivative of the native enzyme was prepared by the addition of calculated amounts of zinc nitrate to an apo preparation at pH 6.0 followed by incubation in the cold for 12 to 24 hours (Valentine and Pantoliano, 1981). The reduced form of the enzyme was prepared by the addition of a solution of NaBH₄ for 8 min. The reaction was stopped by the addition of minute quantities of 1 M acetic acid to decrease the pH to a value between 4 and 5 (Viglino et al., 1985).

The apo protein and the zinc-only derivative of Cu,Zn-SOD were characterized by the activity assay and by AA to determine the metal ion content.

III. 2.2. Preparation of arginine and lysine modified SOD

Native bovine Cu,Zn-SOD was modified at Arg-141 by adding phenylglyoxal dissolved in bicine buffer pH 8.3 to a solution of native SOD and stirring in a water bath at 25 °C for 3 h. The sample was then purified by column chromatography using Sephadex G-25, followed by dialysis against distilled water and lyophilized (Malinowski and Fridovich, 1979).

Native bovine Cu,Zn-SOD was modified at the lysine residues by the addition of solid succinic anhydride to a solution of native protein at 25 °C, while maintaining the pH of 8 - 9 by the addition of NaOH. This solution was then dialyzed against distilled water and lyophilized (Marmocchi et al., 1982).

III. 2.3. Cell Culture on Microcarrier Beads

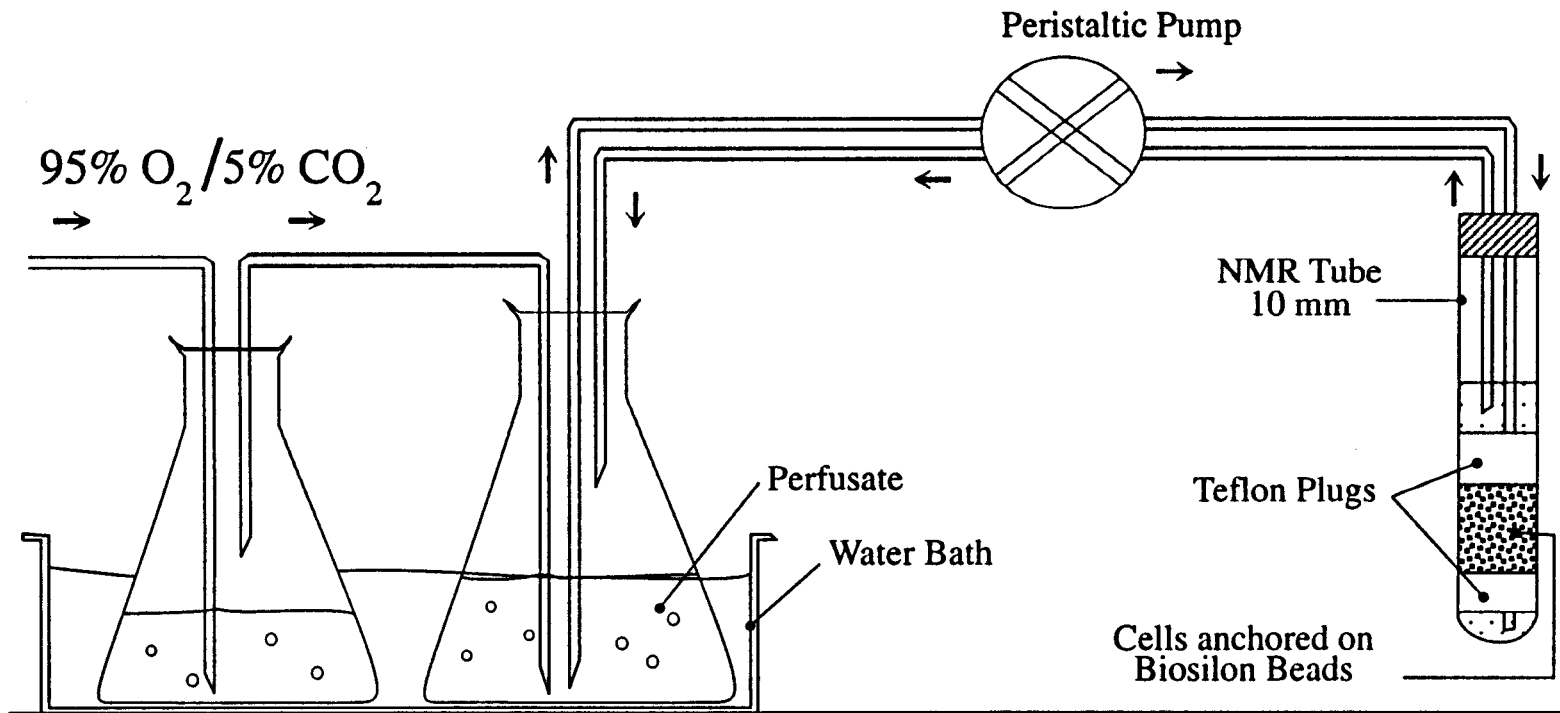
For NMR experiments with cells in suspension, about 1.5×10^8 cells were transferred to an NMR tube and suspended in 4-6 mL modified growth medium containing LiCl and SR. For NMR experiments with cells anchored on Biosilon beads, about 1.5×10^7 cells were seeded onto about 1 g of Biosilon beads suspended in regular growth medium taken in two 100 x 15 mm culture dishes, and allowed to grow to confluency for 5-6 days in a humidified atmosphere of 5% CO₂, 95% air. The culture dishes were gently shaken periodically. The growth medium was replaced at 24-48 hour intervals depending on the cell density. At the time of the NMR experiment, the beads were slowly transferred to an NMR tube containing the modified medium used in the NMR experiment. A vortex plug was placed at the bottom of the NMR tube so that the NMR window is covered entirely with cells on beads.

The cells in the NMR tube were maintained viable by perfusing the cells with fresh oxygenated medium maintained at 37 °C in a water bath. The perfusion apparatus is shown in Figure 3. A peristaltic pump was used to maintain the flow of the medium into and out of the NMR tube. The cell viability was calculated by the Trypan blue dye exclusion method (Patterson, 1979), and monitored by ³¹P NMR spectroscopy.

III. 2.4. Preparation of SH-SY5Y neuroblastoma cells for Electron Microscopy

Samples for scanning electron micrographs were processed according to standard procedures. SH-SY5Y cells were allowed to grow on the surface of Biosilon beads for about 2 days giving a semi confluent culture of cells on the beads. The samples were placed in Karnovsky's fixative (Karnovsky, 1965) containing 2.5% glutaraldehyde, 2% paraformaldehyde in 0.1 M sodium cacodylate buffer at pH 7.4 and allowed to fix overnight. They were then

Figure 3. Schematic representation of the apparatus required for perfusion of cells for the NMR study of SH-SY5Y cells



rinsed thoroughly in the above buffer solution. Postfixation was done in 1% OsO₄ at pH 7.4. After dehydration in ethanol, critical point drying was performed in liquidCO₂ with a Polaron E-2000 critical point dryer. The specimens were then sputter coated with gold-palladium (60% gold, 40% palladium) alloy to a thickness of approximately 30 nm in argon atmosphere by using a Hummer IV sputtering system from Anatech Ltd. Photographs were taken with a Cambridge Instruments Stereoscan 240 scanning electron microscope (SEM) operated at 15kV.

III. 2.5. Preparation of SH-SY5Y neuroblastoma cell membranes

SH-SY5Y neuroblastoma cell membranes were prepared by standard procedures with slight modification (Costa et al., 1991). The cells were grown to confluency in T-75 cm² flasks and harvested using Puck's D₁ solution and centrifuged to pellet the cells. The cells were homogenized in a hypotonic buffer (5 mM Tris-HCl, 0.1 mM EDTA, 0.2 mM dithiothreitol, pH 7.5 - TED) and centrifuged at 1000 x g for 10 min at 4 °C. The resultant supernatant was centrifuged at 37,000 x g for 10 min at 4 °C. The pellet was washed twice with the hypotonic buffer to obtain purified cell membranes. 50-100 µL of TED buffer was added to reduce the viscosity of the membrane sample.

III. 2.6. Preparation of Shift Reagents

Dy(PPP)₂⁷⁻ was prepared from Dy(NO₃)₃ and Na₅PPP according to standard procedures (Mota de Freitas, 1993). To prepare 5 mL of a 20 mM Dy(PPP)₂⁷⁻, 0.0438 g Dy(NO₃)₃ was dissolved in 1-2 mL water. Dissolve 0.1103 g Na₅PPP in 2 mL water. The Na₅PPP solution was added to the Dy(NO₃)₃ drop by drop till a clear solution was obtained. The solution was then transferred to a volumetric flask and the total volume was then made up to 5 mL.

To prepare 5 mL of $0.125 \text{ M Dy(TTHA)}^{3-}$, 0.2741 g $\text{Dy(NO}_3)_3$ and 0.3090 g H_6TTHA were added to 3 mL water and titrated with 30 μL aliquots of 2.5 M NaOH with constant stirring till all the salts were dissolved. The pH was maintained below 8.0 during the titration. The solution was then transferred to a 5 mL volumetric flask and the total volume made up to 5 mL (Mota de Freitas, 1993).

III. 2.7. Determination of protein concentration

Protein concentrations were determined by the Lowry assay at 750 nm (Lowry et al., 1951). The Folin - Ciocalteu Folin Reagent (2.0 N) was purchased from Sigma and diluted 1 to 2 with distilled water. Standards of bovine Cu,Zn-SOD were prepared and used for the experiments with SOD, while bovine serum albumin (BSA) was used as standards for other experiments.

III. 2.8. Activity assay for Cu,Zn-SOD

The activity of the native Cu,Zn-SOD and its derivatives were measured by the xanthine oxidase - cytochrome-c assay (McCord and Fridovich, 1969). O_2^- was generated in situ by the action of xanthine oxidase on xanthine, which then reduces cytochrome-c leading to an increase in absorbance at 550 nm. SOD, when present, removes the O_2^- produced, and the amount of SOD required to inhibit the rate of reduction of cytochrome-c by 50% is defined as 1 unit of activity.

III. 2.9. Extraction of phospholipids from SH-SY5Y cell membranes

Phospholipids from SH-SY5Y cell membranes were extracted according to standard

procedures. Briefly, 0.95 mL of packed SH-SY5Y cell membranes were added slowly to anhydrous methanol (17 mL) and stirred for 15 mins. Chloroform (33 mL) was added to above mixture and stirred for an additional 15 mins. The extracting solvents contained 50 mg/L of butylated hydroxytoluene (BHT) as an antioxidant. Celite was added to the extract, and filtered using a sintered glass funnel. The solids were washed with 50 mL of a chloroform:methanol mixture (2:1). Then 20 mL of 0.1 M KCl was then added to the filtrate and mixed thoroughly in a separatory funnel to remove non-lipid impurities. The bottom organic layer was taken and the solvent removed using a rotary evaporator at 30 °C (Meneses and Glonek, 1988). The lipid film obtained was suspended in a solvent mixture of chloroform/methanol/EDTA reagent (125:8:3).

III. 3. Data Analysis

III. 3.1. Determination of Binding Constants of Phosphates to Native Cu,Zn-SOD, and of Li⁺ to SH-SY5Y Cell Membranes

The binding constants of various polyphosphates to native Cu,Zn-SOD, and of Li⁺ to SH-SY5Y cell membranes were calculated using James-Noggle plots (James and Noggle, 1969). The observed T₁ relaxation values represent the weighted average of free and bound phosphate or Li⁺. This can be represented by the following expression:

$$R_1 = (1/T_1) = R_{1\text{free}} X_{\text{free}} + R_{1\text{bound}} X_{\text{bound}} \quad (1)$$

$$\begin{aligned} (\Delta R)^{-1} &= (R_{\text{obs}} - R_{\text{free}})^{-1} \\ &= K_b^{-1} \{ [B](R_{\text{bound}} - R_{\text{free}}) \}^{-1} + [P] \{ [B](R_{\text{bound}} - R_{\text{free}}) \}^{-1} \end{aligned} \quad (2)$$

where R₁, R_{free}, and R_{bound} were the observed, free and bound relaxation rates of P or M⁺ ions in the solution, X_{free} and X_{bound} were the mole fractions of free and bound P (or M⁺ ions), [P]

(or $[M^+]$) and $[B]$ were the total concentration of P (phosphate ions) (or M^+ , Li^+ ions) and binding sites, respectively. This equation assumes one to one stoichiometry for binding of phosphate (or Li^+) to the protein (or nerve cell membranes); and $[B] \ll [P]$ (James and Noggle, 1969). In the case of experiments with biological phosphates, the R^{-1} used is the calculated value due to paramagnetic contributions from Cu(II), obtained by subtracting the value observed for the oxidized protein from the value measured with a reduced protein (Mota de Freitas et al., 1987).

III. 3.2. Determination of concentrations of various vanadate species

The concentrations of the vanadate monomer (V_1), dimer (V_2) and tetramer (V_4) were calculated by integrating the 1D ^{51}V NMR spectra using the integration routines included in the software of the Varian VXR-300. Control samples containing 2 mM vanadate were used to quantify the observable vanadium species. Aqueous solutions of vanadate contain different concentrations of the vanadate monomer, dimer, tetramer and pentamer; this depends on the vanadium concentration, pH, ionic strength and temperature of the solution (Crans et al., 1990; Crans and Schelble, 1990; Wittenkeller et al., 1991).

$$[V_2] = K_{12}[V_1]^2 \quad (3)$$

$$[V_4] = K_{14}[V_1]^4 \quad (4)$$

From the mole fraction of each vanadate species in the standard samples and from the total vanadate concentration, the concentrations of the individual anions were determined. Using the oligomer concentrations calculated from the standard 2 mM vanadate samples, the equilibrium constants, K_{12} and K_{14} were determined (from equations 3 and 4). For samples containing protein, the concentration of V_1 , $[V_1]$, was calculated from integrations in the ^{51}V NMR spectra.

The concentration of each vanadate species was then calculated from the mole fraction of each vanadate species in the protein-vanadate sample and from the total vanadate concentration. $[V_x\text{-SOD}]$, the total concentration of vanadium atoms in protein-vanadate complex, is determined as

$$[V_x\text{-SOD}] = [V_{\text{total}}] - [V_1]_{\text{obs}} - 2[V_2]_{\text{calc}} - 4[V_4]_{\text{calc}} \quad (5)$$

A plot of $[V\text{-protein}]$ vs $[\text{protein}]$ is then constructed, the slope of the curve is the number of vanadium atoms bound to the vanadate-protein complex.

The line widths of the phosphate and vanadate resonances reported represent the line width at half-height after subtracting the line broadening applied during acquisition in each case.

III. 3.3. Determination of Li^+ transport rates in SH-SY5Y cells

For transport studies with cells in suspension, the amount of Li^+ in cells (A_i) and in extracellular pools (A_o) were obtained by integrating the respective Li^+ resonances using the integration routines in the NMR spectrometer. The areas A_i and A_o were used to obtain a first-order rate constant, k , from the plots of $\ln [A_i/(A_i + A_o)]$ versus time (Abraha and Mota de Freitas, 1992). For transport studies with perfused cells anchored on microcarrier beads, first-order rate constants for Li^+ influx were obtained from the slope of the plot $\ln(A_{\infty}-A_t)$ vs time, while first-order rate constants for Li^+ efflux were obtained from the slope of the plot $\ln(A_t-A_{\infty})$ where A_{∞} is the amount of Li^+ in the cells at time ∞ , and A_t is the amount of Li^+ present in the cells at time t . The rate constant for Li^+ influx in the presence of the ionophore is pseudo-first-order with respect to both Li^+ and the ionophore.

III. 4. Instrumentation

III. 4.1. Nuclear Magnetic Resonance Spectrometer

^7Li , ^{13}C , ^{23}Na , ^{31}P , ^{35}Cl , ^{51}V , and ^{133}Cs NMR measurements were made at 116.5, 75.4, 79.4, 121.4, 29.4, 78.9 and 39.3 MHz, respectively, on a Varian VXR-300 NMR spectrometer equipped with a multinuclear probe. For experiments with aqueous solutions, samples were locked with 15% - 20% D_2O and the rate of spinning used was 16 Hz. The experiments with microcarrier beads and cells were run non-spinning. The temperature of the probe was maintained at 23 °C or at 37 °C. Table 1 lists the NMR parameters for the nuclei investigated in this project.

^{51}V and ^{31}P NMR chemical shifts are reported relative to an external reference of V-DEA complex (Crans and Shin, 1988) and 85% H_3PO_4 , respectively.

Spin-lattice relaxation time (T_1) measurements were performed using the inversion recovery method while the spin-spin relaxation time (T_2) measurements were done by the Carr-Purcell-Meiboom-Gill method (Gadian, 1982).

III. 4.2. Atomic Absorption Spectrophotometer

Cu^{2+} , Zn^{2+} and Li^+ absorption measurements were made at 324.8, 213.9 and 670.8 nm, respectively, on a Perkin Elmer 5000 spectrophotometer equipped with a graphite furnace and flame source.

III. 4.3. UV/Vis Spectrophotometer

An IBM UV/VIS 9420 or a Jasco V-550 spectrophotometer was used to determine protein concentrations and to determine the activity of the native and modified superoxide

Table 1. NMR Parameters of Nuclei Investigated at 7.0 T.

	⁷ Li	¹³ C	²³ Na	³¹ P	³⁵ Cl	⁵¹ V	¹³³ Cs
Frequency/MHz	116.5	75.4	79.4	121.4	29.4	78.9	39.3
SW/KHz	4.5,10	17	15	10	8	73	10
AT/s	1.5	0.86	1.5	0.75	0.5	0.15	1
PW 90/ μ s	27 ^a ,32 ^b ,14 ^c	13	28	13	78	78	38
Flip angle/ degree	45	60/90	45/90	45/90	90	90	45/90

^a90° pulse in low ionic strength solutions (1-20 mM) in 10 mm probe

^b90° pulse in high ionic strength solutions (500 mM) in 10 mm probe

^c90° pulse in low ionic strength solution in 5 mm probe

dismutase enzyme.

III. 4.4. Centrifuge

SH-SY5Y cells were harvested using Puck's D₁ and separated using a Beckman J2-21 centrifuge equipped with a J-20A fixed angle rotor.

III. 4.5. Scanning Electron Microscope

Scanning electron micrographs of SH-SY5Y cells anchored on Biosilon beads were obtained on a Cambridge Instruments Stereoscan 240 scanning electron microscope.

III. 4.6. Vapor Pressure Osmometer

A Wescor Vapor Pressure Osmometer model 5500 was used to measure the osmolarity of all suspension media. The osmolarity of the media was adjusted to 340 ± 5 mOsm using sucrose.

III. 4.7. Lyophilizer

The arginine and lysine-modified Cu,Zn-SOD were prepared and then dried to a powdered form using a FDX Flexi-Dry freezer dryer model 1-54.

III. 4.8. pH Meter

An Orion pH meter was used to check the pH of different samples, buffers and media.

CHAPTER IV

RESULTS

Numerous anion binding studies of the metalloenzyme Cu,Zn-SOD have been conducted to determine the nature and sites of interactions of superoxide anion, which is the natural substrate of Cu,Zn-SOD. The vanadate tetramer is the largest anion shown to bind to Cu,Zn-SOD. This study was carried out to determine the interactions of Cu,Zn-SOD with large biologically-relevant polyphosphate anions such as the adenine nucleotides present in living cells; and the interactions of vanadate with reduced and metal depleted derivatives of Cu,Zn-SOD.

^7Li NMR spectroscopy has been used previously to understand Li^+ interactions using human RBCs as model cells. This methodology has been extended to study Li^+ interactions in human neuroblastoma cells.

In this chapter, we present the results on (a) ^{31}P NMR studies of the interactions of adenine nucleotides and synthetic polyphosphates with native Cu,Zn-SOD, (b) the interactions of vanadate with reduced and different metal-depleted forms of the enzyme Cu,Zn-SOD using ^{51}V NMR, and (c) ^7Li NMR studies of Li^+ transport and binding in cultured SH-SY5Y human neuroblastoma cells.

IV. 1. Interactions of native Cu,Zn-SOD with biologically relevant phosphates and synthetic polyphosphates

IV.1.1. Interactions of adenine nucleotides and 2,3 BPG with native Cu,Zn-SOD

The interactions of the different biologically-relevant phosphates with bovine Cu,Zn-SOD in its oxidized, native form were followed by the changes in the values of the ^{31}P NMR chemical shifts, spin-lattice (T_1) relaxation times and line widths of the phosphate resonances in the absence and presence of native Cu,Zn-SOD. The ^{31}P chemical shifts, line widths and T_1 relaxation times of the phosphate resonances of ATP, ADP, AMP, sodium triphosphate (Na_3PPP), sodium diphosphate (Na_2PP), sodium phosphate (P_i) and 2,3-BPG were obtained in the absence and in the presence of 0.15 mM native Cu,Zn-SOD (Table 2). The chemical shifts of the phosphate resonances of the different compounds studied did not show any significant changes upon addition of Cu,Zn-SOD, whereas the line widths showed an increase in all cases. These observations suggest that these phosphates do interact with the protein. In the case of ATP, the T_1 values of all resonances decreased upon addition of the enzyme, with the largest decrease ($T_1 = 0.7 \pm 0.1$ s from $T_1 = 5.3 \pm 0.4$ s) being in the case of the γ resonance. The T_1 values of the α and β resonances of ATP also decreased, the β resonance having a larger decrease than that of the α resonance. The T_1 values of the phosphate resonances of 5 mM ATP were the same in the absence and in the presence of 0.15 mM reduced Cu,Zn-SOD. These observations indicate that the terminal phosphate group of ATP undergoes more paramagnetic relaxation than the α and β phosphates. Because the phosphates of ATP are attached to each other in a linear arrangement the terminal phosphate is capable of approaching to a greater extent the paramagnetic Cu^{2+} center present at the base of the solvent channel of the protein. This observation is also noticed in the cases of BPG and ADP where the phosphate

Table 2. ^{31}P NMR parameters of the interactions of 0.15 mM bovine Cu,Zn-SOD with biologically relevant phosphates at 5 mM.^a

Ligand ^b	without enzyme			with oxidized enzyme			
	δ	$\Delta\nu_{1/2}$	T_1	δ	$\Delta\nu_{1/2}$	T_1	
ATP	α	-6.7±0.2	3.4±0.1	2.7±0.1	-6.6±0.3	10.4±0.2	2.1±0.1
	β	-17.9±0.2	5.0±0.2	3.8±0.1	-17.9±0.4	19.2±0.5	2.3±0.1
	γ	-2.7±0.2	4.0±0.1	5.3±0.4	-2.6±0.3	17.3±1.9	0.7±0
ADP	α	-6.4±0.1	2.2±0.1	3.7±0.1	-6.5±0.1	11.7±0.5	1.7±0.1
	β	-2.3±0.1	1.9±0.2	6.0±0.1	-2.5±0.1	12.9±0.4	0.95±0.1
AMP		8.2±0.3	0.8±0.1	5.8±0.1	8.4±0.1	9.0±1.3	2.0±0.1
PPP	T	-3.5±0.3	2.3±0.4	7.9±0.4	-3.5±0.2	7.8±0.9	2.5±0.1
	C	-17.7±0.3	3.1±0.4	6.3±0.1	-17.8±0.2	8.5±0.6	3.3±0.1
PP		-3.2±0.1	0.7±0.1	10.4±0.1	-3.3±0.1	2.9±0.1	2.6±0.1
P_i		6.4±0.1	0.6±0.1	13.0±0.1	6.4±0.1	60.7±5.3	0.82±0.1
BPG	P_2	6.0±0.1	1.8±0.3	6.1±0.1	6.0±0.1	10.4±0.7	1.2±0
	P_3	7.2±0.1	1.2±0.3	6.6±0.1	7.2±0.1	13.3±0.9	1.0±0.1

Table 2 (cont.) ^aAll samples contained 50 mM HEPES pH 7.0, 0.1 mM EDTA, 20% D₂O at 23±1 °C. The values reported in the table are the mean ± SD of two separately prepared samples. δ is in ppm, $\Delta\nu_{1/2}$ is in Hz and T_1 in s. The experimental errors for δ are 0.2 ppm, $\Delta\nu_{1/2}$ are 2 Hz, and for T_1 are 0.3 s. The chemical shifts reported are relative to an external reference of 85% H₃PO₄. The line widths reported represent the widths of the resonances at half-height after subtracting the value of line broadening used. ^bFor ATP, α , β and γ represent the three phosphate groups, for ADP α and β represent the two phosphate groups, T and C are the terminal and central phosphates of the triphosphate, and P₂ and P₃ are the phosphate groups attached to C2 and C3 atoms of 2,3 BPG, respectively.

group on the third C of glycerate or the β phosphate of ADP have smaller relaxation values in the presence of Cu,Zn-SOD.

IV.1.2. Interactions of synthetic polyphosphates with native Cu,Zn-SOD

The interactions of the synthetic phosphates, triphosphate (PPP), diphosphate (PP) and inorganic phosphate (P_i), with native Cu,Zn-SOD were also investigated by ^{31}P NMR spectroscopy (Table 2) to determine whether the adenosine group contributed toward binding of polyphosphates to the native protein. Upon addition of 0.15 mM native Cu,Zn-SOD, similar decreases in the T_1 values were observed for the terminal phosphates of ATP and PPP or for ADP and PP. In contrast, the decreases in the T_1 values observed upon addition of 0.15 mM native SOD were smaller for AMP relative to P_i ; this may be due to the presence of the adenosine group in AMP which is absent in the case of P_i .

IV.1.3. ^{31}P NMR measurements of biological phosphates to determine their binding constants to Cu,Zn-SOD

Table 3 shows the changes in the spin-lattice (T_1) relaxation values of the α , β and γ phosphate groups of ATP in the presence of 0.08 mM native Cu,Zn-SOD. As the concentration of ATP increased, the T_1 values of all the three phosphate resonances of the nucleotide increased; the T_1 values of the α and β resonances reached a maximum at ATP concentrations much lower than those concentrations for the γ ATP resonance to reach a maximum. This is due to the γ phosphate being present closer to the Cu^{2+} center of the enzyme. Individual T_1 values represent a weighted average of the free and bound phosphate, and as the concentration of the phosphate ligand increases, there are larger amounts of free ligand, giving rise to an

Table 3. ^{31}P NMR T_1 measurements in the presence of 0.08 mM native Cu,Zn-SOD with increasing concentrations of ATP in 0.05 M HEPES, pH 7.0, 0.1 mM EDTA, 20% D_2O at 23 ± 1 °C.

[ATP]/mM	T_1/s		
	α	β	γ
1	2.0 ± 0.2	2.1 ± 0.4	0.39 ± 0.07
2	2.2 ± 0.1	1.7 ± 0.4	0.48 ± 0.06
3	2.1 ± 0.1	2.3 ± 0.3	0.73 ± 0.08
5	2.1 ± 0.4	2.9 ± 0.4	0.80 ± 0.04
7	2.2 ± 0.1	2.7 ± 0.2	1.03 ± 0.03
10	2.4 ± 0.1	2.8 ± 0.2	1.23 ± 0.05
12	2.5 ± 0.1	2.9 ± 0.1	1.40 ± 0.04
15	2.5 ± 0.1	3.3 ± 0.1	1.90 ± 0.02
18	2.4 ± 0.1	3.2 ± 0.1	2.29 ± 0.06
21	2.5 ± 0.1	3.2 ± 0.1	2.96 ± 0.16
25	2.5 ± 0.1	3.5 ± 0.1	3.36 ± 0.04
30	2.5 ± 0.1	3.3 ± 0.1	3.57 ± 0.07

increase in the T_1 values.

Similar measurements were conducted to determine the changes in the T_1 values of ADP (in the presence of 0.08 mM Cu,Zn-SOD), AMP (in the presence of 0.15 mM Cu,Zn-SOD), diphosphate (in the presence of 0.25 mM Cu,Zn-SOD) and P_i (in the presence of 0.15 mM Cu,Zn-SOD). Changes in the α and β resonances with increasing concentrations of ADP (Table 4) show that the α T_1 values reach a maximum at lower concentrations of ADP when compared to the β resonance. This is again due to the ability of the β phosphate group to be closer to the active site Cu^{2+} in the enzyme. AMP, diphosphate and P_i all give a single ^{31}P NMR resonance. Diphosphate gives only one ^{31}P resonance as both the phosphates are magnetically equivalent and have similar chemical shift values. Tables 5 - 8 give the T_1 values of the phosphate resonances of AMP, 2,3-BPG, diphosphate and P_i , respectively, in the presence of a fixed concentration of Cu,Zn-SOD and varying amounts of the respective phosphate.

The ^{31}P NMR T_1 relaxation times of different phosphates with Cu,Zn-SOD were used to calculate binding constants of the respective phosphates to the protein. The binding constants were calculated as explained in the Methods section and are given in Table 9. The T_1 values of the terminal phosphate of the polyphosphates were considered for determining the binding constant for the respective phosphate, as there was a greater range in T_1 values for terminal phosphates with increasing concentrations of the phosphate ligand, which is required to determine binding constants. Considering the adenine nucleotides studied, ATP has the highest binding constant of $575 M^{-1}$ when compared to ADP ($K_b = 500 M^{-1}$) and AMP ($K_b = 470 M^{-1}$). The K_b of 2,3-BPG was determined to be $574 M^{-1}$ while that of diphosphate was higher ($770 M^{-1}$) compared to those of adenine nucleotides and 2,3-BPG. Inorganic phosphate was shown to have the lowest binding constant to Cu,Zn-SOD. The binding constant of PPP

Table 4. ^{31}P NMR T_1 measurements in the presence of 0.08 mM native Cu,Zn-SOD with increasing concentrations of ADP in 0.05 M HEPES, pH 7.0, 0.1 mM EDTA, 20% D_2O at 23 ± 1 °C.

[ADP]/mM	T_1 /s	
	α	β
1	1.6 ± 0.4	0.73 ± 0.1
3	1.8 ± 0.5	1.00 ± 0.1
4	2.1 ± 0.2	1.60 ± 0.1
5	2.3 ± 0.1	2.10 ± 0.1
6	2.2 ± 0.2	1.90 ± 0.1
7	2.1 ± 0.1	1.80 ± 0.1
10	2.4 ± 0.1	1.90 ± 0.1
13	2.4 ± 0.1	2.29 ± 0.1
17	2.8 ± 0.1	2.68 ± 0.1
21	2.7 ± 0.1	3.34 ± 0.2
25	3.0 ± 0.1	3.52 ± 0.1
30	3.1 ± 0.1	3.80 ± 0.1
34	3.2 ± 0.1	3.95 ± 0.1

Table 5. ^{31}P NMR T_1 measurements in the presence of 0.15 mM native Cu,Zn-SOD with increasing concentrations of AMP in 0.05 M HEPES, pH 7.0, 0.1 mM EDTA, 20% D_2O at 23 ± 1 °C.

[AMP]/mM	T_1 /s
1	1.05 ± 0.1
3	1.55 ± 0.1
5	1.59 ± 0.1
7	1.88 ± 0.1
9	2.28 ± 0.2
12	2.71 ± 0.1
15	2.54 ± 0.1
29.5	3.01 ± 0.1

Table 6. ^{31}P NMR T_1 measurements in the presence of 0.15 mM native Cu,Zn-SOD with increasing concentrations of 2,3-BPG in 0.05 M HEPES, pH 7.0, 0.1 mM EDTA, 20% D_2O at 23 ± 1 °C.

[2,3-BPG]/mM	T_1/s	
	P_2	P_3
2	0.60 ± 0.05	0.56 ± 0.05
4	1.08 ± 0.06	1.05 ± 0.03
6	1.44 ± 0.03	1.22 ± 0.04
8	1.78 ± 0.06	1.52 ± 0.08
10	1.98 ± 0.12	1.78 ± 0.06
15	2.49 ± 0.05	2.23 ± 0.05
20	2.91 ± 0.06	2.64 ± 0.05
25	3.13 ± 0.03	2.80 ± 0.03
30	3.15 ± 0.07	3.02 ± 0.06
40	3.20 ± 0.06	3.18 ± 0.05
60	3.11 ± 0.02	3.23 ± 0.02
80	3.12 ± 0.03	3.33 ± 0.03

Table 7. ^{31}P NMR spin-lattice relaxation times in the presence of 0.25 mM native Cu,Zn-SOD with increasing concentrations of diphosphate in 0.05 M HEPES, pH 7.0, 20% D_2O at 23 ± 1 °C.

[PP]/mM	T_1 /s
2	1.23 ± 0.1
5	1.78 ± 0.1
10	2.66 ± 0.4
20	3.10 ± 0.1
30	3.84 ± 0.1
40	4.39 ± 0.1
50	5.34 ± 0.2
100	7.34 ± 0.6

Table 8. ^{31}P NMR spin-lattice relaxation times in the presence of 0.15 mM native Cu,Zn-SOD with increasing concentrations of inorganic phosphate in 0.05 M HEPES, pH 7.0, 20% D_2O at 23 ± 1 °C.

$[\text{P}_i]/\text{mM}$	T_1/s
5	0.90 ± 0.06
10	1.08 ± 0.08
50	1.87 ± 0.02
100	2.53 ± 0.02
200	4.00 ± 0.03
315	4.49 ± 0.03
700	6.29 ± 0.05

Table 9. Binding constants of the biological phosphates to native Cu,Zn-SOD^a

Ligand	K_d / M^{-1}	r^2
ATP ^b	575	0.99
ADP ^c	500	0.90
AMP	470	0.90
2,3 BPG ^d	574	0.99
PP	770	0.96
P	59	0.96

All samples contained 50 mM HEPES pH 7.0, 0.1 mM EDTA, 20% D₂O at 23 ± 1 °C. The concentration of Cu,Zn-SOD was kept constant, and the concentrations of the respective biological phosphate was varied. ^aThe binding constants were calculated using equation 1 in the Methods section. ^b T_1 values of the γ phosphate resonance of ATP, ^c T_1 values of the β phosphate resonance of ADP, and ^d T_1 values of P_3 phosphate resonance of 2,3-BPG, respectively, were used to calculate the binding constants.

to native SOD could not be calculated by this method. This may be due to the T_1 values obtained for the terminal phosphate groups of PPP. The T_1 values obtained are average values of the terminal phosphate group close to the Cu^{2+} and the one which is at the opposite end of the phosphate chain of PPP.

IV.1.4. ^{31}P NMR measurements of biological phosphates and synthetic polyphosphates in the presence of chemically modified Cu,Zn-SODs

To determine the site(s) of interaction between the different phosphate ligands and the native protein, chemically modified proteins were used. Figure 4 shows the ^{31}P NMR spectra of ATP in the absence and presence of native and modified Cu,Zn-SOD. The spectra of free ATP in solution is similar to the spectra of ATP in the presence of lysine-modified and arginine-modified Cu,Zn-SOD, while there appears to be broadening of the β and γ phosphate resonances of ATP in the presence of the native Cu,Zn-SOD. The T_1 values of the ^{31}P NMR phosphate resonances in the presence and absence of native and chemically modified Cu,Zn-SOD are given in Table 10. The similar ^{31}P T_1 values of the phosphate resonances of the free ligands in solution and in the presence of lysine-modified Cu,Zn-SOD indicate that these large phosphates interact at the positively charged lysine residues present at the mouth of the solvent channel of each subunit. Lys-120 and Lys-134 residues are further away (12 Å and 13 Å, respectively) from the paramagnetic Cu^{2+} center when compared to Arg-141 (5 Å) (Tainer et al., 1982). The ^{31}P T_1 values for the phosphates in the presence of arginine modified SOD are thus lower as indicated in Table 10. The ^{31}P T_1 values are hence distance-dependent. Chemical modification of these essential amino acid residues are known to reduce activity (Malinowski and Fridovich, 1979; Marmocchi et al., 1982) and anion affinities towards the protein (Mota

Figure 4. ^{31}P NMR spectra of 5 mM ATP in 50 mM HEPES pH 7.4, 0.1 mM EDTA, 20% D_2O at 23 ± 1 °C in the absence of Cu,Zn-SOD (A), and in the presence of 0.15 mM native Cu,Zn-SOD (B), 0.15 mM lysine-modified Cu,Zn-SOD (C) and 0.15 mM arginine-modified Cu,Zn-SOD (D).

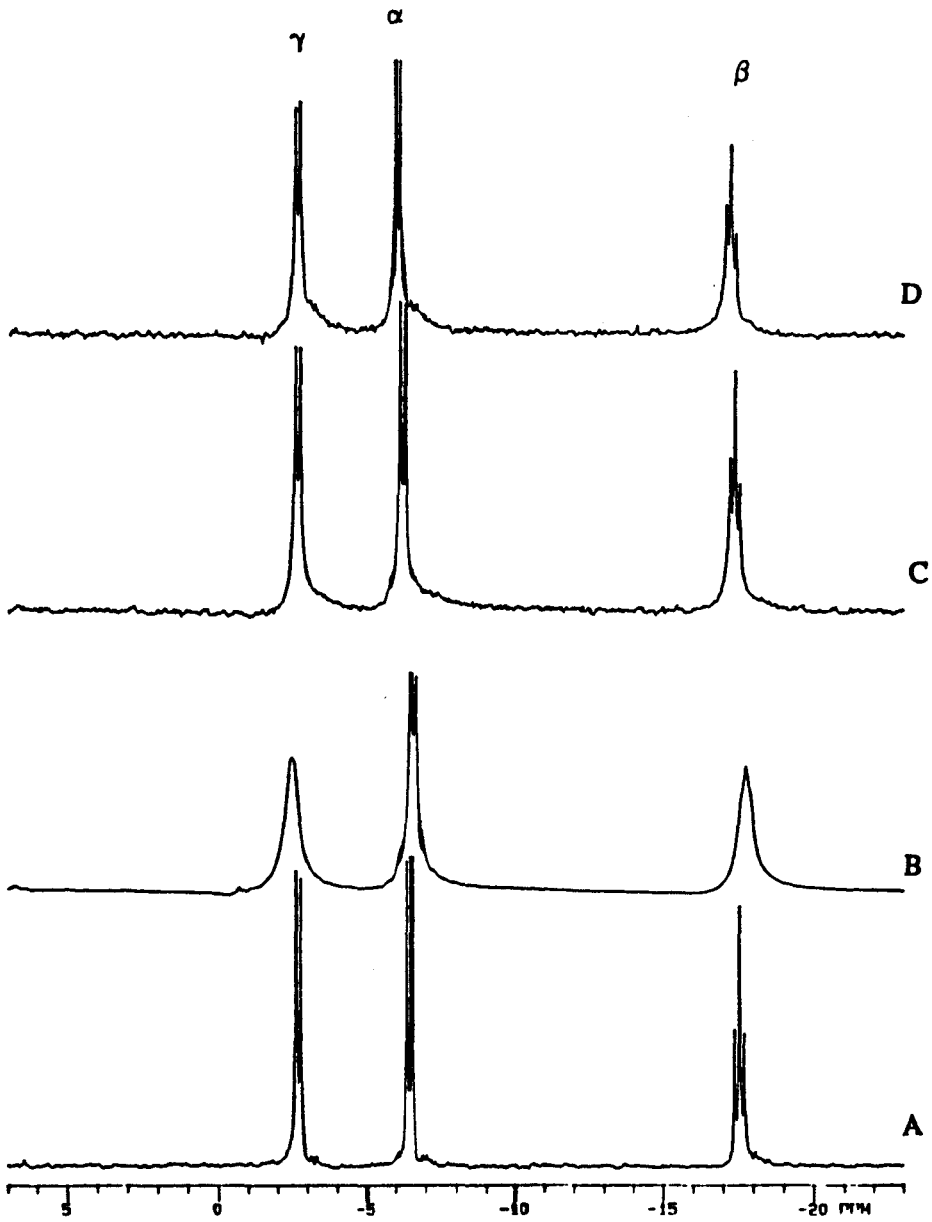


Table 10. ^{31}P T_1 values (in s) of biological phosphates in the presence and absence of native and chemically modified Cu,Zn-SOD.^a

	Free ligand	w/native SOD	w/lys-mod	w/arg-mod
ATP α	2.6 ± 0.2	1.7 ± 0.1	2.7 ± 0.1	2.3 ± 0.1
β	3.8 ± 0.4	2.2 ± 0.1	3.5 ± 0.4	3.4 ± 0.5
γ	5.3 ± 0.3	0.5 ± 0.1	5.7 ± 0.4	3.5 ± 0.3
ADP α	3.9 ± 0.1	1.6 ± 0.1	3.7 ± 0.3	2.9 ± 0.1
β	5.9 ± 0.7	1.1 ± 0.1	5.7 ± 0.6	3.3 ± 0.2
AMP	5.4 ± 0.5	2.4 ± 0.2	4.1 ± 0.1	3.3 ± 0.1
PPP T-P	8.2 ± 0.2	2.4 ± 0.1	7.8 ± 0.1	7.0 ± 0.4
C-P	6.7 ± 0.4	3.0 ± 0.2	5.5 ± 0.4	6.5 ± 0.6
PP	10.7 ± 0.3	2.5 ± 0.1	8.8 ± 0.4	8.0 ± 0.3
P_i	12.8 ± 1.1	0.99 ± 0.1	8.4 ± 0.3	6.8 ± 0.3
BPG P_2	6.0 ± 0.2	1.6 ± 0.1	6.3 ± 0.2	5.4 ± 0.3
P_3	6.3 ± 0.2	1.3 ± 0.1	6.3 ± 0.2	5.9 ± 0.2

^aAll samples contained 50 mM HEPES pH 7.0, 0.1 mM EDTA, 20% D_2O at 23 ± 1 °C. The concentration of all the ligands used was 5 mM, and the enzyme concentration was 0.15 mM.

de Freitas and Valentine, 1984; Mota de Freitas et al., 1990b). These amino acid residues play a major role in anion binding to SOD, and are the sites of interactions between large polyphosphates and SOD.

IV.1.5. ^{13}C NMR measurements of biological phosphates in the presence of native Cu,Zn-SOD

Using ^{13}C NMR spectroscopy (Tables 11 and 12) we observed no significant changes in either the chemical shifts or in the line widths of the carbon resonances from the base and the sugar moieties upon addition of 0.15 mM native enzyme to 10 mM ATP or 10 mM AMP solutions. Higher concentrations of nucleotides were used in the ^{13}C NMR experiments because of the lower sensitivity. These nucleotides are known to form base stacks at higher concentrations (Scheller et al., 1981).

IV.1.6. Effect of adenine nucleotides and synthetic polyphosphates on the activity of native Cu,Zn-SOD.

The effects of the different adenine nucleotides and synthetic polyphosphates on the activity of the enzyme Cu,Zn-SOD was characterized and tabulated in Table 13. The activity of native Cu,Zn-SOD was inhibited by 10 % in the presence of 10 mM ATP at $I = 0.153$. NaF was not required to adjust the ionic strength of the ATP solution. ADP at 20 mM and AMP at 20 mM did not affect the activity of the enzyme at $I = 0.150$. However, P_i at 10 mM exhibited a 35 % inhibition in the activity at $I = 0.150$ when NaF was used to adjust ionic strength. Alternatively, when HEPES was substituted for NaF to adjust the ionic strength of the assay system, P_i at 10 mM and 20 mM exhibited a lower inhibitory effect than in solutions

Table 11. ^{13}C NMR chemical shifts and line widths of the C atoms of 10 mM ATP in the absence and in the presence of 0.15 mM Cu,Zn-SOD.^{a,b}

		δ/ppm^c		$\Delta\nu_{1/2}/\text{Hz}$	
		No SOD	+ SOD	No SOD	+ SOD
Base	C ₂	155.4	155.4	1.6	2.0
	C ₄	151.7	151.7	2.0	4.1
	C ₅	121.2	121.3	3.2	2.3
	C ₆	158.2	158.2	4.3	3.6
	C ₈	142.5	142.4	2.4	3.5
Sugar	C ₁ '	89.2	89.2	1.9	2.1
	C ₂ '	73.0	73.1	1.9	1.7
	C ₃ '	76.9	76.8	1.6	1.9
	C ₄ '	86.8	86.9	1.8	2.0
	C ₅ '	67.7	67.7	3.8	3.0

^a The sample contained 10 mM ATP at pH 7.4, 20 % D₂O; neither HEPES nor EDTA were used. ^b C₂, C₄, C₅, C₆, and C₈ refer to the base carbon atoms; C₁' to C₅' are the sugar carbon atoms. ^c The chemical shifts are reported with reference to an external standard of CDCl₃. The errors in δ are less than 0.2 ppm, and in $\Delta\nu_{1/2}$ are less than 1.5 Hz. The ^{13}C assignments were made as previously reported (Jones et al., 1970).

Table 12. ^{13}C NMR chemical shifts and line widths of the C atoms of 10 mM AMP in the absence and in the presence of 0.15 mM Cu,Zn-SOD.^{a,b}

		δ/ppm^c		$\Delta\nu_{1/2}/\text{Hz}$	
		No SOD	+ SOD	No SOD	+ SOD
Base	C ₂	155.3	155.2	1.7	1.7
	C ₄	151.5	151.5	1.1	1.3
	C ₅	121.1	121.1	2.0	2.6
	C ₆	158.1	158.1	2.7	2.3
	C ₈	142.6	142.6	2.1	2.0
Sugar	C ₁ '	89.3	89.3	2.2	1.7
	C ₂ '	73.4	73.3	2.5	1.6
	C ₃ '	77.1	77.1	2.4	1.6
	C ₄ '	87.4	87.4	2.8	2.0
	C ₅ '	66.0	66.0	6.5	6.1

^a The samples contained 10 mM AMP at pH 7.4, 20 % D₂O; neither HEPES nor EDTA were used. ^b C₂, C₄, C₅, C₆, and C₈ refer to the base carbon atoms; C₁' to C₅' are the sugar carbon atoms. ^c The chemical shifts are reported with reference to an external standard of CDCl₃. The errors in δ are less than 0.2 ppm, and in $\Delta\nu_{1/2}$ are less than 1.5 Hz. The ^{13}C assignments were made as previously reported (Jones et al., 1970).

containing NaF (Table 13). Hence NaF might contribute to the inhibition of SOD when used to adjust ionic strengths (Beyer et al., 1986). PP did have any effect on the SOD activity even at 20 mM.

IV.2. Interactions of metal-depleted and reduced forms of Cu,Zn-SOD with vanadate

IV.2.1. Interactions of apo Cu,Zn-SOD with vanadate

^{51}V NMR chemical shifts and line widths of the different forms of vanadate namely monomer (V_1), dimer (V_2) and tetramer (V_4) present in a 2 mM vanadate solution in the absence and in the presence of 0.03 mM - 0.2 mM apo enzyme form of Cu,Zn-SOD (where Cu^{2+} and Zn^{2+} are removed) are provided in Table 14. Figure 5 shows ^{51}V NMR spectra of 2 mM vanadate with increasing concentrations of the apo enzyme. There were no significant changes in the chemical shift values of the vanadate monomer, dimer and tetramer with increasing concentrations of the apo enzyme. Addition of the apo enzyme (0.03 - 0.2 mM) to the vanadate solution, however, does lead to an increase in line widths of the vanadate tetramer (from 69 - 181 Hz). Much smaller changes in the line widths of the vanadate monomer (66 - 89 Hz) and dimer (113 - 152 Hz) resonances were observed. The intensity of the vanadate tetramer decreases to a greater extent than those of the monomer and dimer. The concentrations of the vanadate species in the presence of increasing concentrations of apo SOD are given in Table 15. The concentration of the tetramer decreases from 0.216 mM to 0.097 mM, while that of the monomer decreases from 0.886 mM to 0.724 mM, and that of the dimer decreases from 0.125 to 0.083 mM.

Table 13. Inhibition of native Cu,Zn-SOD by adenine nucleotides and synthetic phosphates^a

Phosphate	Conc./mM	I ^b	% inhibition
ATP	10	0.153	10
ADP	10	0.150	0
	20	0.153	0
AMP	20	0.150	0
PP	10	0.150	0
	20	0.153	0
	10	0.3	0
	20	0.3	0
P _i	10	0.150	35
	10	0.150 ^c	20
	20	0.150	44
	20	0.150 ^c	30

^an=3^bI stands for ionic strength which was adjusted to the reported values with NaF.^cI was adjusted with HEPES buffer.

Table 14. Chemical shifts and line widths of monomeric(V_1), dimeric(V_2) and tetrameric(V_4) forms of 2 mM vanadate in the presence of E_2E_2SOD (apo enzyme) in 0.10 M HEPES, pH 7.4 at 20 ± 1 °C.^a

	V_1	V_2	V_4
No E_2E_2SOD			
δ/ppm	-553.2 ± 0.3	-568.1 ± 0.2	-574.4 ± 0.2
$\Delta v_{1/2}/Hz$	66 ± 8	113 ± 9	69 ± 7
0.03 mM E_2E_2SOD			
δ/ppm	-553.2 ± 0.3	-568.1 ± 0.3	-574.4 ± 0.2
$\Delta v_{1/2}/Hz$	65 ± 3	114 ± 11	80 ± 9
0.06 mM E_2E_2SOD			
δ/ppm	-553.3 ± 0.3	-568.2 ± 0.3	-574.4 ± 0.2
$\Delta v_{1/2}/Hz$	72 ± 10	144 ± 68	92 ± 13
0.10 mM E_2E_2SOD			
δ/ppm	-553.2 ± 0.3	-568.1 ± 0.3	-574.4 ± 0.2
$\Delta v_{1/2}/Hz$	69 ± 3	125 ± 71	117 ± 17
0.13 mM E_2E_2SOD			
δ/ppm	-553.4 ± 0.4	-568.3 ± 0.3	-574.4 ± 0.2
$\Delta v_{1/2}/Hz$	80 ± 7	134 ± 33	145 ± 32
0.16 mM E_2E_2SOD			
δ/ppm	-553.3 ± 0.4	-568.2 ± 0.3	-574.4 ± 0.2
$\Delta v_{1/2}/Hz$	80 ± 12	155 ± 39	159 ± 37
0.20 mM E_2E_2SOD			
δ/ppm	-553.2 ± 0.5	-568.1 ± 0.3	-574.3 ± 0.1
$\Delta v_{1/2}/Hz$	89 ± 15	152 ± 45	181 ± 40

^aChemical shifts and line widths are expressed as mean \pm SD of 3 separate trials.

Figure 5. ^{51}V NMR spectra of 2 mM vanadate in 0.1M HEPES, pH 7.4, at 20 ± 1 °C in the absence (A) and in the presence of 0.06 mM (B), 0.13 mM (C), and 0.20 mM apo Cu,Zn-SOD. Line broadening of 20 Hz was applied to improve the S/N ratio.

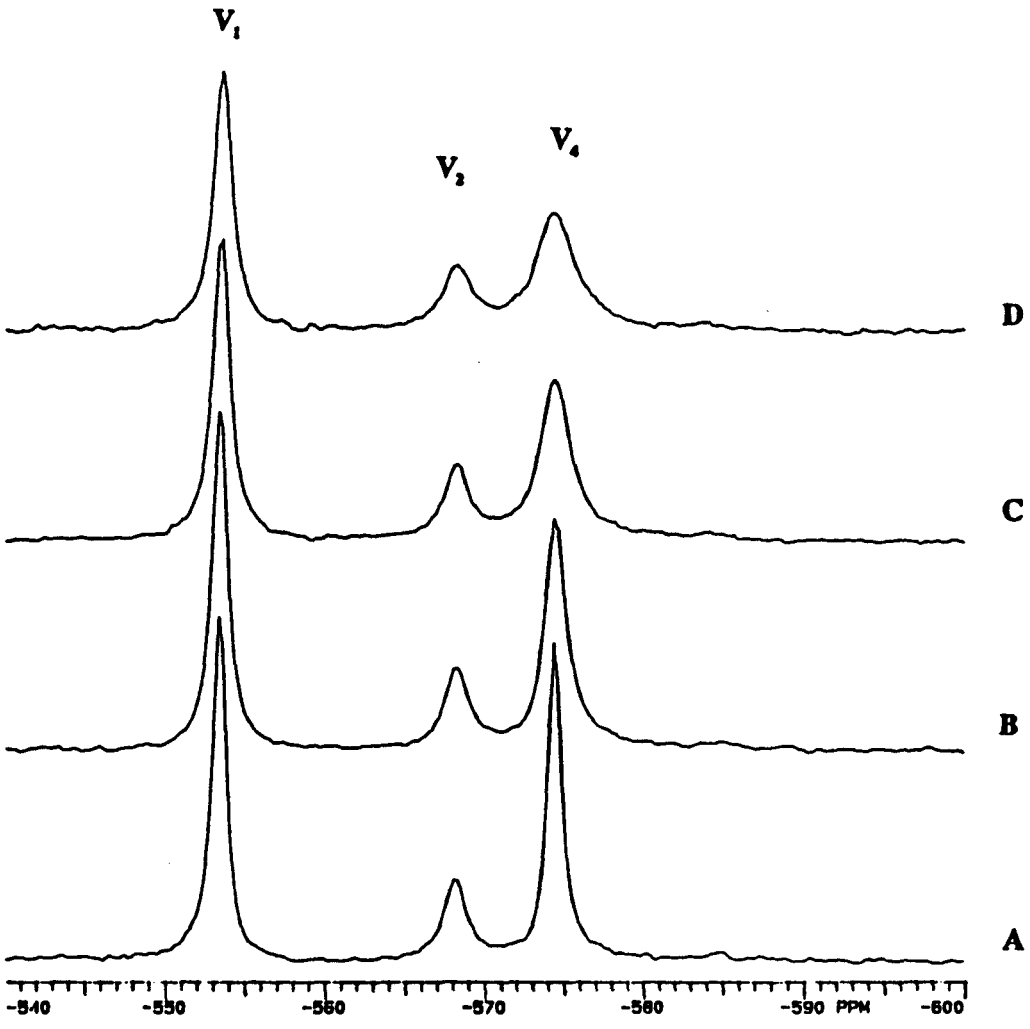


Table 15. Concentrations (mM) of vanadate species in the presence of increasing concentrations of E₂E₂SOD (apo enzyme) at pH 7.4 at 20 °C in 0.1 M HEPES containing 2 mM total vanadate.^a

[E ₂ E ₂ SOD]	[V ₁]	[V ₂]	[V ₄]	[V _x E ₂ E ₂ SOD]
0.00	0.886	0.125	0.216	0.000
0.03	0.886	0.125	0.216	0.000
0.06	0.758	0.091	0.116	0.596
0.10	0.720	0.082	0.094	0.740
0.13	0.748	0.089	0.110	0.634
0.16	0.726	0.084	0.098	0.714
0.20	0.724	0.083	0.097	0.722

^aThe concentrations of the vanadate species were calculated by using Equation 5 of the Methods Sections.

VI.2.2. Interactions of the zinc-only form of Cu,Zn-SOD with vanadate

Table 16 lists the ^{51}V NMR chemical shifts and line widths of the vanadate monomer, dimer and tetramer in the absence and in the presence of increasing concentrations of the zinc-only form of Cu,Zn-SOD. This protein derivative has an empty site at the Cu^{2+} binding domain of the enzyme. Addition of the zinc-only derivative of Cu,Zn-SOD to a 2 mM solution of vanadate did not significantly affect the ^{51}V NMR chemical shifts of the vanadate monomer, dimer and tetramer. There were significant changes in the line widths and intensities of the vanadate tetramer upon addition of higher concentrations of the zinc-only form of SOD. The line widths of the vanadate tetramer increased from 79 Hz to 336 Hz. Smaller changes in the line widths and intensities were observed in the case of the vanadate monomer and dimer; the line width of the monomer increased from 69 Hz to 91 Hz while that of the dimer increased from 108 Hz to 174 Hz. The concentrations of the different vanadate species in the presence of varying concentrations of the zinc-only derivative of Cu,Zn-SOD are given in Table 17.

IV.2.3. Interactions of reduced Cu,Zn-SOD with vanadate

Figure 6 shows the ^{51}V NMR chemical shifts and line widths of the vanadate monomer, dimer and tetramer in the absence and in the presence of increasing concentrations of reduced Cu,Zn-SOD, and these values are tabulated in Table 18. While no significant differences were observed in the ^{51}V NMR chemical shifts of the vanadate monomer, dimer and tetramer in the presence of 0.03 - 0.2 mM reduced Cu,Zn-SOD, significant increases in the line widths of the vanadate tetramer (71 Hz to 491 Hz) were observed upon addition of the reduced protein. Smaller changes were seen in line widths in the case of the vanadate monomer (69 Hz to 123

Table 16. Chemical shifts and line widths of monomeric(V_1), dimeric(V_2) and tetrameric(V_4) forms of 2 mM vanadate in the presence of E_2Zn_2SOD (zinc-only form of Cu,Zn-SOD) in 0.10 M HEPES, pH 7.4 at 20 ± 1 °C.^a

	V_1	V_2	V_4
No E_2Zn_2SOD			
δ/ppm	-552.7 ± 0.1	-567.9 ± 0	-574.2 ± 0
$\Delta v_{1/2}/Hz$	69 ± 7	108 ± 21	79 ± 10
0.03 mM E_2Zn_2SOD			
δ/ppm	-552.8 ± 0.3	-567.9 ± 0.2	-574.2 ± 0.2
$\Delta v_{1/2}/Hz$	79 ± 5	122 ± 12	122 ± 5
0.06 mM E_2Zn_2SOD			
δ/ppm	-552.8 ± 0.2	-567.9 ± 0	-574.3 ± 0.4
$\Delta v_{1/2}/Hz$	77 ± 3	131 ± 9	163 ± 12
0.10 mM E_2Zn_2SOD			
δ/ppm	-553.1 ± 0.1	-568.0 ± 0.1	-574.3 ± 0.5
$\Delta v_{1/2}/Hz$	79 ± 5	149 ± 25	230 ± 3
0.13 mM E_2Zn_2SOD			
δ/ppm	-553.1 ± 0.2	-567.9 ± 0	-574.4 ± 0.4
$\Delta v_{1/2}/Hz$	82 ± 7	145 ± 25	269 ± 18
0.16 mM E_2Zn_2SOD			
δ/ppm	-553.2 ± 0.2	-568.1 ± 0.1	-574.5 ± 0.4
$\Delta v_{1/2}/Hz$	86 ± 10	163 ± 38	306 ± 6
0.20 mM E_2Zn_2SOD			
δ/ppm	-553.1 ± 0.3	-567.8 ± 0.4	-574.1 ± 0.1
$\Delta v_{1/2}/Hz$	91 ± 5	174 ± 12	336 ± 10

^aChemical shifts and line widths are expressed as mean \pm SD of 3 separate trials.

Table 17. Concentrations (mM) of vanadate species in the presence of increasing concentrations of E_2Zn_2SOD at pH 7.4 at 20 °C in 0.1 M HEPES containing 2 mM total vanadate.^a

$[E_2Zn_2SOD]$	$[V_1]$	$[V_2]$	$[V_4]$	$[V_xE_2Zn_2SOD]$
0.00	0.876	0.128	0.217	0.000
0.03	0.848	0.120	0.190	0.152
0.06	0.798	0.106	0.149	0.394
0.10	0.756	0.095	0.120	0.574
0.13	0.738	0.091	0.109	0.644
0.16	0.746	0.093	0.114	0.612
0.20	0.682	0.078	0.079	0.846

^aThe concentrations of the vanadate species were calculated by using Equation 5 of the Methods Sections.

Hz) and dimer resonances (121 Hz to 226 Hz). Significant decreases in intensities, and hence concentrations, were observed for the vanadate tetramer, while such differences were not observed for the vanadate monomer and dimer. Concentrations of vanadate monomer, dimer and tetramer in the presence of increasing concentrations of reduced Cu,Zn-SOD are provided in Table 19.

IV.2.4. Interactions of native Cu,Zn-SOD with vanadate

The interactions of native Cu,Zn-SOD with vanadate were also followed using ^{51}V NMR spectroscopy. The ^{51}V NMR chemical shifts and line widths of the 3 vanadate species in the absence and in the presence of varying concentrations of native Cu,Zn-SOD are given in Table 20. On addition of increasing concentrations of the protein, the ^{51}V NMR chemical shifts of the vanadate monomer, dimer and tetramer were similar to those obtained in the absence of protein. The line widths of the vanadate tetramer increases to a larger extent (78 Hz to 475 Hz), when compared to those of vanadate monomer (66 Hz to 149 Hz) and vanadate dimer (108 Hz to 235 Hz). These changes in line widths are larger compared to those obtained for reduced Cu,Zn-SOD, the zinc-only derivative and the apo enzyme derivative of native Cu,Zn-SOD. The concentrations of the different vanadate species in the absence and in the presence of increasing concentrations of native SOD are tabulated in Table 21.

Figure 7 shows the ^{51}V NMR spectra of 2 mM vanadate solution in the absence and in the presence of 0.20 mM of the different metal depleted derivatives of native Cu,Zn-SOD. The presence of the native enzyme has the maximum effect on the intensity and line width of the vanadate tetramer, while smaller effects are observed in the presence of the reduced, the zinc-only derivative and the apo enzyme form of Cu,Zn-SOD. This observation can be qualitatively

Figure 6. ^{51}V NMR spectra of 2 mM vanadate in 0.1M HEPES, pH 7.4, at 20 ± 1 °C in the absence (A) and in the presence of 0.06 mM (B), 0.13 mM (C), and 0.20 mM reduced Cu,Zn-SOD (D). Line broadening of 20 Hz was applied to improve the S/N ratio.

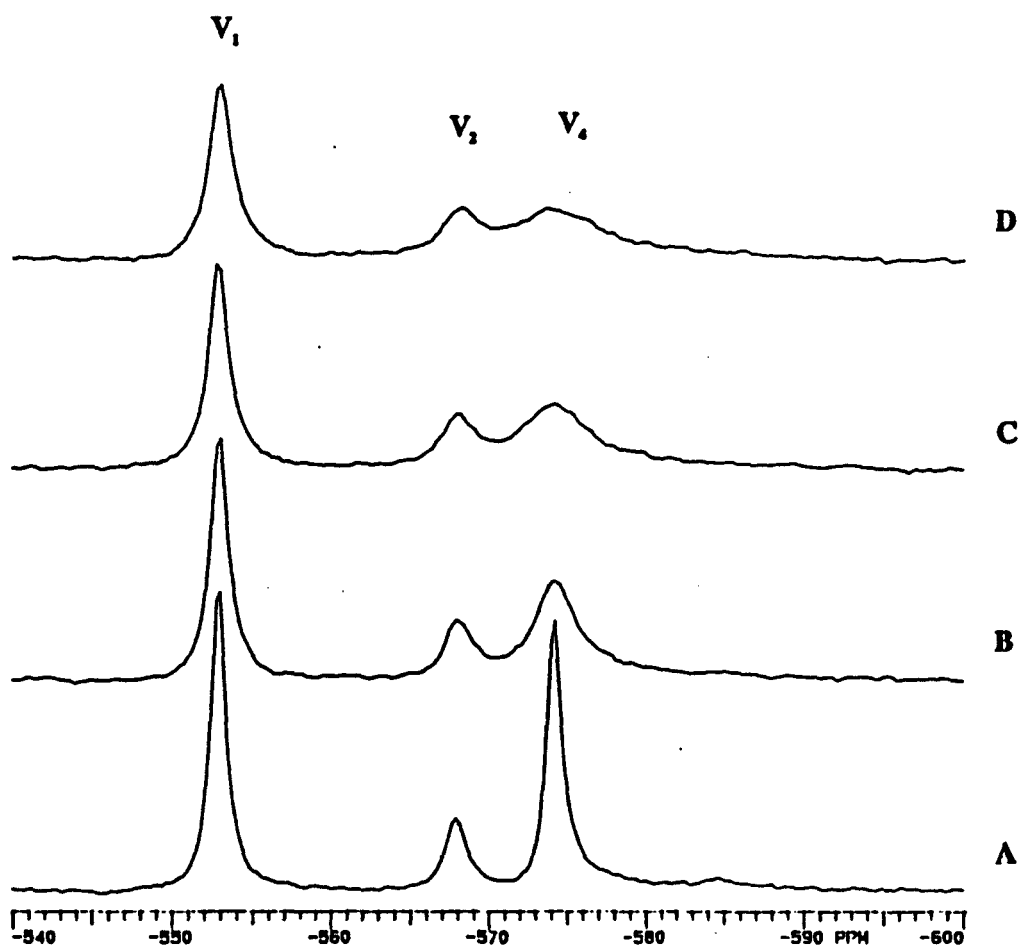


Table 18. Chemical shifts and line widths of monomeric(V_1), dimeric(V_2) and tetrameric(V_4) forms of 2 mM vanadate in the presence of Reduced Cu_2Zn_2SOD in 0.10 M HEPES, pH 7.4 at 20 ± 1 °C.^a

	V_1	V_2	V_4
No reduced Cu_2Zn_2SOD			
δ /ppm	-553.2 ± 0.3	-568.1 ± 0.2	-574.4 ± 0.2
$\Delta v_{1/2}$ /Hz	69 ± 7	121 ± 8	71 ± 5
0.03 mM reduced Cu_2Zn_2SOD			
δ /ppm	-552.9 ± 0.3	-568.1 ± 0.1	-574.4 ± 0.2
$\Delta v_{1/2}$ /Hz	86 ± 7	138 ± 14	168 ± 9
0.06 mM reduced Cu_2Zn_2SOD			
δ /ppm	-553.0 ± 0.2	-568.1 ± 0.1	-574.3 ± 0.2
$\Delta v_{1/2}$ /Hz	92 ± 15	172 ± 5	237 ± 8
0.10 mM reduced Cu_2Zn_2SOD			
δ /ppm	-553.1 ± 0.2	-568.3 ± 0.3	-574.5 ± 0.5
$\Delta v_{1/2}$ /Hz	98 ± 8	188 ± 13	333 ± 9
0.13 mM reduced Cu_2Zn_2SOD			
δ /ppm	-553.0 ± 0.1	-568.1 ± 0.1	-574.4 ± 0.1
$\Delta v_{1/2}$ /Hz	109 ± 6	203 ± 25	371 ± 30
0.16 mM reduced Cu_2Zn_2SOD			
δ /ppm	-553.0 ± 0.3	-568.3 ± 0.1	-574.6 ± 0.2
$\Delta v_{1/2}$ /Hz	115 ± 7	200 ± 13	415 ± 47
0.20 mM reduced Cu_2Zn_2SOD			
δ /ppm	-553.1 ± 0.2	-568.2 ± 0.1	-574.2 ± 0.2
$\Delta v_{1/2}$ /Hz	123 ± 2	226 ± 4	491 ± 14

^aChemical shifts and line widths are expressed as mean \pm SD of 3 separate trials

Table 19. Concentrations (mM) of vanadate species in the presence of increasing concentrations of Reduced Cu,Zn SOD at pH 7.4 at 23 °C in 0.10 M HEPES containing 2 mM total vanadate.^a

[Red.SOD]	[V ₁]	[V ₂]	[V ₄]	[V _x Red.SOD]
0.00	0.888	0.130	0.213	0.000
0.03	0.762	0.096	0.115	0.586
0.06	0.808	0.108	0.146	0.392
0.10	0.790	0.103	0.133	0.472
0.13	0.782	0.101	0.128	0.504
0.16	0.720	0.085	0.092	0.742
0.20	0.692	0.079	0.078	0.838

^aThe concentrations of the vanadate species were calculated by using Equation 5 of the Methods Sections.

Table 20. Chemical shifts and line widths of monomeric(V_1), dimeric(V_2) and tetrameric(V_4) forms of 2 mM vanadate in the presence of native Cu_2Zn_2SOD in 0.10 M HEPES, pH 7.4 at 20 ± 1 °C.^a

	V_1	V_2	V_4
No native Cu_2Zn_2SOD			
δ/ppm	-553.7 ± 0.3	-568.4 ± 0.3	-574.7 ± 0.4
$\Delta v_{1/2}/Hz$	66 ± 6	108 ± 1	78 ± 4
0.03 mM native Cu_2Zn_2SOD			
δ/ppm	-552.7 ± 0.3	-568.4 ± 0.3	-574.6 ± 0.2
$\Delta v_{1/2}/Hz$	91 ± 4	135 ± 6	168 ± 27
0.06 mM native Cu_2Zn_2SOD			
δ/ppm	-553.7 ± 0.3	-568.4 ± 0.3	-574.6 ± 0.4
$\Delta v_{1/2}/Hz$	96 ± 3	140 ± 13	233 ± 15
0.10 mM native Cu_2Zn_2SOD			
δ/ppm	-553.6 ± 0.4	-568.4 ± 0.5	-574.5 ± 0.5
$\Delta v_{1/2}/Hz$	101 ± 3	189 ± 4	315 ± 7
0.13 mM native Cu_2Zn_2SOD			
δ/ppm	-553.7 ± 0.3	-568.6 ± 0.2	-575.3 ± 0.3
$\Delta v_{1/2}/Hz$	112 ± 13	182 ± 85	354 ± 22
0.16 mM native Cu_2Zn_2SOD			
δ/ppm	-553.6 ± 0.3	-568.5 ± 0.4	-574.6 ± 0.2
$\Delta v_{1/2}/Hz$	124 ± 9	240 ± 2	455 ± 3
0.20 mM native Cu_2Zn_2SOD			
δ/ppm	-553.6 ± 0.4	-568.6 ± 0.6	-574.8 ± 0.1
$\Delta v_{1/2}/Hz$	149 ± 6	235 ± 22	475 ± 50

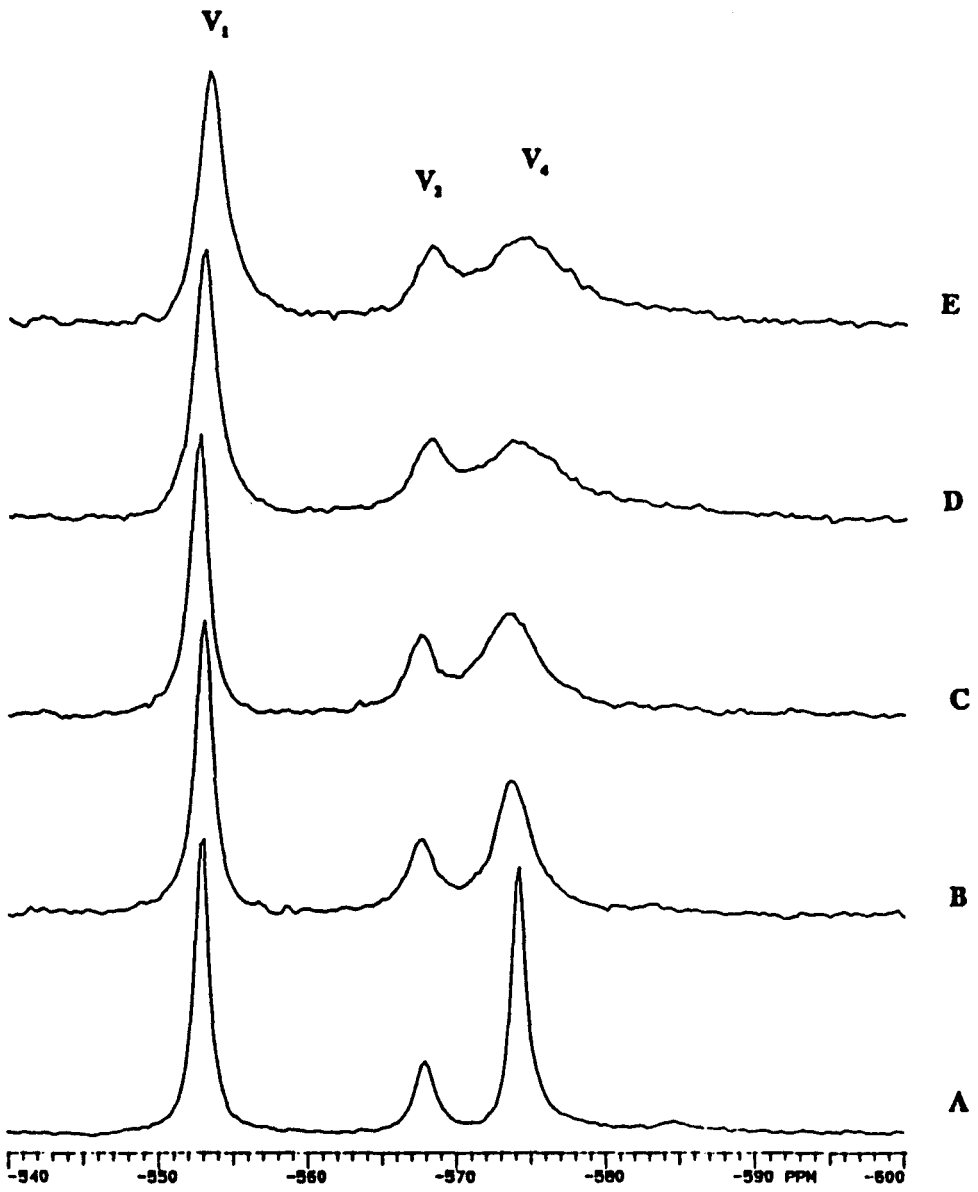
^aChemical shifts and line widths are expressed as mean \pm SD of 2 separate trials.

Table 21. Concentrations (mM) of vanadate species in the presence of increasing concentrations of native Cu,Zn SOD at pH 7.4 at 23 °C in 0.10 M HEPES containing 2 mM total vanadate.^a

[Native SOD]	[V ₁]	[V ₂]	[V ₄]	[V _x Native SOD]
0.00	0.908	0.143	0.202	0.000
0.03	0.818	0.116	0.134	0.414
0.06	0.810	0.114	0.128	0.450
0.10	0.702	0.086	0.072	0.838
0.13	0.700	0.085	0.072	0.842
0.16	0.668	0.078	0.059	0.940
0.20	0.542	0.051	0.026	1.252

^aThe concentrations of the vanadate species were calculated by using Equation 5 of the Methods Sections.

Figure 7. ^{51}V NMR spectra of 2 mM vanadate in 0.1 M HEPES, pH 7.4 in the absence of any protein (A) and in the presence of 0.20 mM apo Cu,Zn-SOD (B), zinc-only SOD (C), reduced Cu,Zn-SOD (D) and native Cu,Zn-SOD (E). Line broadening of 20 Hz was used to improve the S/N ratio.



interpreted as the vanadate tetramer interacting with the metal-depleted derivatives of Cu,Zn-SOD.

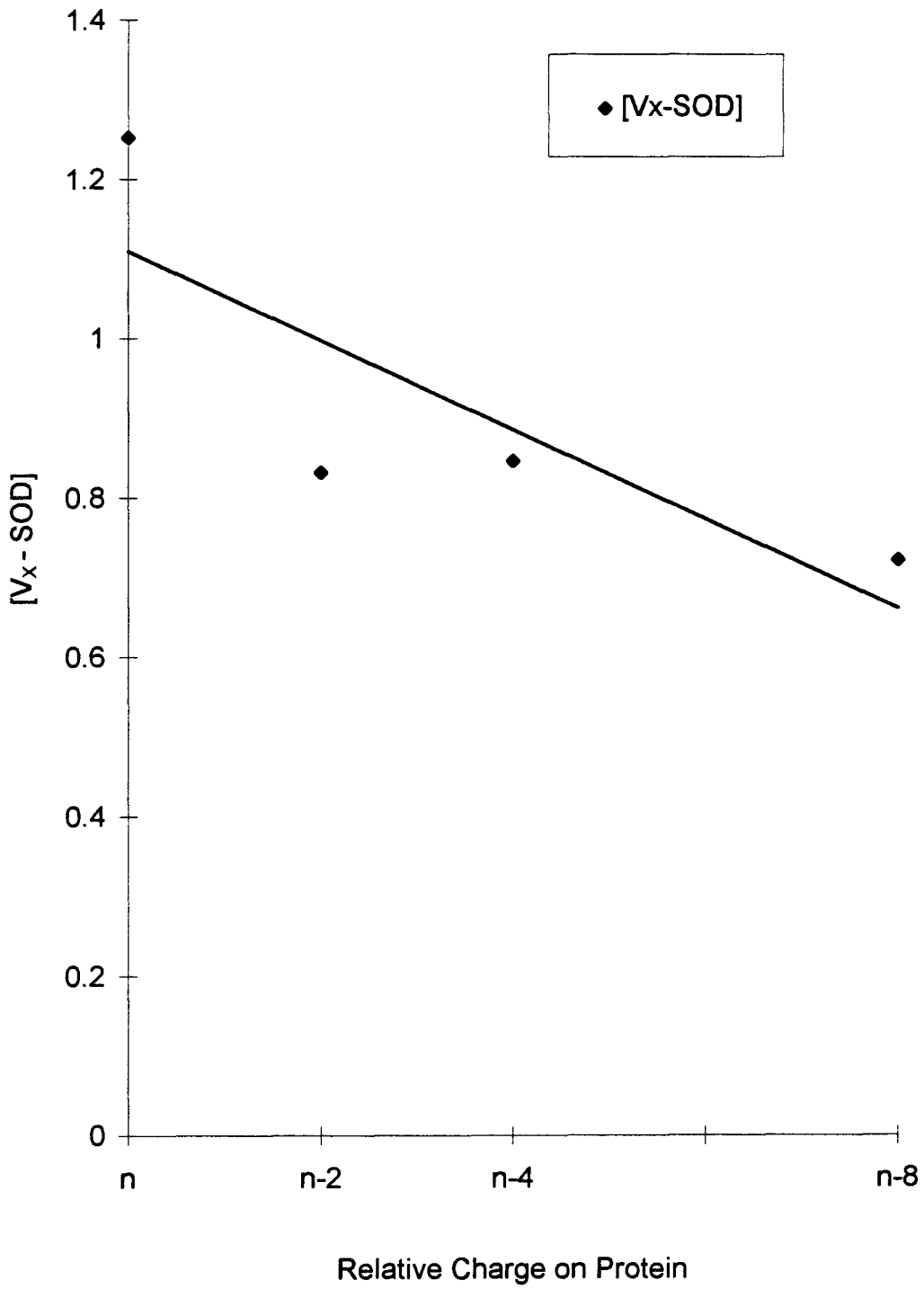
Figure 8 indicates the change in concentrations of vanadate-protein complex as a function of relative charge on the protein. Reduced SOD, the zinc-only derivative and the apo enzyme form of SOD represent progressive removal of positive charges/metal ions from the protein, rendering the protein more negatively charged. Since the apo enzyme form of SOD is more negatively charged than all the other protein derivatives studied, the interactions of vanadate with apo protein form would be weaker compared to the other protein derivatives; this is evident from the values of the vanadate-protein (protein-derivative) concentrations calculated. The concentrations of vanadate-protein complex increase with an increase in the relative positive charge on the protein derivative.

Tetrameric vanadate was shown to interact with native Cu,Zn-SOD at the lysine residues present at the mouth of the solvent channel of each subunit of the enzyme (Wittenkeller et al., 1991). In the case of the reduced and zinc-only derivatives of Cu,Zn-SOD, the tetrameric vanadate would bind at the lysine residues as in the case of the native enzyme. Since apo SOD has a random coil structure, and hence other positively charged residues could be exposed and bind vanadate.

IV.3. Li⁺ transport and binding in cultured nerve cell lines

Initial experiments were conducted using the glioma cell line U 373-MG, which was cultured in Dr. David Petering's laboratory at the University of Wisconsin at Milwaukee. The effect of the shift reagents Dy(PPP)₂⁷⁻ and Dy(TTHA)³⁻, and LiCl on cell viability was studied in monolayer cultures. These studies indicated that at least 65 % of the cells were viable after

Figure 8. Plot of $[V_x\text{Protein}]$ vs relative charge on the protein (derivative) for a 2 mM vanadate solution in the presence of 0.2 mM protein (derivative) ($r^2 = 0.70$).



24 hours (data not included). These cells were to be grown on Cytodex-1 microcarrier beads. However, ^7Li NMR spectra of cell-free suspensions of Cytodex-1 beads in a buffer with a shift reagent showed the presence of two ^7Li resonances, indicating that these beads were permeable to Li^+ .

IV.3.1. Characterization of microcarrier beads to determine suitability for alkali metal ion transport using NMR

Four different types of commercially available microcarrier beads namely Cytodex-1, CultiSpher-G, Biosilon and glass beads were used to characterize their alkali metal ion and shift reagent permeabilities. The physical properties and chemical composition of these beads are given in Table 22. The ^7Li , ^{23}Na and ^{133}Cs NMR chemical shifts and line widths of buffered solutions containing alkali metal ions in the absence and in the presence of microcarrier beads are given in Table 23. The three different shift reagents used were 5 mM $\text{HTm}(\text{DOTP})^4$, 5 mM $\text{Dy}(\text{PPP})_2^{7-}$ and 7 mM $\text{Dy}(\text{TTHA})^{3-}$. Figure 9 shows the ^7Li (A) and ^{23}Na (B) spectra of cell-free suspensions in a 5 mM HEPES buffer pH 7.4 containing 5 mM $\text{HTm}(\text{DOTP})^4$. The presence of Cytodex-1 or CultiSpher-G beads in the buffer gave rise to two separate ^7Li or ^{23}Na resonances, whereas only one ^7Li or ^{23}Na resonance was observed in solutions containing Biosilon or glass beads. Lower resolution was observed with solutions in ^7Li when compared to that of ^{23}Na NMR spectra of suspensions of Cytodex-1 and CultiSpher-G. The ^7Li and ^{23}Na isotropic shifts followed the order $\text{HTm}(\text{DOTP})^4 \approx \text{Dy}(\text{PPP})_2^{7-} > \text{Dy}(\text{TTHA})^{3-}$.

When two separate resonances were observed for Cytodex-1 and CultiSpher-G beads, their assignment to the intrabead space and extrabead space was made by removal of the top half of the beads from the NMR tube and replaced by the suspension medium. In the case of

Table 22. Composition and Physical Properties of Microcarrier Beads Used.

Bead Type	Composition		Permeable	Density (g cm ⁻³)	Diameter(μm)
	Inside	Surface			
Cytodex-1	Dextran	DEAE	Yes	1.03	131 - 220
CultiSpher-G	Gelatin	Charged Residues	Yes	1.00	120 - 180
Biosilon	Polystyrene	Charged Residues	No	1.05	1.6 - 300
Glass	Glass	Glass	No	1.04	90 - 150

Cytodex-1, the downfield shifted resonance corresponds to the intrabead space, while the opposite is true for CultiSpher-G.

^7Li and ^{23}Na NMR measurements were conducted in suspensions of Cytodex-1 at three different concentrations of $\text{Dy}(\text{PPP})_2^{7-}$ (Table 24). An increase in SR concentration resulted in increased downfield shifts and broadening for both intra- and extrabead resonances of Cytodex-1.

Discrimination of ^{133}Cs chemical shifts does not generally require shift reagents (Wittenkeller et al., 1992). ^{133}Cs NMR spectra in solutions containing one of the four types of beads in the absence and presence of $\text{Dy}(\text{TTHA})^{3-}$ indicated that in the presence of Cytodex-1 and CultiSpher-G beads, separate ^{133}Cs resonances were observed in the absence and in the presence of shift reagent, while only one ^{133}Cs resonance was observed in case of Biosilon and glass beads (Figure 10).

^{35}Cl NMR was used to determine the permeability of Cytodex-1 to Cl^- . Figure 11 shows the ^{35}Cl NMR spectra of cell-free suspensions of Cytodex-1 beads in the absence and presence of 10 mM $\text{Co}(\text{NO}_3)_2$ or 3 mM Mn^{2+} . Two unresolved ^{35}Cl NMR resonances are observed in the case of the bead suspension devoid of Co^{2+} or Mn^{2+} . In the presence of Co^{2+} , one broad ^{35}Cl resonance is observed, but both resonances become invisible in the presence of the paramagnetic Mn^{2+} . This is due to the permeability of the beads to Co^{2+} , Mn^{2+} and Cl^- . These permeability studies along with the fact that Biosilon beads are smaller in size compared to the other types of beads in this study, make them suitable for NMR studies of perfused cells by providing larger cell densities.

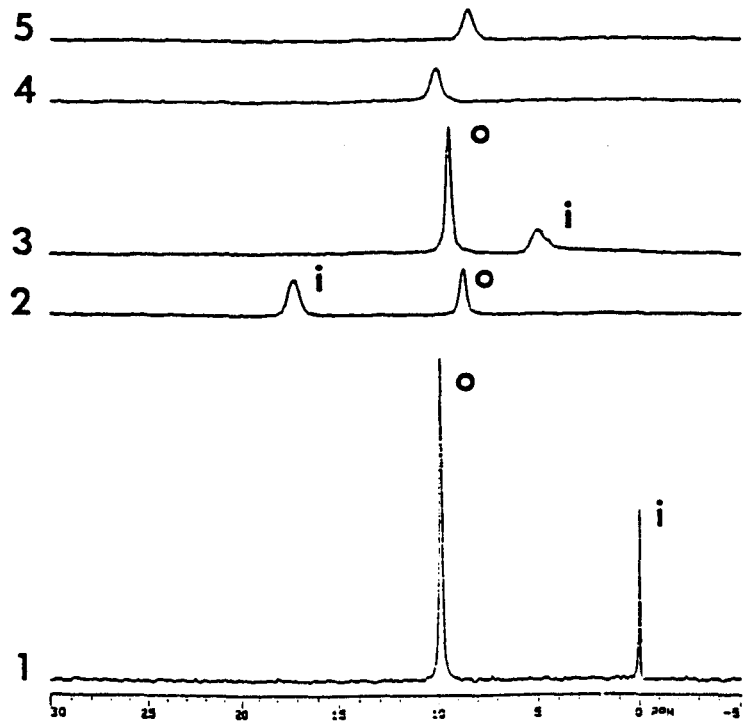
Table 23. NMR Parameters of Buffered Solutions Containing Alkali Metal Ions in the Absence and Presence of Microcarrier Beads.^a

	Inner-tube/Outer-tube		Cytodex-1		CultiSpher-G		Biosilon		Glass	
	$\delta_i(\Delta v_{1/2i})$	$\delta_o(\Delta v_{1/2o})$	$\delta_i(\Delta v_{1/2i})$	$\delta_o(\Delta v_{1/2o})$	$\delta_i(\Delta v_{1/2i})$	$\delta_o(\Delta v_{1/2o})$	$\delta_i(\Delta v_{1/2i})$	$\delta_o(\Delta v_{1/2o})$	$\delta_i(\Delta v_{1/2i})$	$\delta_o(\Delta v_{1/2o})$
A. ⁷Li NMR^b										
with HTm(DOTP) ⁴⁻ ^c	0.0(7.0)	9.8(17)	16.6(71)	8.5(43)	4.7(89)	9.2(34)	- ^s	9.5(83)	- ^s	8.6(71)
with Dy(PPP) ₂ ⁷⁻ ^d	0.0(5.2)	-6.5(15)	-17.6(160)	-5.2(183)	-3.5(87)	-6.4(46)	- ^s	-6.6(136)	- ^s	-6.6(123)
with Dy(TTHA) ³⁻ ^e	0.0(11)	2.0(8.0)	-1.9(62) ^f	2.7(76) ^f	- ^s	1.8(65)	- ^s	1.4(201)	- ^s	1.4(189)
B. ²³Na NMR^b										
with HTm(DOTP) ⁴⁻ ^c	0.0(12)	13.2(28)	23.8(97)	11.8(40)	7.2(68)	12.8(66)	- ^s	12.7(60)	- ^s	12.4(58)
with Dy(PPP) ₂ ⁷⁻ ^d	0.0(12)	-13.0(27)	-29.9(204)	-9.3(162)	-7.5(113)	-12.6(54)	- ^s	-12.4(117)	- ^s	-14.3(102)
with Dy(TTHA) ³⁻ ^e	0.0(11)	3.3(13)	4.5(50) ^f	3.3(91) ^f	-2.6(45) ^f	3.3(57) ^f	- ^s	2.7(138)	- ^s	2.5(127)
C. ¹³³Cs NMR^a										
without SR	- ⁱ	-0.1(1.3)	-3.1(4.5)	-3.9(5.5)	-3.3(15)	-3.9(7.0)	- ^s	-4.2(7.5)	- ^s	-4.5(6.5)
with Dy(TTHA) ³⁻	-4.2(2.0)	-0.3(2.0)	2.1(14)	-0.5(24)	^j	-0.7(23)	- ^s	-0.7(45)	- ^s	-0.7(51)

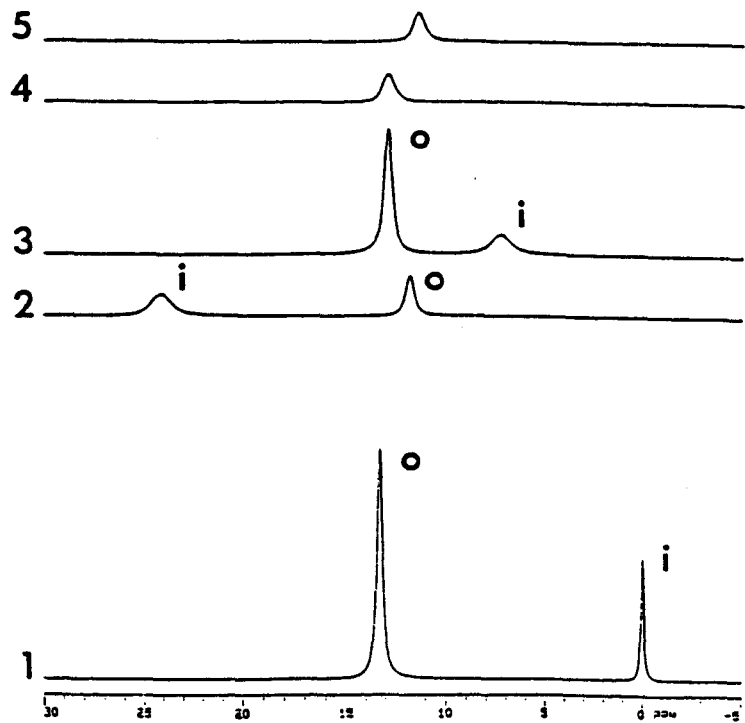
Table 23 (cont.)

^aThe reported NMR parameters are an average for the two separately prepared samples. Chemical shifts in ppm are followed by line widths in Hz in parentheses. The meaning of the symbols i and o is the same as for Fig. 1. The reported line widths at half-height intensity were corrected by subtraction of the line broadening used to obtain each spectrum. Errors in chemical shift and line width are less than 0.1 ppm and 1.0 Hz, respectively. ^bThe chemical shifts of ⁷Li and ²³Na are reported relative to the resonances from a solution containing 10 mM LiCl, 140 mM NaCl, and 5 mM HEPES, pH 7.4, without SR placed in an inner coaxial tube, whereas the outer tube contained a similar buffered solution plus SR (5 mM HTm(DOTP)⁴⁻ or 5 mM Dy(PPP)₂⁷⁻ or 7 mM Dy(TTHA)³⁻). ^cThe solution composition was 10 mM LiCl, 140 mM NaCl, 5 mM HTm(DOTP)⁴⁻, and 5 mM HEPES, pH 7.4. ^dThe solution composition was 10 mM LiCl, 140 mM NaCl, 5 mM Dy(PPP)₂⁷⁻, 5 mM HEPES, pH 7.4. ^eThe solution composition was 10 mM LiCl, NaCl, 7 mM Dy(TTHA)³⁻, 5 mM HEPES, pH 7.4. ^fPartially resolved resonance. ^gResonance not resolved. ^hThe ¹³³Cs chemical shifts are reported relative to an external reference of 150 mM CsCl containing 20% D₂O; the solution composition for bead-suspension measurements without SR was 10 mM CsCl, 140 mM NaCl, and 5 mM HEPES, pH 7.4. For the measurements in the presence of SR, 7 mM Dy(TTHA)³⁻ was added to the same medium. ⁱNo inner coaxial tube was used.

Figure 9. (A) ^7Li and (B) ^{23}Na NMR spectra of a solution containing 10 mM LiCl, 140 mM NaCl, 5 mM HTm(DOTP) $^{4-}$, 5 mM HEPES, pH 7.4, in the absence of beads (spectra 1) and in the presence of Cytodex-1 beads (spectra 2), CultiSpher-G beads (spectra 3), Biosilon beads (spectra 4), and glass beads (spectra 5). An inner-outer tube combination was used for spectra 1, whereas regular 10 mm NMR tubes without a coaxial tube were used for spectra 2 through 5. The symbols i and o denote NMR resonances originating from the internal bead volume and from the medium, respectively, except for spectra 1 where i denotes the inner tube resonance and o denotes the outer tube resonance.



A



B

Table 24. NMR parameters of buffered solutions containing Na⁺ and Li⁺ in the absence and presence of Cytodex-1 beads, with different concentrations of Dy(PPP)₂⁷⁻

Dy(PPP) ₂ ⁷⁻ /mM	Inner-tube/Outer-tube		Cytodex-1	
	$\delta_i(\Delta\nu_{1/2i})$	$\delta_o(\Delta\nu_{1/2o})$	$\delta_i(\Delta\nu_{1/2i})$	$\delta_o(\Delta\nu_{1/2o})$
A. ⁷Li NMR				
5	0.0(9)	-5.6(20)	-4.7(146)	-13.8(118)
7	0.0(10)	-7.2(21)	-6.2(181)	-16.0(130)
10	0.0(6)	-9.2(28)	-8.4(223)	-17.5(135)
B. ²³Na NMR				
5	0.0(15)	-12.0(26)	-10.1(116)	-26.9(153)
7	0.0(12)	-15.9(32)	-13.9(143)	-31.9(163)
10	0.0(12)	-21.0(38)	-18.8(176)	-37.5(183)

Chemical shifts in ppm are followed by line widths in Hz in parenthesis. The reported line widths at half-height intensity were corrected by subtraction of the line broadening used for obtaining each spectrum.

Figure 10. ^{133}Cs NMR spectra of a solution containing 10 mM CsCl, 140 mM NaCl, 5 mM HEPES, pH 7.4, in the presence of (A) Cytodex-1 beads (B) CultiSpher-G beads (C) Biosilon Beads, or (D) Glass beads. The symbols i and o represent intra- and extrabead ^{133}Cs resonance.

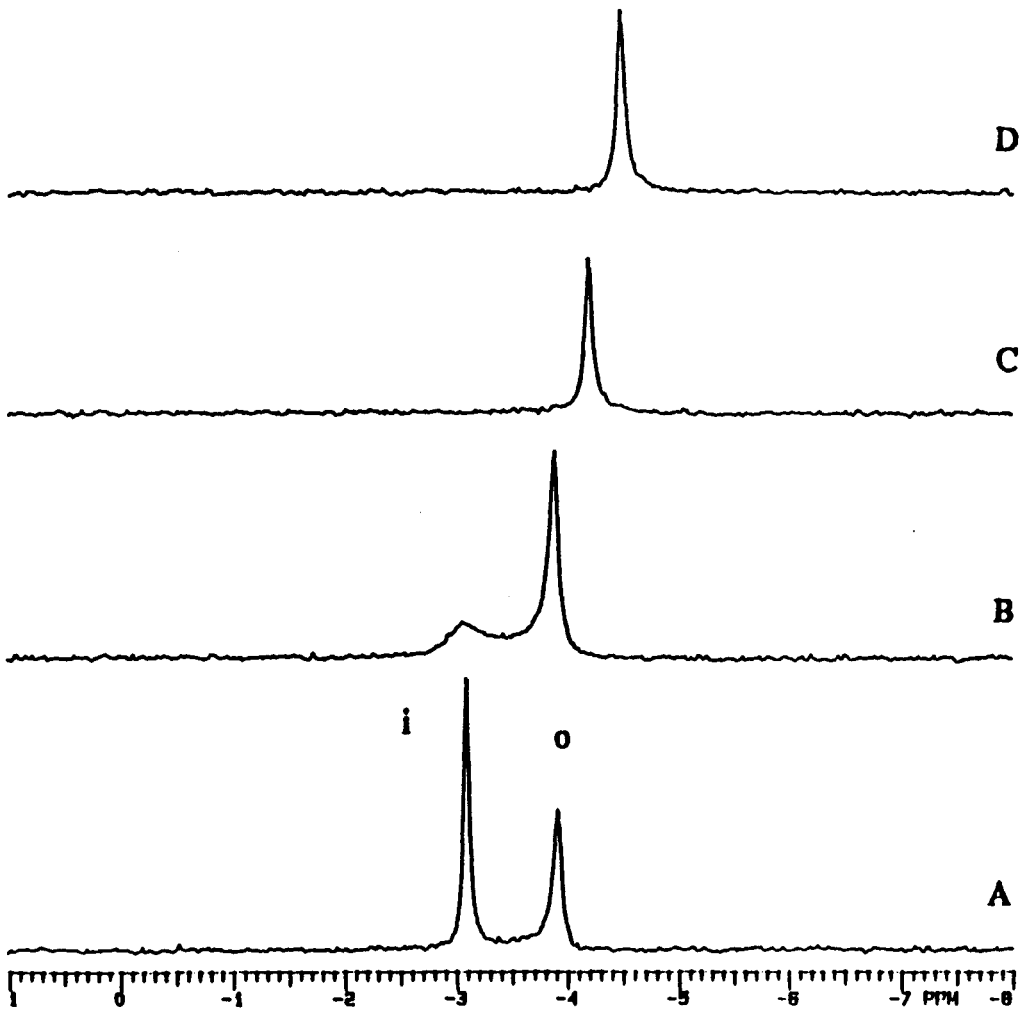
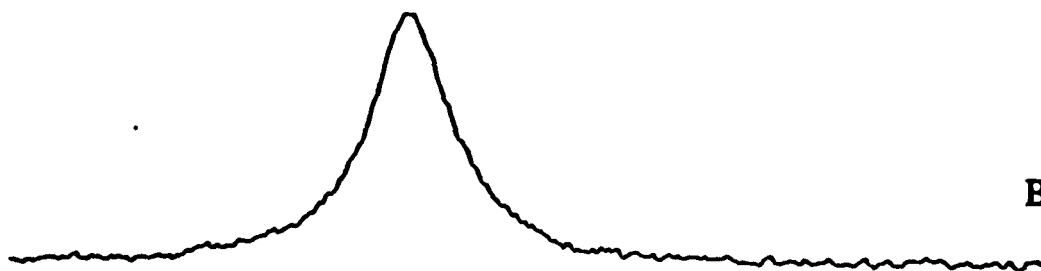


Figure 11. ^{35}Cl NMR spectra of a solution containing 10 mM LiCl, 140 mM NaCl, 5 mM HEPES, pH 7.4, in the presence of Cytodex-1 beads. (A) Spectrum in the absence of Co^{2+} or Mn^{2+} (B) Spectrum in the presence of 10 mM Co^{2+} (C) Spectrum in the presence of 3 mM Mn^{2+} .

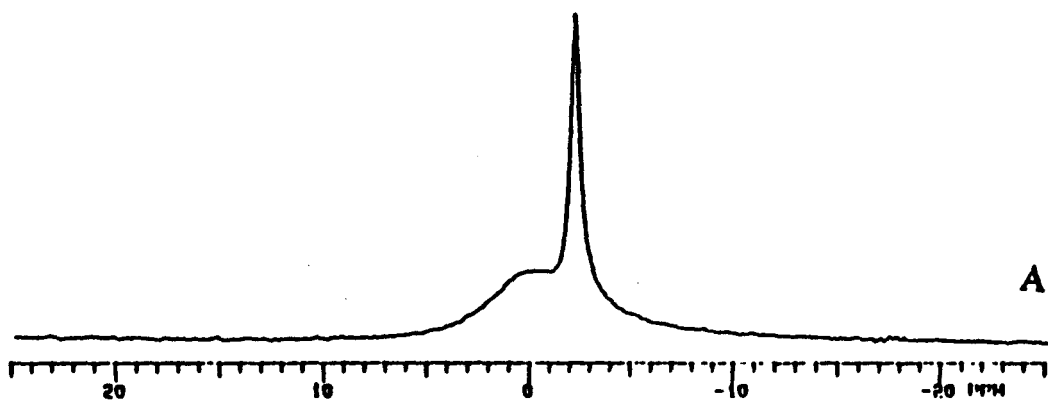
C



B



A



IV.3.2. Viability of SH-SY5Y cells in the presence of different shift reagents and LiCl

The inability of the U 373-MG glioma cells to grow on Biosilon beads prompted us to choose another cell line, namely the human neuroblastoma SH-SY5Y cells, to study Li^+ interactions in nerve cells. First, the viability of these cells in the presence of LiCl alone and in the presence of individual shift reagents and LiCl were determined in non-confluent monolayer cultures. The results are shown in Table 25. There were no significant differences observed in cell viability in the presence of LiCl alone when compared to control cultures (85-95% viable). However, in the presence of the shift reagents and LiCl, small decreases in viability of the cells were observed. Though the shift reagents have similar effects on cell viability within the period of time studied, the morphology of the cells was altered in the presence of $\text{Dy}(\text{PPP})_2^{7-}$ within an hour. The cells lost their characteristic shape, were seen to round off and gradually detach from the base of the plate. The cell morphology was maintained in the presence of $\text{HTm}(\text{DOTP})^{4-}$ and $\text{Dy}(\text{TTHA})^{3-}$ up to 5 hours (Figure 12).

IV.3.3. Li^+ transport in SH-SY5Y cells in suspension

Li^+ transport into SH-SY5Y cells was first followed in cell suspensions. Two shift reagents $\text{HTm}(\text{DOTP})^{4-}$ and $\text{Dy}(\text{PPP})_2^{7-}$ were used. The cells were first allowed to settle prior to the acquisition of spectra. 5 mM $\text{HTm}(\text{DOTP})^{4-}$ was sufficient to differentiate between the intracellular and the extracellular ^7Li resonances. We were able to follow increases in the intracellular ^7Li resonance with time (Figure 13). The rate constants calculated were similar when either 5 mM $\text{HTm}(\text{DOTP})^{4-}$ or 5 mM $\text{Dy}(\text{PPP})_2^{7-}$ were used (Table 26). However, the cell viability of neuroblastoma cells in suspension decreased to below 70% after 45 min. A

Table 25. Viability of SH-SY5Y cells in monolayers in the presence of different shift reagents and LiCl.^a Values expressed as % (mean \pm error, n=3^b) of total number of cells.

Shift Reagent Time	LiCl	HTm(DOTP) ^{4c}	Dy(PPP) ₂ ^{7-d}	Dy(TTHA) ^{3-e}
1 hr	86.3 \pm 3.2	81.0 \pm 1.4	87.5 \pm 6.4	82.0 \pm 6.0
2 hr	85.8 \pm 1.3	78.8 \pm 0.4	80.1 \pm 7.2	86.4 \pm 5.1
3 hr	85.6 \pm 3.0	80.2 \pm 1.6	80.3 \pm 3.9	85.8 \pm 3.4
5 hr	85.2 \pm 4.1	82.5 \pm 7.8	78.9 \pm 0.6	82.5 \pm 4.0

^a[LiCl] = 5mM

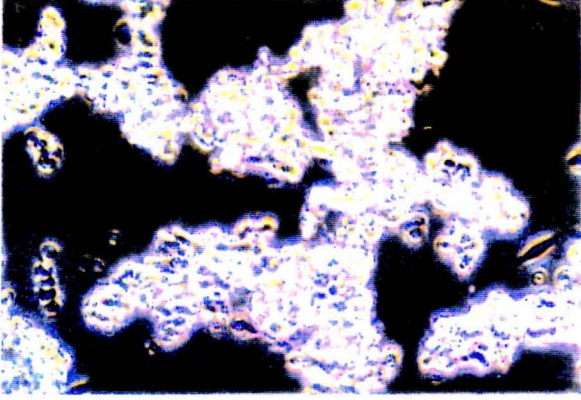
^bvariation of 3 separate samples each counted in 7-8 fields

^c[HTm(DOTP)⁴⁻] = 5 mM

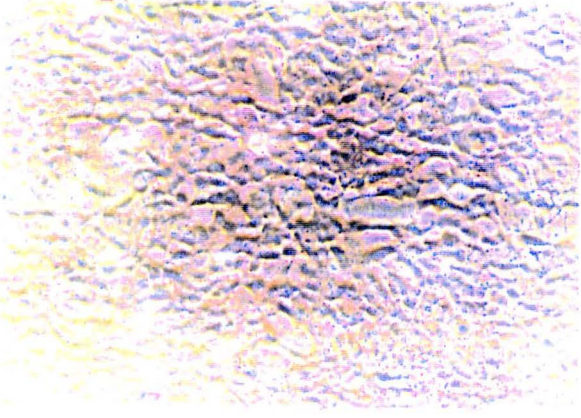
^d[Dy(PPP)₂⁷⁻] = 5 mM

^e[Dy(TTHA)³⁻] = 10 mM

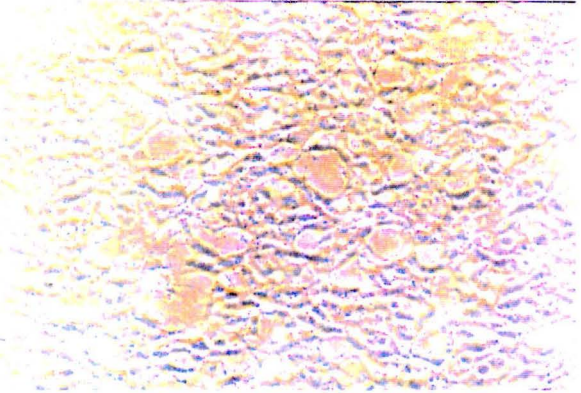
Figure 12. Morphology of SH-SY5Y cells in the absence of LiCl and shift reagent (A); in the presence of 5 mM LiCl and 5 mM HTm(DOTP)⁴⁻ for 5 hours (B); and in the presence of 5 mM LiCl and 5 mM Dy(PPP)₂⁷⁻ for 2 hours (C).



C



B



A

decrease in the viability was also reflected in the collapse of the chemical shift separation between the intra- and extracellular ^7Li NMR resonances.

IV.3.4. Li^+ transport in SH-SY5Y cells anchored on Biosilon beads

The viability of SH-SY5Y cells in suspensions cannot be maintained during the course of a Li^+ transport experiment as indicated in the previous section. Hence SH-SY5Y cells were immobilized and allowed to grow on non-permeable Biosilon beads. Photoelectron micrographs were obtained to visualize these cells anchored on Biosilon beads (Figure 14). Morphologically, these cells appear to retain their shape when anchored on beads. Li^+ transport was monitored in SH-SY5Y cells anchored on Biosilon beads and perfused with a modified growth medium.

Li^+ influx was monitored in the absence and in the presence of the ionophore DB14C4 (Figure 15). The rate constant for Li^+ influx was determined to be $0.036 \pm 0.001 \text{ min}^{-1}$; this rate constant was enhanced by a factor of 2 in the presence of 0.3 mM DB14C4 (Table 27, A). Li^+ efflux was followed in SH-SY5Y cells anchored on Biosilon beads, and loaded with Li^+ prior to the start of perfusion. The rate constant for Li^+ efflux was calculated to be $0.018 \pm 0.0025 \text{ min}^{-1}$ (Table 27, B).

The viability of SH-SY5Y cells during the course of NMR experiments was monitored using ^{31}P NMR spectroscopy. A typical ^{31}P NMR spectrum of SH-SY5Y cells immobilized on Biosilon microcarrier beads and perfused with medium is shown in Figure 16. ^{31}P NMR spectra were obtained every 70 mins for over 6 hrs after the start of perfusion and the phosphocreatine and ATP levels were obtained. The ratio of phosphocreatine to β -ATP was calculated and was found to decrease from 2.1 to 0.84. The levels of phosphocreatine was

Figure 13. ^7Li NMR spectra of packed SH-SY5Y human neuroblastoma cells in suspension in DME medium containing 5 mM HTm(DOTP) $^{4-}$ after the addition of 5 mM LiCl at 10 mins (A), at 20 mins (B), and at 30 mins (C). Line broadening of 15 Hz was applied to improve the S/N ratio. The symbols i and o denote intracellular and extracellular ^7Li NMR resonances.

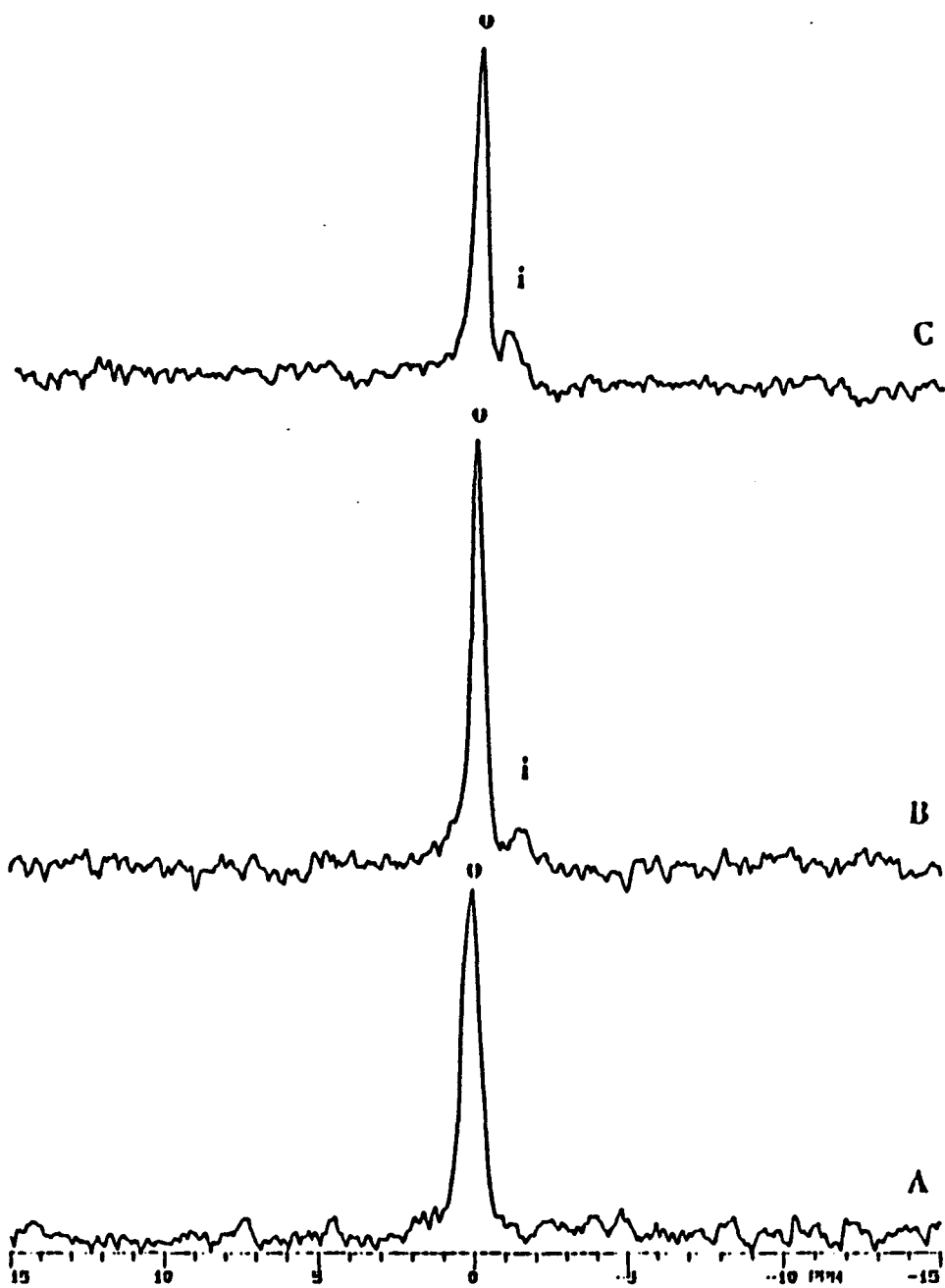


Table 26. Li⁺ influx into SH-SY5Y human neuroblastoma cells in suspension^a

Shift reagent	Rate Constant (min ⁻¹)
HTm(DOTP) ⁴⁻	0.050 ± 0.016
Dy(PPP) ₂ ⁷⁻	0.046 ± 0.013

^aThe cells were suspended in culture medium containing 5 mM LiCl and 5 mM shift reagent (n=2). The rate constants were determined as described in the Methods Section.

Figure 14. Scanning electron micrograph of SH-SY5Y cells anchored on Biosilon microcarrier beads. The amplification factor was 194. The scale bar equals 200 μM .

Figure 15. ^7Li NMR spectra of Li^+ influx into SH-SY5Y human neuroblastoma cells anchored on Biosilon beads in DME medium containing 15 mM LiCl , 5 mM HTm(DOTP)^+ , and 0.3 mM DB14C4. The spectra of Li^+ influx were obtained at 25 mins (A), at 36 mins (B) at 47 mins (C) and at 53 mins (D). Line broadening of 10 Hz was used to improve the S/N ratio. The

symbol used indicates the intra- and extracellular ^7Li NMR resonances

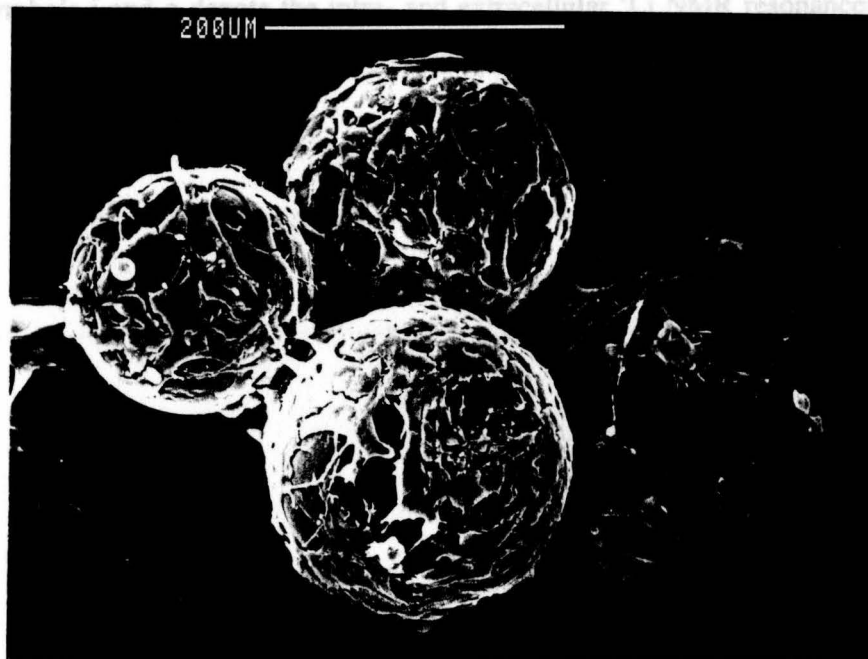


Figure 15. ^7Li NMR spectra of Li^+ influx into SH-SY5Y human neuroblastoma cells anchored on Biosilon beads in DME medium containing 15 mM LiCl , 3 mM HTm(DOTP)^4 , and 0.3 mM DB14C4 . The spectra of Li^+ influx were obtained at 25 min (A), at 36 mins (B) at 47 mins (C) and at 53 mins (D). Line broadening of 10 Hz was used to improve the S/N ratio. The symbols i and o denote the intra- and extracellular ^7Li NMR resonances.

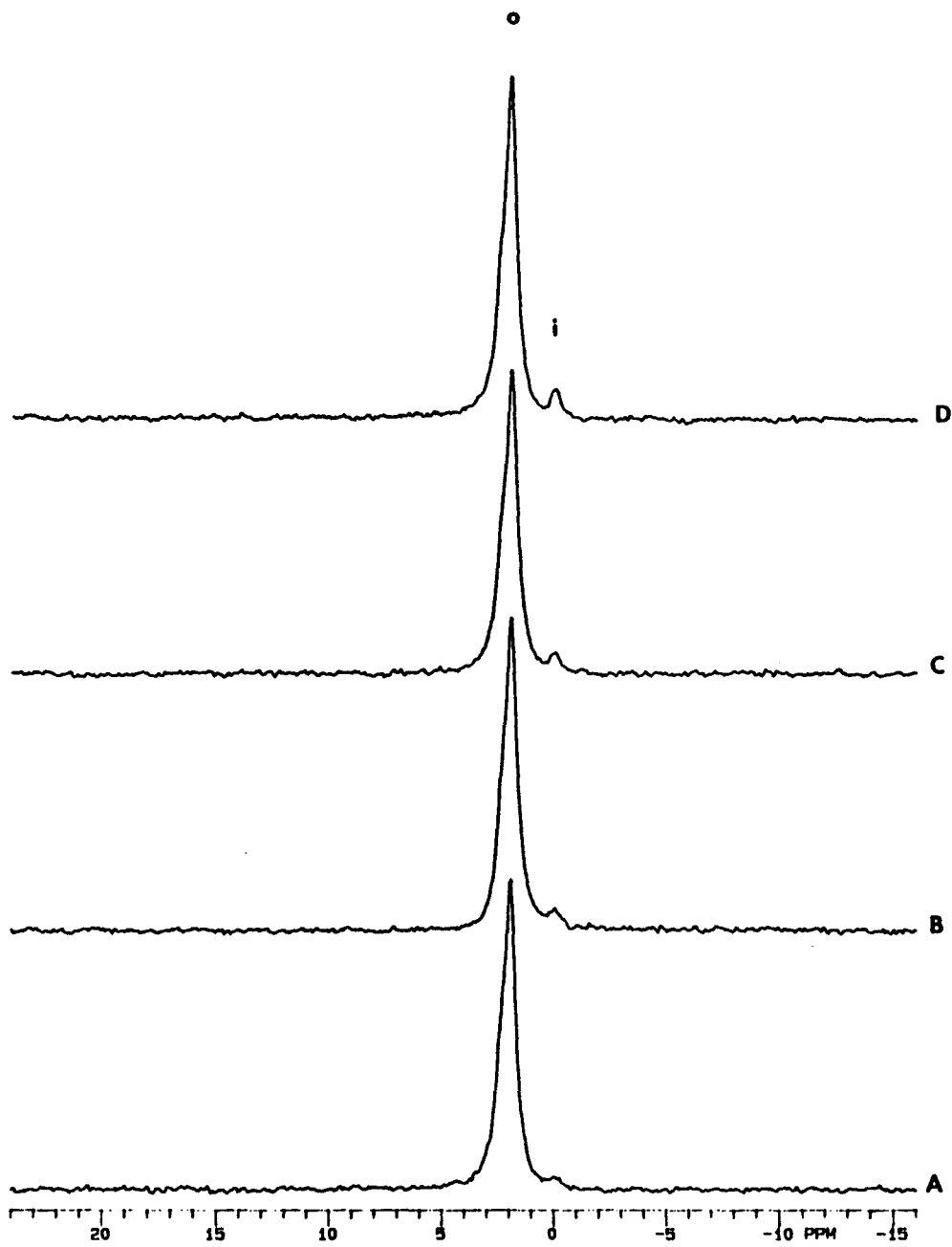


Table 27. Li⁺ transport rates in SH-SY5Y cells anchored on Biosilon beads^a

A. Li ⁺ influx	Rate Constant/ min ⁻¹
a) no ionophore present	0.036 ± 0.001 (n=2)
b) 0.3 mM DB14C4	0.068 ± 0.001 (n=2)
B. Li ⁺ efflux	0.018 ± 0.0025 (n=2)

^aThe cells anchored on Biosilon beads were perfused with DME medium containing 2 mM LiCl (for efflux experiments), or 15 mM LiCl (for influx experiments), and 3 mM HTm(DOTP)⁺. The rate constants were determined as described in the Methods Section.

maintained during the course of the experiment; an unexplained increase in ATP was, however, observed. Hence the cells were shown to be viable during the course of the transport experiments.

IV. 3.5. ^7Li NMR relaxation times in SH-SY5Y cells

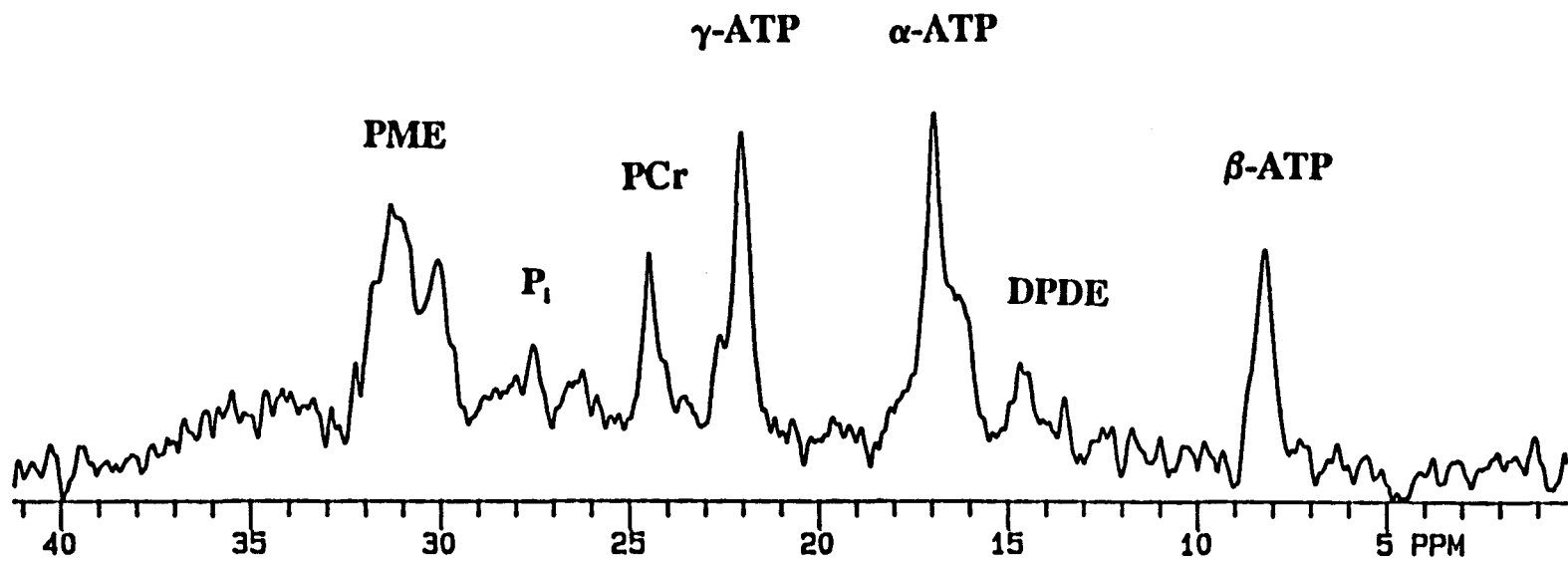
The ^7Li NMR spin-lattice (T_1) and spin-spin (T_2) relaxation times were obtained after a steady-state was reached following Li^+ uptake into SH-SY5Y cells. The T_1 and T_2 values obtained are provided in Table 28. ^7Li NMR relaxation times were obtained for both cells in suspension and for cells anchored on Biosilon beads. The value of R for both cells in suspension and for cells anchored on microcarrier beads have the same order of magnitude, and is much larger than 1, indicating that Li^+ binds to sites within SH-SY5Y cells.

One of the potential binding sites of Li^+ within the cells is the cell membranes. The interaction of Li^+ with purified membrane preparations was followed by ^7Li NMR relaxation measurements. ^7Li T_1 and T_2 values were obtained with increasing concentrations of Li^+ (Table 29). As the concentration of Li^+ is increased, both T_1 and T_2 values increase. A typical Li^+ titration of cell membranes with increasing concentrations of Li^+ is shown in Table 29. The R ratio (T_1/T_2) decreases from 53 to 8 as Li^+ is varied from 1 mM to 500 mM.

Using James Noggle plots, a binding constant (K_b) was calculated using T_1 values and was found to be $255 \pm 16.5 \text{ M}^{-1}$ ($n=2$). Similar K_b values were obtained with T_2 measurements. These results indicate that Li^+ transported into the neuroblastoma cells interact with intracellular components, and one such component is the cell membrane.

The phospholipids from SH-SY5Y cell membranes were extracted and quantified by ^{31}P NMR spectroscopy (Figure 17) using established procedures (Mota de Freitas et al., 1994a).

Figure 16. ^{31}P NMR spectrum of SH-SY5Y human neuroblastoma cells anchored on Biosilon beads perfused with DME medium containing 15 mM LiCl and 3 mM HTm(DOTP)⁴⁻. Line broadening of 20 Hz was used to improve the S/N ratio. The different phosphorus containing metabolites in the spectrum are: phosphomonoesters (PME); P_i (inorganic phosphate); phosphocreatine (PCr); γ -ATP; α -ATP; diphosphodiester; and β -ATP. These assignments were made by comparison of the ^{31}P chemical shifts obtained to the values reported in literature for other cell systems (Gillies et al., 1986) and by spiking the spectrum with known phosphorus compounds.



The ^{31}P NMR resonances obtained were identified by spiking the lipid extract with known amounts of pure phospholipids. The phospholipid analysis of these membranes indicated that PC and PE accounted for about 90% of the total phospholipids in the cell membranes. The phospholipid composition was determined to be: PE and PE_p 36%, PS 2.8%, PI 6.6%, PC 50.1% and X (unidentified) 4.5%.

Table 28. ^7Li NMR relaxation measurements in SH-SY5Y cells

	T_1/s	T_2/s	$R=T_1/T_2$
Cell suspension ^a	6.52 ± 0.014	0.038 ± 0.0035	171 (n=2)
Cells on beads ^b	3.50 ± 0.31	0.031 ± 0.007	113 (n=2)

^aThe cells were suspended in DME medium containing 5 mM LiCl and 5 mM shift reagent.

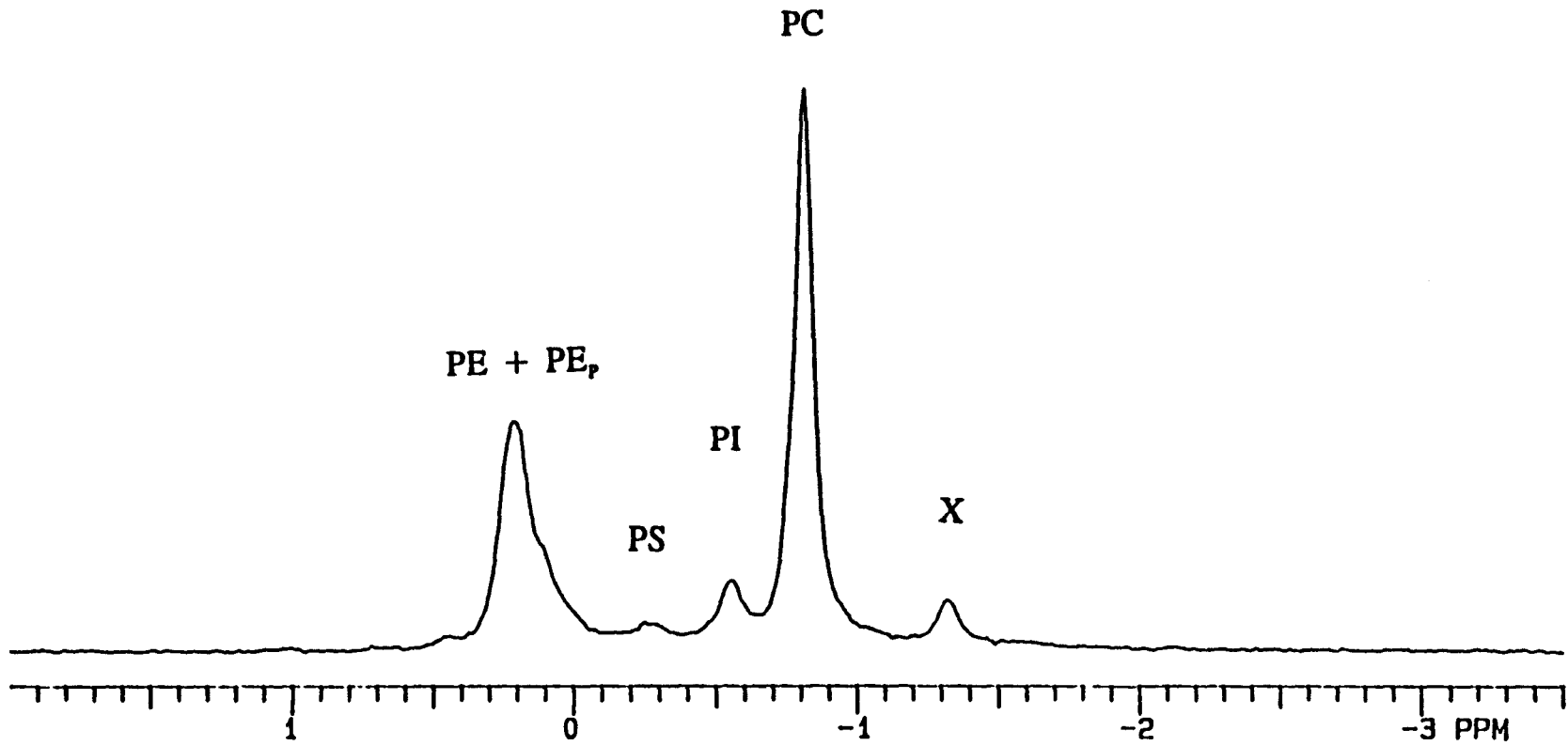
^bThe cells were anchored on Biosilon beads and perfused with DME medium containing 15 mM LiCl and 3 mM HTm(DOTP)⁴⁻.

Table 29. ^7Li NMR relaxation measurements with SH-SY5Y cell membranes

$[\text{Li}^+]/\text{mM}$	T_1/s	T_2/s	$R=T_1/T_2$
1	5.22 ± 0.38	0.098 ± 0.016	53
2	5.93 ± 0.47	0.143 ± 0.022	41
3	7.16 ± 0.30	0.169 ± 0.013	42
4	6.80 ± 0.13	0.196 ± 0.019	35
5	7.76 ± 0.30	0.192 ± 0.014	39
6	7.97 ± 0.36	0.210 ± 0.020	39
500	15.51 ± 0.17	1.89 ± 0.037	8

Binding constant (K_b) of Li^+ to SH-SY5Y membranes was $255 \pm 17 \text{ M}^{-1}$ ($n=2$).

Figure 17. ^{31}P NMR spectrum of phospholipid extract from SH-SY5Y cell membranes. The lipids were dissolved in a solvent mixture containing chloroform/methanol/0.2 mM EDTA in the ratio 125:8:3. The assignments of each resonance are: PE phosphatidyl ethanolamine; PE_p PE plasmalogen; PS phosphatidyl serine; PI phosphatidyl inositol; PC phosphatidyl choline; X unknown. The chemical shifts are reported relative to that of PC, at -0.84 ppm. The relative amounts of each phospholipid expressed as a % of total membrane phospholipids are PE + PE_p 36%, PS 2.8%, PI 6.7%, PC 50.1% and X 4.5%.



CHAPTER V

DISCUSSION

V. 1. Interactions of native Cu,Zn-SOD with biologically relevant phosphates

The natural substrate of SOD is O_2^- , an anion (Fridovich, 1995). Anion binding studies of Cu,Zn-SOD have provided information on the mode of binding of O_2^- and anionic inhibitors such as CN^- , N_3^- and halides (Rigo et al., 1977). Larger anions such as phosphate and vanadate have also been shown to interact with SOD (Mota de Freitas and Valentine, 1984; Mota de Freitas et al., 1987; Wittenkeller et al., 1991). Hence, this study was carried out to determine whether adenosine phosphate metabolites which are generally present in the cell interact with Cu,Zn-SOD. ATP, ADP, AMP and 2,3-BPG are phosphate-containing metabolites present in all living cells under normal physiological conditions. The interactions of Cu, Zn-SOD with the adenosine phosphates, 2,3-BPG, triphosphate and diphosphate were followed by the differences in the ^{31}P NMR spin-lattice (T_1) relaxation times and line widths of the respective phosphate resonances in the absence and presence of native Cu,Zn-SOD (Table 2). Addition of native Cu,Zn-SOD to the individual phosphates did not significantly alter the chemical shifts of the phosphate resonances of the different phosphates studied. However, the line widths of the individual phosphate resonances increased while the corresponding T_1 values decreased in the presence of native Cu,Zn-SOD (Table 2). These changes in NMR parameters indicate that these biologically relevant phosphates interact with native Cu,Zn-SOD. The presence of inorganic phosphate in a solution containing Cu,Zn-SOD did not alter the visible or ESR

spectrum of native Cu,Zn-SOD (Mota de Freitas and Valentine, 1984). No changes were envisaged in the visible or ESR spectra of Cu,Zn-SOD in the presence of each of the phosphate anions examined in this study as these large phosphate anions were larger anions than inorganic phosphate and would not bind to the Cu(II) center as the smaller anions like N_3^- and CN^- .

In the presence of native Cu,Zn-SOD, the T_1 value of the γ phosphate of ATP decreased to a larger extent than those of the α and β resonances. Similarly, the T_1 value of the β phosphate of ADP decreased to a greater extent than the α phosphate in the presence of the native enzyme. The decrease in T_1 is due to the proximity of the phosphate group to the paramagnetic Cu(II) in the native protein. The above observations indicate that the terminal phosphates of ATP and ADP undergo greater paramagnetic relaxation than the phosphate groups present proximal to the adenosine moiety.

The P_2 and P_3 phosphate groups of 2,3-BPG both undergo paramagnetic relaxation in the presence of native Cu, Zn-SOD (Table 2), but the T_1 values are similar in the presence of native SOD. This may be due to the ability of both the phosphate groups to move closer to the paramagnetic center in the protein. 2,3-BPG does not have the large adenosine moiety present as in case of the adenosine phosphates and hence the phosphate groups on two adjacent C atoms might be able to move closer to the Cu(II) in the protein. However, as in the case of ATP and ADP, the phosphate on the C_3 of BPG undergoes greater paramagnetic relaxation when compared to that of the phosphate on the C_2 of BPG. In the case of AMP, there is a lower decrease in the T_1 values of the phosphate group in the presence of the native enzyme when compared to the decreases in T_1 values of the γ and β resonances of ATP and ADP respectively (Table 2). AMP has only one phosphate group attached to the adenosine moiety, the presence of which might sterically hinder the interactions of the lone phosphate group on

AMP.

The terminal phosphates of triphosphate are magnetically equivalent, and were observed to undergo greater paramagnetic relaxation than the central phosphate. For diphosphate, with two magnetically equivalent phosphates, only one phosphate resonance is observed, which undergoes paramagnetic relaxation in the presence of native Cu,Zn-SOD. The T_1 values of the phosphate resonances depend on the distance between the phosphate group and the Cu(II) center in the protein (Mota de Freitas et al., 1987). Hence the terminal phosphate groups of ATP, ADP and triphosphate undergo greater paramagnetic relaxation than the phosphate groups directly attached to the adenosine group. Similarly, the phosphate group on C_3 of 2,3-BPG undergoes greater paramagnetic relaxation than the phosphate group on C_2 as explained earlier.

The binding constants of the different polyphosphates to native Cu,Zn-SOD were determined (Table 9). Among the biologically relevant phosphates, ATP had a higher binding constant (575 M^{-1}), when compared to ADP (500 M^{-1}) and AMP (470 M^{-1}). ATP has a larger net negative charge than ADP and AMP, and hence there would be greater local interaction at the Lys residues, when compared to that of ADP or AMP. 2,3-BPG has a binding constant similar to ATP. This may be due to the relative configurations of the two phosphate groups of 2,3-BPG near the solvent channel of SOD such that strong interactions are possible with the enzyme. The COO^- group of BPG would be oriented away from the protein. Further, 2,3-BPG lacks the large adenosine moiety of ADP which may play a role in the interactions of ADP with SOD. The binding constant of P_i was calculated to be 59 M^{-1} . This binding constant value is slightly higher than the one reported for the same pH (Mota de Freitas et al., 1987) and may be due to the presence of EDTA in solution. The presence of an additional phosphate group in diphosphate led to much stronger interactions with a higher binding constant (770

M^{-1}). The adenosine group in ADP may sterically hinder the interactions of the two phosphate groups present on ADP, when compared to the structure of diphosphate.

To determine the site(s) at which the phosphates interact with the native Cu,Zn-SOD, functionally relevant amino acids with positively charged side chains namely Arg-141, Lys-120 and Lys-134 were chemically modified as previously described (Malinowski and Fridovich, 1979; Marmocchi et al., 1982). The Arg- and Lys-modified enzymes were first characterized by the activity assay (McCord and Fridovich, 1969). The SOD activities of the Arg- and Lys-modified protein derivatives were less than 15% of that of the native enzyme. It was previously shown by polyacrylamide gel electrophoresis that arginine- and lysine-modified proteins with 15% residual activity did not contain the native enzyme as a contaminant, and that the residual activity was inherent to the chemically modified protein (Marmocchi et al., 1982).

The ^{31}P NMR T_1 relaxation times of the different phosphates were obtained in the absence and in the presence of chemically modified Cu,Zn-SOD. The ^{31}P T_1 values of the phosphates in the presence of native SOD is determined by the paramagnetic Cu^{2+} present at the active site of the enzyme. This relaxation induced by the paramagnetic Cu^{2+} is distance dependent, and is proportional to $1/r^6$, where r is the distance between Cu^{2+} and the phosphate nucleus (Mota de Freitas et al., 1987). The ^{31}P T_1 values of the α , β and γ phosphate of ATP are similar in the absence and in the presence of Lys-modified SOD, indicating that the phosphate groups of ATP interact at the Lys-120 and Lys-134 residues. However, in the presence of the arginine-modified SOD, the T_1 value of the γ phosphate is lower than that obtained in the absence of the modified derivative (Table 10). Arg-141 is present 5 Å away from the Cu^{2+} center, while Lys-120 and Lys-134 are present 12 Å and 13 Å, respectively, from the Cu^{2+} (Tainer et al., 1982). Hence in the presence of Arg-modified SOD, the γ phosphate

of ATP is able to position itself closer to the paramagnetic Cu(II) center of SOD, resulting in lower T_1 values when compared to those obtained in presence of Lys-modified SOD. The ^{31}P T_1 values are hence shown to be affected by the proximity of the phosphate group to Cu^{2+} present in the protein. Further, the modification introduced at the Arg-141 residue, leads to lower interaction between ATP and the Arg-modified protein when compared to that between ATP and native SOD, as observed from the differences in the ^{31}P T_1 values of the γ phosphate resonance. Chemical modification of Arg-141 maintains the overall charge on the protein, while a decrease in anion affinities have been reported (Mota de Freitas and Valentine, 1984). Succinylation of lysine residues of native SOD leads to the formation of a protein derivative which is more negatively charged, with reduced anion affinities (Mota de Freitas et al., 1990b). Studies using mutant human Cu,Zn-SOD where Arg-143 was replaced with Ile-143 indicated that the specific activity of the mutant was drastically reduced when compared to the wild type (Beyer et al., 1987) and reduced anion binding to this mutant SOD (Bertini et al., 1991). The specific activity of the double mutant *Xenopus laevis* Cu,Zn-SOD where Lys-120 and Lys-134 were replaced by Leu and Thr was also reduced (Polticelli et al., 1995). Though reduced anion affinities of the chemically modified proteins may arise from chemical modification, these positively charged amino acid residues are essential for activity and binding of anions, as inferred from studies with mutant SODs. Along with the present studies, it can be deduced that ATP interacts at Arg-141, Lys-120 and Lys-134 residues of Cu,Zn-SOD.

Similar results with the terminal β -phosphate resonance of ADP was observed in the absence and presence of chemically modified protein (Table 10). 2,3-BPG also interacts through the P_2 and P_3 phosphate groups at the Arg-141, Lys-120 and Lys-134 residues as can be inferred from the T_1 values of the phosphate groups in the absence and presence of modified

proteins. From the NMR relaxation measurements of the synthetic polyphosphates triphosphate and diphosphate, these phosphates were also shown to interact with SOD at the Lys and Arg residues (Table 9). Inorganic phosphate was shown to interact with the SOD at the Arg-141 residues from activity studies, and affinity constants of N_3^- and CN^- to Arg-modified proteins were lower when compared to those obtained for native SOD (Mota de Freitas and Valentine, 1984). ATP, ADP and 2,3-BPG are larger anions when compared to inorganic phosphate, and hence these anions may span the distance between arginine and the lysines residues, interacting at the positively charged side chains of Arg-141, Lys-120 and Lys-134 residues present at the solvent channel of the native protein, 5 Å, 12 Å and 13 Å away from Cu^{2+} as obtained from X-ray crystallographic studies (Figure 2). Earlier studies using ^{51}V NMR (Wittenkeller et al., 1991) indicated that the vanadate tetramer interacts with Cu,Zn-SOD. Using chemically modified proteins, the vanadate tetramer was shown to bind to the positively charged side chains of Lys-120 and Lys-134. Along with the present study, it can be concluded that large anions interact with Cu,Zn-SOD primarily at Arg-141, Lys-120 and Lys-134 located along the solvent channel.

To determine whether the adenosine groups of ATP, ADP and AMP contribute to the interactions between these phosphates and native Cu,Zn-SOD, the ^{13}C NMR chemical shifts and line widths of the C atoms on the adenosine moiety were obtained in the absence and in the presence of native Cu,Zn-SOD. These experiments were conducted with a nucleotide concentration of 10 mM due to lower sensitivity of the NMR experiment (Tables 11 and 12). Higher concentrations of nucleotides were not used as it has been previously observed that the nucleotides undergo base stacking at higher concentrations (Scheller et al., 1981). No significant changes were observed in the ^{13}C NMR chemical shifts or in the line widths of the

^{13}C NMR resonances from the adenosine group (Tables 11 and 12). Hence, there may not be any specific interactions between the adenosine group in the adenine nucleotides and the native protein. Another possibility is that the adenosine group may interact via the N atoms present on the base ring. These large polyphosphates thus interact with native Cu,Zn-SOD through the phosphate groups.

V. 2. Biologically relevant phosphates and activity of native Cu,Zn-SOD

Inorganic phosphate was shown to inhibit the activity of native Cu,Zn-SOD, while the activity of chemically modified SODs was inhibited only to a small extent (Mota de Freitas and Valentine, 1984). The activity of the enzyme in the presence of the different polyphosphate compounds mentioned earlier was determined by the xanthine oxidase-cytochrome c assay (Table 13). The assays were conducted at constant ionic strength, which was adjusted with NaF or HEPES. This precaution was taken as the activity and anion binding of SOD was found to vary with ionic strength of the medium (McAdam et al., 1977; Cudd and Fridovich, 1982). P_i at 10 mM inhibited the activity of native Cu,Zn-SOD by 35% in the presence of NaF, 20 mM P_i decreased the activity by 44% in the presence of NaF. However, the SOD activity was decreased to a lower extent when HEPES was used to adjust the ionic strength of solutions. NaF was reported interfere with the xanthine oxidase reaction with xanthine (Beyer et al., 1986). A higher percentage of inhibition by P_i in the presence of NaF may be due to fluoride interference of O_2^- generation by xanthine oxidase (Beyer et al., 1986). The results obtained in the presence of NaF are similar to those obtained earlier (Mota de Freitas and Valentine, 1984). Hence, it is possible that P_i , at concentrations present in cells, are capable of inhibiting the activity of SOD.

ATP at 10 mM inhibited the activity of native SOD by 10% (Table 13). NaF was not used to adjust the ionic strength of ATP solutions. Hence the reduction in SOD activity by ATP can be attributed only to the presence of ATP. The phosphate chain of ATP may align itself in a manner at the solvent channel of the enzyme such that there is steric interference to the passage of the substrate O_2^- towards the base of the solvent channel of the enzyme where the catalytic Cu^{2+} center is present (Figure 1). Moreover, the negative charges on the phosphate chain may also play a role in repelling the negatively charged O_2^- ions. At $I=0.15$, the activity of native SOD was not affected in the presence of other phosphates (Table 13). The other adenosine phosphates have one or two phosphate groups whose size may not be suitably large enough to physically block the solvent channel of the protein. Inorganic phosphate is small enough to move into the solvent channel of the native SOD and neutralize the charge at the Arg-141 residue leading to a decrease in activity of the enzyme. The essential positively charged residues are responsible for guiding the substrate to the $Cu(II)$ present at the base of the solvent channel.

V. 3. Interactions of metal-depleted and reduced forms of Cu,Zn-SOD with vanadate

^{51}V NMR spectroscopy has been used to determine vanadate concentrations in aqueous solutions, and allows for simultaneous detection and quantification of the different vanadate species present in the solution (Crans and Simone, 1991; Wittenkeller et al., 1991). Apo Cu,Zn-SOD is a metal free derivative of the native Cu,Zn-SOD where both the Cu^{2+} and Zn^{2+} have been removed and the metal binding domains in the protein remain empty (E_2E_2 -SOD). This derivative was characterized first by AA to determine the metal content in the derivative and by the activity assay. The apo enzyme derivatives had $< 3\%$ Cu^{2+} , $< 4\%$ Zn^{2+} and an

activity of < 5% of the native enzyme. Line width changes of the different vanadate species namely the vanadate monomer (V_1), dimer (V_2) and tetramer (V_4) in the presence of apo Cu,Zn-SOD (Table 14 and Figure 5) indicate that the tetramer interacts most strongly with the enzyme derivative. In the presence of 0.03 mM - 0.20 mM apo Cu,Zn-SOD, the vanadate tetramer shows the largest line broadening (from 69 Hz to 181 Hz), while the monomer and dimer shows much smaller changes (66 Hz - 89 Hz for the monomer and 113 Hz - 152 Hz for the dimer). These trends are similar to those obtained for native Cu,Zn-SOD (Wittenkeller et al., 1991) but the extent to which the apo enzyme interacts is lower, based on the observed effects on line widths of V_4 . No significant changes were observed in the chemical shift values of the vanadate monomer, dimer and tetramer in the presence of the apo enzyme. The intensity of vanadate tetramer decreases with an increase in protein concentration. Earlier studies with native Cu,Zn-SOD (Wittenkeller et al., 1991) indicated that there were no significant changes in viscosity of the solution or in the T_1 values of the different vanadate species on addition of native Cu,Zn-SOD to a vanadate solution. Hence the observed changes in line widths are due to exchange kinetics between the vanadate species in solution and the protein derivative. The concentrations of V_1 , V_2 and V_4 were obtained by integration of the ^{51}V NMR spectra. The concentration of V_1 was obtained from the ^{51}V NMR spectra, while those of V_2 and V_4 were calculated as described in the Methods section. Calculated concentrations of V_2 and V_4 were smaller than the corresponding observed values. This is due to the presence of observable V-protein complexes in the ^{51}V NMR spectra (Wittenkeller et al., 1991).

The interactions of the zinc-only derivative of Cu,Zn-SOD with vanadate were also characterized by ^{51}V NMR spectroscopy. The zinc-only derivative of the native Cu,Zn-SOD is one wherein the Cu^{2+} is removed and the Cu^{2+} binding site is empty ($\text{E}_2\text{Zn}_2\text{-SOD}$). As in the

case of the apo derivative, the zinc-only derivative of Cu,Zn-SOD was first characterized by AA and was found to contain $< 3\%$ Cu^{2+} and $> 98\%$ Zn^{2+} . The residual activity was determined to be $< 5\%$ of the native enzyme. Cu^{2+} is required for the activity of Cu,Zn-SOD (Fridovich, 1995). On addition of increasing concentrations of this protein derivative to a vanadate solution, the chemical shift values of the V_1 , V_2 and V_4 did not show any significant change (Table 16). Similar results were observed with the apo enzyme form of Cu,Zn-SOD. Line widths of V_1 , V_2 and V_4 in the presence of increasing concentrations of the zinc-only derivative (Table 16) indicate that the line width of V_4 increases from 79 - 336 Hz in the presence of 0.20 mM protein derivative. This is in comparison to the increase seen in the case of V_4 in the presence of the apo derivative (69- 181 Hz). Smaller changes in the line widths of the V_1 and V_2 were observed in the presence of the zinc-only derivative. The intensities of the vanadate species decrease with increase in protein concentration, the decrease being higher in the case of V_4 . These changes are reflected in the concentrations of the vanadate species (Table 17). This observation along with the change in line widths of V_4 indicate that V_4 interacts more strongly with the zinc-only derivative than V_1 and V_2 . V_4 interacts more strongly with the zinc-only derivative than with the apo enzyme form because of higher net positive charge due to the presence of two Zn^{2+} ions per dimer in the zinc-only derivative. Further, the zinc-only derivative maintains the native structure of the enzyme, thus allowing the V_4 to interact at the positively charged amino groups of Lys-120 and Lys-134 residues that are present in the solvent channel of the protein.

During the catalytic cycle of the O_2^- dismutation reaction, Cu(II) present at the active site of Cu,Zn-SOD undergoes alternate reduction and reoxidation. The interactions of reduced Cu,Zn-SOD [where Cu is present as Cu(I)] with vanadate was also followed using ^{51}V NMR

spectroscopy. Reduced Cu,Zn-SOD was formed by the addition of NaBH₄ and the reaction was stopped by the addition of acetic acid (Viglino et al., 1985). Borate is the end-product of the reaction between NaBH₄ and acetic acid. ⁵¹V NMR control spectra were obtained wherein the solution contained 2 mM vanadate and 0.6 mM borate to ascertain whether there were any interactions between borate and vanadate anions. No significant changes in chemical shift values or in the areas of the different vanadate species were observed in the presence of borate when compared to solutions without borate. Hence borate does not interfere in the interactions of vanadate with Cu,Zn-SOD. With increasing concentrations of reduced Cu,Zn-SOD, the chemical shift values of the different vanadate species were similar to those obtained with a vanadate solution in the absence of any protein (Table 18). However, addition of reduced Cu,Zn-SOD to the vanadate solution yielded significant increases in line widths of the V₄ tetramer from 71 Hz to 491 Hz. The line width of V₁ increased from 69 Hz to 123 Hz, and that of V₂ increased from 121 Hz to 226 Hz (Table 18). The intensity of V₄ decreased to a much greater extent when compared to that of V₁ and V₂. The V₂ and V₄ resonances are not clearly resolved in the presence of 0.20 mM reduced SOD (Figure 6). The reduced Cu,Zn-SOD has 2 positive charges more than that in the zinc-only derivative. This would lead to an increase in the interactions between vanadate and the reduced protein when compared to that of the zinc-only derivative. Similar results were obtained for native Cu,Zn-SOD with increase in the line widths of V₄ (78 Hz to 475 Hz) when compared to the changes for V₁ (66 Hz to 149 Hz) and V₂ (108 Hz to 235 Hz) on addition of 0.2 mM native enzyme. Figure 7 shows the ⁵¹V NMR spectra of 2 mM vanadate solution in the absence and in the presence of different Cu,Zn-SOD derivatives or native protein at a concentration of 0.20 mM. It is observed that the ⁵¹V NMR spectra in the presence of native and reduced Cu,Zn-SOD are similar with large increases

in line widths of V_4 and a significant decrease in the intensities of the V_2 and V_4 . Smaller increases in line widths of the V_4 were observed for the apo and Zn-only derivative. V_4 appears to interact most strongly with the native protein and all protein derivatives, but the extent of interaction depends upon the protein derivative present. Reduced Cu,Zn-SOD, the zinc-only derivative and apo enzyme form of Cu,Zn-SOD are derivatives obtained by the progressive removal of two positive charges/metal ions respectively, from the native protein. The concentrations of the protein-vanadate complex depends on the protein derivative present in solution (Figure 8). Hence, there is a decrease in protein-vanadate interactions depending upon the overall charge present on the protein.

The effect of metal ions on the metal binding domain of SOD was examined by the addition of Zn^{2+} to an apo derivative of SOD (Lippard et al., 1977). The 1H spectra of reduced Cu,Zn-SOD was similar to that obtained for an apo protein to which one equivalent Zn^{2+} was added per subunit of protein. The presence of Zn^{2+} is thus responsible for much of the native structure of the protein. The apo protein does not possess an organized structure, as is present in the zinc-only, reduced and in native protein. This would lead to a decrease in interaction between the apo derivative and vanadate, as the arginine and lysines may not be present close to each other to provide a fixed electrostatic region for anion interaction.

As low vanadate concentrations are usually used to study protein-vanadate interactions, the major species involved would be V_1 . Oligomeric vanadate has also been shown to interact with proteins. The activity of glucose-6-phosphate dehydrogenase was observed to be inhibited by both V_2 and V_4 (Crans and Schelbe, 1990), while that of glycerol-3-phosphate dehydrogenase was inhibited by V_4 . The enzymes known to interact with vanadate are phosphate-dependent. SOD is not a phosphate-dependent enzyme, but has been shown to

interact strongly with vanadate (Wittenkeller et al., 1991). This study examined the influence of overall charge on a protein on protein-vanadate interactions.

V. 4. Characterization of microcarrier beads

Nuclear magnetic resonance (NMR) spectroscopy has emerged as an important non-invasive tool for observing both the structure and physiology of intact biological systems. NMR spectroscopy has been applied to determine different intracellular organic and inorganic compounds providing information on cell metabolism in live cells and in organs (Balaban, 1984). However, NMR is a relatively insensitive technique and requires cell metabolites to be present in relatively high concentrations to be detected. Also, NMR sensitivity depends on the nucleus being detected. Hence high cell densities are required to perform NMR experiments. Cells such as erythrocytes can be obtained at high cell densities, and can be maintained viable in a nutrient-containing suspension. RBCs have been used by us as a model cell system to understand the interactions of Li^+ in cells (Espanol and Mota de Freitas, 1987; Mota de Freitas et al., 1994b). Other cells such as mammalian liver cells and neuronal cells which have higher metabolic rates, cannot be maintained viable in suspension during the course of an NMR experiment. These cells have to be immobilized in the NMR tube and perfused continuously with fresh oxygenated medium. Different methods of cell immobilization have been used in the past such as anchoring the cells on microcarrier beads, entrapment in gel threads, hollow dialysis fiber and mesh support systems and the spheroid technique (Egan, 1987; Kaplan et al., 1992; Swergold, 1992).

In this study, neuroblastoma cells anchored on microcarrier beads were used to monitor Li^+ transport and binding properties. Initially, the cation and SR permeabilities of four different

commercially available microcarrier beads were characterized; Cytodex-1, CultiSpher-G, Biosilon and glass beads which were chosen to provide different size, matrix composition and charge distribution (Table 22).

Cytodex-1 and CultiSpher-G beads contain hydrophilic matrices (cross-linked dextran and gelatin polymer, respectively); the Biosilon matrix is made of hydrophobic polystyrene polymeric material. The placement of charged groups throughout the matrix also varies. Whereas the glass beads are uncharged, the Cytodex-1 matrix has an even distribution of dextran-modified DEAE positively charged groups throughout the matrix. The CultiSpher-G beads have an evenly distributed matrix of positive charges from arginyl and lysyl residues, whereas Biosilon beads have charged residues at the surface of the uncharged polystyrene matrix. These beads were suspended in different buffered solutions as indicated in the footnotes to Table 23. The presence of Cytodex-1 or CultiSpher-G beads in the buffered solution gave rise to two separate ${}^7\text{Li}$ or ${}^{23}\text{Na}$ resonances, whereas only one ${}^7\text{Li}$ or ${}^{23}\text{Na}$ resonance was observed in solutions containing Biosilon or glass beads in the presence and absence of SRs (Figure 9). Because the ${}^7\text{Li}$ shifts induced by $\text{Dy}(\text{TTHA})^{3-}$ are typically less than those for ${}^{23}\text{Na}$ (Ramasamy et al., 1989), it is not surprising that less resolution was observed in ${}^7\text{Li}$ than in ${}^{23}\text{Na}$ NMR spectra of suspensions of Cytodex-1 and CultiSpher-G containing $\text{Dy}(\text{TTHA})^{3-}$ (Table 20). The ${}^7\text{Li}$ and ${}^{23}\text{Na}$ isotropic shifts followed the order $\text{HTm}(\text{DOTP})^4 - \text{Dy}(\text{PPP})_2^{7-} > \text{Dy}(\text{TTHA})^{3-}$, in agreement with published data (Buster et al., 1990; Ramasamy et al., 1992). The pattern of chemical shift discrimination in ${}^7\text{Li}$ or ${}^{23}\text{Na}$ NMR spectra was similar in solutions containing one of the four different types of beads (Table 22), indicating that this phenomenon is independent of the type of SR used. When two separate resonances were observed, their assignment to the intrabead (i) and extrabead (o) space was

made by removal of the top half of the beads from the NMR tube and replacement with suspension medium as previously described (Shedd and Spicer, 1991). In the case of Cytodex-1, the most downfield shifted signal corresponds to the intrabead space, where the SRs are more concentrated than in the extrabead space. The opposite is true for CultiSpher-G, where the partitioning of the SRs favors the extrabead space, in a similar way to what was observed for Sephadex G50 (Shedd and Spicer, 1991).

Because discrimination of ^{133}Cs chemical shifts does not generally require SRs (Wittenkeller et al., 1992), the ^{133}Cs NMR spectra were obtained in solutions containing one of the four types of beads in the absence and presence of $\text{Dy}(\text{TTHA})^{3-}$. Cytodex-1 and CultiSpher-G beads gave separate ^{133}Cs NMR resonances in the absence and presence of SR, whereas Biosilon and glass beads yielded only one ^{133}Cs NMR resonance in the presence and absence of SR (Table 23, Figure 10), indicating that this phenomenon is general for alkali metal NMR resonances and occurs regardless of the presence of SRs in the medium.

In the presence of SRs in the medium, it has been shown (Shedd and Spicer, 1991) that anionic SRs are distributed between the intra- and extrabead spaces, yielding metal ion NMR spectra which depend on the charge and type of SR, and on the charge distribution, size exclusion (porosity), and shape of the bead matrix. ^7Li and ^{23}Na NMR measurements were conducted in suspensions of Cytodex-1 beads at three different concentrations of $\text{Dy}(\text{PPP})_2^{7-}$ (Table 24); an increase in SR concentration resulted in increased downfield shifts and broadening for both the intra- and extrabead resonances of Cytodex-1 suspensions. Therefore, the physical basis for the discrimination between the alkali metal NMR resonances in cell-free suspensions of Cytodex-1 and CultiSpher-G is in their cation and anion permeabilities, because ion-impermeable beads, such as Biosilon and glass, give only one alkali metal NMR resonance.

One of the NMR parameters shown in Table 23 is the peak line width, $\Delta\nu_{1/2}$. The broadening of the resonances in the presence of SRs is attributed to magnetic susceptibility field gradient effects (Brindle et al., 1979; Glasel and Lee, 1974) arising from the presence of SR in the heterogeneous bead suspensions, but not from its sequestration into the beads, because no significant differences in line widths are apparent between permeable and impermeable beads. Such pronounced line broadening was not observed in samples of SR solution alone (paramagnetic relaxation effects) or in samples of beads in salt solutions without SR.

Partially resolved ^{35}Cl NMR resonances were observed in suspensions of Cytodex-1 beads in the absence of either Co^{2+} or Mn^{2+} . When Co^{2+} or Mn^{2+} was, however, added to Cytodex-1 bead suspensions, only one ^{35}Cl NMR resonance was observed with Co^{2+} , but it became invisible in the presence of Mn^{2+} , indicating that Cl^- , Co^{2+} , and Mn^{2+} are permeable to Cytodex-1 beads (Figure 11). Because Cytodex-1 beads are permeable to large anionic species such as SRs (Shedd and Spicer, 1991) and alkali metal ions as described above, it is not surprising that this bead type is also permeable to small ions such Cl^- , Co^{2+} , and Mn^{2+} .

The relative permeabilities of Cytodex-1 and CultiSpher-G beads to cations and anions are presumably associated with the chemical composition of the materials used to manufacture these beads (Table 22). Although the densities of the microcarrier beads used in this study were similar, their diameters and thus the corresponding volumes excluded for cell growth varied greatly (Table 22). Biosilon beads, with their characteristically smaller sizes, will therefore yield the highest cell densities and the highest sensitivities for NMR studies of perfused cells. Based on considerations of ion permeability, magnetic susceptibility, size, matrix composition, and charge distribution, Biosilon beads were the microcarriers of choice for immobilization of cells used in ion transport NMR studies.

V. 5. Li⁺ transport and binding in cultured neuroblastoma cells

This study was initiated to apply multinuclear NMR spectroscopy to monitor the interactions of Li⁺ in nerve cells. The human neuroblastoma SH-SY5Y cells were used as the model cell system. SH-SY5Y cells are a clonal derivative of the SK-N-SH cell line and consists solely of the neuroblast phenotype (Biedler et al., 1973). These cells have been used in the past as a model system to investigate G protein function in the brain (Carter and Medzihradsky, 1993; Laugwitz et al., 1993), and to determine the effects of Li⁺ on the phosphatidylinositol turnover (Stubbs and Agranoff, 1993). Further, this cell line has been used to investigate the regulation of cations such as Ca²⁺ (McDonald et al., 1994), Be²⁺ (Faraci et al., 1993), and Rb⁺ (Spinedi et al., 1992), as well as for the study of alterations in membrane composition induced by lithium treatment (Liepkalns et al., 1993; 1994).

The effect of LiCl and shift reagents (SR) on the viability of SH-SY5Y cells were determined in pre-confluent monolayer cultures by the Trypan Blue dye exclusion method (Patterson, 1979). This is a routine test performed to determine cell viability based on the ability of an intact cell membrane to exclude certain dyes; the dye penetrates dead cells and renders them stained when compared to the live cells. The presence of 5 mM LiCl alone in the growth medium did not have any effect on the viability of these cells even after 5 hrs of exposure to LiCl, since control cultures have cell viabilities between 85-95% (Table 25). However, the presence of 5 mM LiCl along with either one of the SR studied led to small decreases in cell viability in 5 hrs. The presence of 10 mM Dy(TTHA)³⁻ along with 5 mM LiCl gave cell viabilities similar to those with LiCl alone. This may be due to the lower charge of -3 present on the SR. Though a small percentage of cell die, the overall morphology of these cells are maintained. However, in the presence of 5 mM Dy(PPP)₂⁷⁻ the characteristic

morphology of the cells is altered within an hour (Figure 12), and soon get detached from the base of the culture plate. Generally cell detachment is accompanied by cell death, though cell viability was maintained in this case at approximately 80% in the presence of LiCl and Dy(PPP)₂⁷⁻ (Table 25). The viability of these cells may be due to the short duration of time following detachment. Longer time periods may lead to cell death. The effects of SR on morphology and cell diameter of human RBCs in the absence of Li⁺ showed that 10 mM Dy(TTHA)³⁻ and 5 mM Dy(DOTP)⁵⁻ did not alter the morphology nor the size of the cells. However, higher concentrations of the SR produced shrunken RBCs with numerous cytoplasmic projections (Ramasamy et al., 1990). 5 mM HTm(DOTP)⁴⁺ or 10 mM Dy(TTHA)³⁻ in the presence of 5 mM LiCl did not alter the gross morphology of SH-SY5Y cells even after 5 hrs of exposure (Figure 12).

It was possible to differentiate between intra- and extracellular Li⁺ in suspensions of SH-SY5Y cells in a modified suspension medium containing 5 mM LiCl and 5 mM SR using ⁷Li NMR spectroscopy (Figure 13). Two different SRs that were used in this study were HTm(DOTP)⁴⁺ and Dy(PPP)₂⁷⁻. It was possible to follow Li⁺ transport into SH-SY5Y cells in suspensions with time (Table 26). The cells were allowed to settle prior to acquisition of the spectra. Figure 13 shows the ⁷Li NMR spectra of Li⁺ uptake into SH-SY5Y cell in suspension. Similar rate constants were obtained when either SR was used. The cell viability, however, decreased to below 70% after 45 min as determined by the Trypan blue dye exclusion method. This decrease in cell viability is also reflected in the collapse of the chemical shift separation between the intra- and extracellular ⁷Li NMR resonances with time (Figure 13). A decreased cell viability leads to a decrease in the intracellular ⁷Li NMR resonance. However, the intensity of the intracellular resonance increased with time, and as the cells were allowed to settle prior

to acquisition, this increase was not due to an increase in the number of cells in the NMR window, but due to increases in intracellular Li^+ concentrations. The large error obtained for rate constants may be partly attributed to the decrease in cell viability with time. The SR $\text{Dy}(\text{TTHA})^{3-}$ upto concentrations of 15 mM in the suspension medium failed to provide a chemical shift separation between the intra- and extracellular ^7Li resonances for cells in suspension. Hence $\text{Dy}(\text{TTHA})^{3-}$ was not used further.

In subsequent experiments, the cell viability during the course of the NMR experiment was maintained by immobilizing the cells on microcarrier beads, followed by continuous perfusion of the anchored cells. The microcarrier beads perform two functions: (a) the beads provide a substratum on which the cells could be anchored upon, and (b) the beads prevent the cells from being washed away during the course of perfusion. Photoelectron micrographs of SH-SY5Y cells anchored on Biosilon beads were obtained (Figure 14). The cells anchored on Biosilon beads appear to be morphologically similar to those on monolayer cultures (Figure 12).

Li^+ transport into SH-SY5Y cells anchored on Biosilon beads and perfused with a modified culture medium was monitored by ^7Li NMR spectroscopy. The perfusate contained 15 mM LiCl and 3 mM $\text{HTm}(\text{DOTP})^4$. A lower concentration of the SR was sufficient to observe two well differentiated ^7Li NMR resonances corresponding to the intra- and extracellular Li^+ pools (Table 27A, B; Figure 15). SR concentrations of 5 mM were required to provide two well defined ^7Li NMR resonances for SH-SY5Y cell suspensions (Table 26, Figure 13). A higher concentration of SR may be required for cells in suspension as these cells may adhere to each other in suspension, with the absence of a uniform concentration of SR around the cells. Further, lower concentrations of SR removes any effect the SR may have on the transport of Li^+ . The presence of 7 mM $\text{Dy}(\text{PPP})_2^{7-}$ as the SR in ^7Li NMR transport studies

of human RBCs was shown to increase the rate of Na^+ - Li^+ exchange rates when compared to 7 mM $\text{Dy}(\text{TTHA})_3^{3-}$ as the SR (Mota de Freitas et al., 1990a). In a recent report of Li^+ transport in human 1321 N1 astrocytomas anchored on Biosilon beads using ^7Li NMR spectroscopy, 5 mM $\text{Dy}(\text{PPP})_2^{7-}$ was used (Bramham et al., 1996). The rates of Li^+ influx reported in SH-SY5Y cells are the sum total of the Li^+ flux into the cells. The actual pathway(s) through which Li^+ influx occurs in this cell line have not been characterized in detail. The different pathways through which Li^+ is transported into these cells can be characterized by using ion channel inhibitors and activators to determine their effects on Li^+ transport. Earlier studies using the mouse neuroblastoma cell line N1E-115 showed that Li^+ uptake was mediated by the Na^+ channels (Richelson, 1977). Other studies using a mixed population of chick glial and neuronal cells indicated the involvement of a Na^+ -dependent Li^+ uptake (Szentistvanyi et al., 1979b) or of Na^+ - Li^+ exchange and the sodium pump in rat neuroblastoma x glioma cells (Reiser and Duhm, 1982). These pathways may also mediate Li^+ transport in SH-SY5Y cells.

One needs to administer 200-1600 mg of Li_2CO_3 to patients for periods up to 2 weeks to achieve therapeutic levels of Li^+ in serum (Jefferson et al., 1985). The rate of Li^+ transport in biological tissues may be enhanced by the use of ^6Li , the lighter isotope, or by Li^+ ionophores (Abraha et al., 1991b; Espanol and Mota de Freitas, 1987; Abraha and Mota de Freitas, 1992). In the presence of the ionophore DB14C4, Li^+ transport into SH-SY5Y cells was followed (Figure 15) and the rate constant for Li^+ influx in these cells increased by a factor of 2 (Table 27, A). This ionophore was shown to enhance Li^+ uptake in human RBCs and in phosphatidylcholine membrane vesicles even in the presence of physiologically relevant concentrations of Na^+ ions (Abraha and Mota de Freitas, 1992). A similar trend was observed

for SH-SY5Y cells as the modified culture medium used to perfuse the cells contained more than 150 mM Na⁺. Hence this ionophore could be used to increase the rate of Li⁺ influx into neuronal tissue (Table 27). Li⁺ efflux from Li⁺-loaded SH-SY5Y cells anchored on Biosilon beads was also monitored by ⁷Li NMR spectroscopy. The pathways mediating both Li⁺ influx and efflux have not been identified, but need to be characterized. To compare the rates of Li⁺ transport in neuroblastoma cells with that in human RBCs, the rates of Li⁺ transport have to be determined in units similar to those for RBCs. This requires the determination of cell volume.

The viability of SH-SY5Y cells was confirmed by following the ³¹P NMR spectra every 70 mins during the course of perfusion. A typical ³¹P NMR spectrum of SH-SY5Y cells anchored on Biosilon beads is shown in Figure 16. The different ³¹P resonances were assigned to the respective metabolites by comparison of their chemical shifts to the ones reported in literature for other cell perfused systems (Gillies et al., 1986) and by spiking the spectrum with known phosphorus compounds. The ratio of phosphocreatine to β-ATP was found to decrease with time. The levels of phosphocreatine were maintained while there were small increases in the levels of ATP. This indicated that the cells were provided with sufficient oxygen to maintain these metabolite levels. Perfusion of cells with oxygenated medium thus maintains cell viability. Human 1321 N1 astrocytoma cells anchored on Biosilon beads were claimed to maintain viability by periodical shaking of the NMR tube (Bramham et al, 1996). The perfusion method is obviously a more effective method to maintain cell viability.

⁷Li NMR spectroscopy has been previously used to monitor Li⁺ interactions in human RBCs and in RBC ghosts (Rong et al., 1993; Mota de Freitas et al., 1991). The T₁/T₂ (R) ratio of Li⁺ inside the RBCs is 20-30, while in SH-SY5Y cells the R ratio is greater than 100 for both cells in suspension and anchored to microcarrier beads (Table 28). ⁷Li T₁ and T₂ values

are similar in free solutions ($R \approx 1$), and it is known from NMR relaxation theory that slow tumbling contribute only toward T_2 , whereas components of motion at the resonance frequency contribute to both T_1 and T_2 (Gadian, 1982). When Li^+ ions are subject to electric field gradients or are immobilized on any substrate, the Li^+ T_1/T_2 ratio increases. The large difference in Li^+ T_1 and T_2 values have been used to probe Li^+ binding in biological samples. The larger T_1/T_2 ratio in case of SH-SY5Y cells is hence indicative of tighter binding of Li^+ in the neuroblastoma cells.

Previous studies on Li^+ interactions in human RBCs show that the RBC membranes is one of the primary binding sites for Li^+ (Rong et al, 1993). The Li^+ T_1/T_2 ratios obtained for SH-SY5Y cells (greater than 100) was larger than that observed for RBCs (Rong et al., 1993). Since the Li^+ T_1/T_2 ratio in intact SH-SY5Y cells was larger than in RBCs, we postulated that Li^+ would interact more strongly in the neuronal cells. Li^+ was shown to interact with the membrane bilayer of human RBCs (Rong et al., 1993; Mota de Freitas et al., 1994). Hence Li^+ binding to purified neuroblastoma cell membranes were studied. The Li^+ binding constant to neuroblastoma cells was calculated to be $255 \pm 17 \text{ M}^{-1}$ ($n=2$), which is comparable to the values obtained for human RBC membranes.

Phospholipids present in SH-SY5Y cell membranes were analyzed using ^{31}P NMR spectroscopy. This method has been used to determine the phospholipid composition in mammalian optic nerve (Greiner et al., 1994), in brain tissue (Edzes et al., 1992), and in erythrocytes (Mota de Freitas et al., 1994a). Phospholipid analysis of SH-SY5Y cells show that phosphatidyl choline (PC) and phosphatidyl ethanolamine (PE) form about 90% of the total membrane phospholipids (Figure 17). However, sphingomyelin (Sph) was not detected in SH-SY5Y cell membranes using ^{31}P NMR. In this regard, the lipid profile of SH-SY5Y cell

membrane is comparable to that of SK-N-SH cells, the parent cell line of SH-SY5Y cells (Stubbs et al., 1992). Further, these are consistent with the observations of Greiner et al. (1994) where the percentage of PC and PE in the retina, brain gray and white matter was greater than 80% of the total phospholipids. Phospholipids in the RBC membranes are asymmetrically distributed, with the inner leaflet containing approximately 10-20% PC, 40-50% PE, 10% Sph, 20-30% phosphatidyl serine (PS) and 1.4% phosphatidyl inositol (PI). The outer leaflet of the RBC membrane contains 40-50% each of PC and Sph, and 10-15% PE (Cullis and Hope, 1985; Schwartz et al., 1984). It has been shown previously that Li^+ binds to the inner leaflet of the RBC membranes (Rong et al.1993), specifically at the anionic phospholipids. As the phospholipid profile of SH-SY5Y cell membranes indicate a much lower percentage of anionic phospholipids when compared to human RBC membranes (about 6% of total phospholipids in SH-SY5Y cell membranes and about 15% of total phospholipids in human RBC membranes), Li^+ interactions with SH-SY5Y cell membranes may not be much higher than that observed in case of RBC membranes, as indicated by the Li^+ binding constant to SH-SY5Y cell membranes (Table 29). The higher Li^+ T_1/T_2 ratios in neuroblastoma cells may be due to Li^+ binding to sub-cellular organelles in addition to cell membranes.

Hence multinuclear NMR spectroscopy along with perfusion techniques have been applied to follow Li^+ interactions in more complex systems such as nerve cells. As cells have to be maintained viable during the experiment, they were anchored on non-permeable microcarrier beads to enable the cells to be perfused. ^7Li NMR relaxation measurements indicate that Li^+ interacts more strongly with SH-SY5Y cells when compared to RBCs.

BIBLIOGRAPHY

- Abraha, A., Mota de Freitas, D., Castro, M.M.C.A., Geraldés, C.F.G.C. Competition between Li^+ and Mg^{2+} for ATP and ADP in aqueous solution: a multinuclear NMR study. J. Inorg. Biochem., 1991a; 42: 191-198.
- Abraha, A., Dorus, E., Mota de Freitas, D. Nuclear magnetic resonance study of differences between ^6Li and ^7Li ions in transport across human red blood cell membranes. Lithium, 1991b; 2: 118-121.
- Abraha, A., Mota de Freitas, D. Ionophore-induced Li^+ transport across human erythrocyte membranes in the presence of a background of Na^+ ions. Lithium, 1992; 3: 203-211.
- Avissar, S., Murphy, D.L., Schreiber, G. Magnesium reversal of lithium inhibition of β -adrenergic and muscarinic receptor coupling to G proteins. Biochem. Pharmacol., 1991; 41: 171-175.
- Avissar, S., Schreiber, G., Danon, A., Belmaker, R.H. Lithium inhibits adrenergic and cholinergic increases in GTP binding in rat cortex. Nature, 1988; 331: 440-442.
- Balaban, R.S. The application of nuclear magnetic resonance to the study of cellular physiology. A. J. Physiol., 1984; 246: C10-C19.
- Banci, L., Bencini, A., Bertini, I., Luchinat, C., Piccioli, M. ^1H NOE and ligand field studies of copper-cobalt superoxide dismutase with anions. Inorg. Chem., 1990; 29: 4867-4873.
- Banci, L., Bertini, I., Bruni, B., Carloni, P., Luchinat, C., Mangani, S., Orioli, P.L., Piccioli, M., Ripniewski, W., Wilson, K.S. X-ray, NMR and molecular dynamics studies on reduced bovine superoxide dismutase: implications for the mechanisms. Biochem. Biophys. Res. Commun., 1994; 202: 1088-1095.
- Banci, L., Bertini, I., Luchinat, C., Scozzafava, A. Nuclear relaxation in the magnetic coupled system $\text{Cu}_2\text{Co}_2\text{SOD}$. Histidine-44 is detached upon anion binding. J. Am. Chem. Soc., 1987; 109: 2328-2334.
- Banci, L., Bertini, I., Luchinat, C., Scozzafava, A. Cyanide and azide behave in a similar fashion versus cuprozinc-superoxide dismutase. J. Biol. Chem., 1989; 264: 9742-9744.
- Belmaker, R.H. Receptors, adenylate cyclase, depression, and lithium. Biol. Psychiatry, 1981; 16: 333-350.

- Berridge, M.J. Inositol trisphosphate and diacylglycerol: Two interacting second messengers. Ann. Rev. Biochem., 1987; 56: 159-193.
- Bertini, I., Lanini, G., Luchinat, C., Messori, L., Monnanni, R., Scozzafava, A. Investigation of $\text{Cu}_2\text{Co}_2\text{SOD}$ and its anion derivatives. ^1H NMR and electronic spectra. J. Am. Chem. Soc., 1985; 107: 4391-4396.
- Bertini, I., Lepori, A., Luchinat, C., Turano, P. Role of Arg-143 in human $\text{Cu}_2\text{Zn}_2\text{SOD}$ studied through anion binding. Inorg. Chem., 1991; 30: 3363-3364.
- Beyer, W.F., Fridovich, I., Mullenbach, G.T., Hallewell, R. Examination of the role of arginine-143 in the human copper and zinc superoxide dismutase by site-specific mutagenesis. J. Biol. Chem., 1987; 262: 11182-11187.
- Beyer, W.F., Jr., Wang, Y., Fridovich, I. Phosphate inhibition of the copper- and zinc-containing superoxide dismutase: A reexamination. Biochemistry, 1986; 25: 6084-6088.
- Biedler, J.L., Helson, L., Spengler, B.A. Morphology and growth, tumorigenicity, and cytogenetics of human neuroblastoma cells in continuous culture. Cancer Res., 1973; 33: 2643-2652.
- Blackburn, N.J., Strange, R.W., McFadden, L.M., Hasnain, S.S. Anion binding to bovine erythrocyte superoxide dismutase studied by x-ray absorption spectroscopy. A detailed structural analysis of the native enzyme and the azido and cyano derivatives using a multiple scattering approach. J. Am. Chem. Soc., 1987; 109: 7162-7170.
- Boyd, D.W., Kustin, K., Niwa, M. Do vanadate polyanions inhibit phosphotransferase enzymes? Biochim. Biophys. Acta, 1985; 827, 472-475.
- Bramham, J., Carter, A.N., Riddell, F.G. The uptake of Li^+ into human 1321 N1 astrocytomas using ^7Li NMR spectroscopy. J. Inorg. Biochem., 1996; 61: 273-284.
- Brindle, K.M., Brown, F.F., Campbell, I.D., Grathwohl, C., Kuchel, P.W. Application of spin-echo nuclear magnetic resonance to whole-cell systems. Biochem. J., 1979; 180: 37-44.
- Buster, D.C., Castro, M.M.C.A., Geraldès, C.F.G.C., Malloy, C.R., Sherry, A.D., Siemers, T.C. $\text{Tm}(\text{DOTP})^5$: A new $^{23}\text{Na}^+$ shift reagent for perfused rat hearts. Magn. Reson. Med., 1990; 15: 25-32.
- Cabantik, Z.I., Rothstein, A. Membrane proteins related to anion permeability of human red cell. I. Localization of disulfonic stilbene binding sites in proteins involved in permeation. J. Membr. Biol., 1974; 15: 207-226.
- Cade, J.F.J. Lithium salts in the treatment of psychotic excitement. Med. J. Aust., 1949; 36: 349-352.

- Canessa, M., Bize, I., Adragna, N. Cotransport of lithium and potassium in human red cells. J. Gen. Physiol., 1982; 80: 149-168.
- Carter, B.D., Mezhiradsky, F. G_o mediates the coupling of the μ opioid receptor to adenylyl cyclase in cloned neural cells and brain. Proc. Natl. Acad. Sci. USA, 1993; 90: 4062-4066.
- Carugo, K.D., Battisoni, A., Carri, M.T., Polticelli, F., Desideri, A., Rotilio, G., Coda, A., Bolognesi, M. Crystal structure of the cyanide-inhibited *Xenopus laevis* Cu,Zn superoxide dismutase at 98 K. FEBS Lett., 1994a; 349: 93-98.
- Carugo, K.D., Polticelli, F., Desideri, A., Rotilio, G., Wilson, K.S., Bolognesi, M. Crystallographic study of azide-inhibited bovine Cu,Zn superoxide dismutase. J. Mol. Biol., 1994b; 240: 179-183.
- Cass, A.E.G., Hill, H.A.O., Hasemann, V., Johansen, J.T. Proton nuclear magnetic resonance spectroscopy of yeast copper, zinc superoxide dismutase. Structural homology with the bovine enzyme. Carlsberg Res. Commun., 1978; 43: 439-449.
- Chasteen, N.D. The biochemistry of vanadium. Struct. Bond., 1983; 53: 105-138.
- Costa, E.M., Hoffman, B.B., Loew, G.H. Opioid agonists binding and responses in SH-SY5Y cells. Life Sciences, 1991; 50: 73-81.
- Crans, D.C., Willging, E.M., Butler, S.R. Vanadate tetramer as the inhibiting species in enzyme reactions in vivo and in vivo. J. Am. Chem. Soc., 1990; 112: 427-432.
- Crans, D.C., Simone, C.M. Non-reductive interaction of vanadate with an enzyme containing a thiol group in the active site: glycerol-3-phosphate dehydrogenase. Biochemistry, 1991; 30: 6734-6741.
- Crans, D.C., Schelble, S.M. Vanadate dimer and tetramer both inhibit glucose-6-phosphate dehydrogenase from *Leuconostoc mesenteroides*. Biochemistry, 1990; 29: 6698-6706.
- Crans, D.C., Shin, P.K. Spontaneous and reversible interaction of vanadium (V) oxyanions with amine derivatives. Inorg. Chem., 1988; 27: 1797-1806.
- Cremona, C.R., Long, G.T., Grammer, J.C. Photocleavage of myosin subfragment 1 by vanadate. Biochemistry, 1990; 29: 7982-7990.
- Csermely, P., Martonosi, A., Levy, G.C., Ejchart, A.J. ^{51}V NMR analysis of the binding of vanadium (V) oligoanions to sarcoplasmic reticulum. Biochem. J., 1985; 230: 807-815.
- Cudd, A., Fridovich, I. Electrostatic interactions in the reaction mechanism of bovine erythrocyte bovine superoxide dismutase. J. Biol. Chem., 1982; 257: 11443-11447.

- Cullis, P.R., Hope, M.J. Physical properties and functional roles of lipids in membranes. In "Biochemistry of Lipids and Membranes", Vance, D.E. and Vance, J.E., (eds.). Benjamin/Cummings, Menlo Park. 1985; pp 25-72.
- DeKoch, R.J., West, D.J., Cannon, J.C., Chasteen, N.D. Kinetics and electron paramagnetic resonance spectra of vanadyl (IV) carboxypeptidase A. Biochemistry, 1974; 13: 4347-4354.
- Desideri, A., Paci, M., Rotilio, G. ^1H and ^{31}P NMR studies of the Binding of low-affinity anions to Cu,Zn superoxide dismutase. J. Inorg. Biochem., 1988; 33: 91-97.
- Djinović, K., Coda, A., Antolini, L., Pelosi, G., Desideri, A., Falconi, M., Rotilio, G., Bolognesi, M. Crystal structure solution and refinement of the semisynthetic cobalt-substituted bovine erythrocyte superoxide dismutase at 2 Å resolution. J. Mol. Biol., 1992; 226: 227-238.
- Duhm, J., Eisenried, F., Backer, B.F. Studies of lithium transport across the red blood cell membrane. I. Lithium uphill transport by the Na^+ dependent Li^+ countertransport system of human erythrocytes. Pflugers Arch., 1976; 364: 147-155.
- Duhm, J.: Lithium transport pathways in erythrocytes; In Emich, H.M., Aldenhoff, J.B., Lux, H.D. (eds.): Basic Mechanisms in the Action of Lithium. Amsterdam, Excerpta Medica, 1981, pp 1-20.
- Easwaran, K.R.K. Interaction between valinomycin and metal ions. In H. Sigel (ed.) Metal Ions in Biological Systems: Antibiotics and their Complexes. New York: Marcel Dekker, Inc., 1985, pp 109-137.
- Edzes, H.T., Teerlink, T., Van der Knapp, M.S., Valk, J. Analysis of phospholipids in brain tissue by ^{31}P NMR at different compositions of the solvent system chloroform-methanol-water. Magn. Res. Med., 1992; 26: 46-59.
- Egan, W.M. The use of perfusion systems for nuclear magnetic resonance studies of cells. In NMR Spectroscopy of Cells and Organisms, edited by R.K. Gupta. Boca Raton: CRC Press, 1987, vol. II, p. 135-161.
- Ehrlich, B.E., Diamond, J.M. Lithium fluxes in human erythrocytes. Am. J. Physiol., 1979; 237: C102-C110.
- Espanol, M.C., Mota de Freitas, D. ^7Li NMR studies of lithium transport in human erythrocytes. Inorg. Chem., 1987; 26: 4356-4359.
- Faraci, W.S., Zorn, S.H., Bakker, A.V., Jackson, E., Pratt, K. Beryllium competitively inhibits brain myo-inositol monophosphatase, but unlike lithium does not enhance agonist-induced inositol phosphate accumulation. Biochem. J., 1993; 291: 369-374.

- Fee, J.A., Gaber, B.P. Anion binding to bovine erythrocyte superoxide dismutase: Evidence for multiple binding sites with qualitatively different properties. J. Biol. Chem., 1972; 247: 60-65.
- Fee, J.A., Ward, R.L. Evidence for a coordination position available to solute molecules on one of the metals at the active center of reduced bovine superoxide dismutase. Biochem. Biophys. Res. Commun., 1976; 71: 427-437.
- Fitzgerald, J.J., Chasteen, N.D. Electron paramagnetic resonance studies of the structure and metal ion exchange kinetics of vanadyl (IV) bovine carbonic anhydrase. Biochemistry, 1974; 13: 4338-4347.
- Frausto da Silva, J.J.R., Williams, R.J.P. Possible mechanism for the biological action of lithium. Nature, 1976; 263: 237-239.
- Fridovich, I. Superoxide dismutases. Adv. Enzymol., 1986; 58: 61-97.
- Fridovich, I. Superoxide radical and superoxide dismutases. Annu. Rev. Biochem., 1995; 64: 97-112.
- Gadian D.G.: NMR and its applications to living systems. Clarendon Press, Oxford, 1982, pp. 23-41.
- Geisler, A., Mørk, A.: The interaction of lithium with magnesium-dependent enzymes. In R.O. Bach and V.S. Gallichio (eds.) Lithium and Cell Physiology. New York: Springer-Verlag, 1990, pp 125-136.
- George, G.N., Coyle, C.L., Hales, B.J., Cramer, S.P. X ray absorption of *Azotobacter vinelandii* vanadium nitrogenase. J. Am. Chem. Soc., 1988; 110: 4057-4059.
- Getzoff, E.D., Cabelli, D.E., Fisher, C.L., Parge, D.E., Viezzoli, M.S., Banci, L., Hallewell, R.A. Faster superoxide dismutase mutants designed by enhancing electrostatic guidance. Nature, 1992; 358: 347-351.
- Gillies, R.J., Chresand, T.J., Drury, D.D., Dale, B.E. Design and application of bioreactors for analysis of mammalian cells by NMR. Rev. Magn. Reson. Med., 1986; 1: 155-179.
- Gilman, A.G. G proteins: Transducers of receptor-generated signals. Ann. Rev. Biochem., 1987; 56: 615-649.
- Glasel, J.A., Lee, K.H. On the interpretation of water nuclear magnetic resonance relaxation times in heterogeneous systems. J. Am. Chem. Soc., 1974; 96: 970-978.
- Goodno, C. Inhibition of myosin ATPase by vanadate ion. Proc. Natl. Acad. Sci. USA, 1979; 76: 2620-2624.

- Greiner, C.A.M., Greiner, J.V., Hebert, E., Berthiaume, R.R., Glonek, T. Phospholipid analysis of mammalian optic nerve tissue: A ^{31}P nuclear magnetic resonance spectroscopic study. Ophthalmic Res., 1994; 26: 264-274.
- Hallcher, L.M., Sherman, W.R. The effects of lithium ion and other agents on the activity of myo-inositol-1-phosphatase from bovine brain. J. Biol. Chem., 1980; 255: 10896-10901.
- Hallewell, R.A., Imlay, K.C., Lee, P., Fong, N.M., Gallegos, C., Getzoff, E.D., Tainer, J.A., Cabelli, D.E., Tekamp-Olson, P., Mullenbach, G.T., Cousens, L.S. Thermostabilization of recombinant human and bovine CuZn superoxide dismutases by replacement of free cysteines. Biochem. Biophys. Res. Commun., 1991; 181: 474-480.
- Hepler, J.R., Gilman, A.G. G proteins. Trends Biochem. Sci., 1992; 17: 383-387.
- Hill, R.L., Steinman, H.M., Abernethy, J.L. Bovine erythrocyte superoxide dismutase subunit structure and sequence location of the intrasubunit disulfide bond. J. Biol. Chem., 1974; 249: 7339- 7347.
- Hinton, J.F., Koepe II, R.E. Complexing properties of gramicidins. In H. Sigel (ed.) *Metal Ions in Biological Systems: Antibiotics and their Complexes*. New York: Marcel Dekker, Inc., 1985, pp 173-206.
- Hoppe, G., Siemroth, J., Damaschun. Alexander von Humboldt and the discovery of vanadium. Chem. Erde, 1990; 50: 81-94.
- Jabusch, J.R., Farb, D.L., Kerschensteiner, D.A., Deutsch, H.F. Some sulfhydryl properties and primary structure of human erythrocyte superoxide dismutase. Biochemistry, 1980; 19: 2310-2316.
- James, T.L., Noggle, J.H. Na nuclear magnetic resonance relaxation studies of sodium ion interaction with soluble RNA. Proc. Natl. Acad. Sci., 1969; 62: 644-649.
- Jefferson, J.W., Greist, J.H., Baudhuin, M.: Lithium in Psychiatry. In R.O. Bach (ed.) *Lithium: Current applications in Science, Medicine, and Technology*. New York: Wiley, 1985, pp 345-352.
- Johansen, J.T., Overballe-Peterson, C., Martin, B., Hasemann, V., Svendsen, I. Complete amino acid sequence of copper zinc superoxide dismutase from *Saccharomyces cerevisiae*. Carlsberg Res. Commun., 1979; 44: 201-217.
- Jones, A.J., Winkley, M.W., Grant, D.M., Robins, R.K. Carbon-13 nuclear magnetic resonance: Naturally occurring nucleosides. Proc. Natl. Acad. Sci. USA, 1970; 65: 27-30.
- Josephson, L., Cantley, Jr., L.C. Isolation of a potent (Na-K)ATPase inhibitor from striated muscle. Biochemistry, 1977; 16: 4572-4578.

- Kaplan, O., Van Zijl, P.C.M., Cohen, J.S. NMR studies of metabolism of cells and perfused organs. In P. Diehl, E. Fluck, H. Gunther, R. Kosfeld, J. Seelig. (eds.) *NMR: Basic Principles and and Progress*, 28: 3-52, 1992.
- Karnovsky, M.J. A formaldehyde-glutaraldehyde fixative of high osmolarity for use in electron microscopy. *J. Cell Biol.*, 1965; 27: 137A.
- Kimura, K., Tanaka, M., Kitazawa, S., Shono, T. Highly selective crown ether dyes for extraction photometry. *Chem Lett.*, 1985; 8: 1239-1240.
- Kimura, K., Yano, H., Kitazawa, S., Shono, T. Synthesis and selectivity for lithium of lipophilic 14-crown-4 derivatives bearing bulky substituents or an additional binding site in the side arm. *J. Chem. Soc. Perkin Trans II*, 1986; 1945-1951.
- Kusthardt, U., Hedman, B., Hodgson, K.O., Hahn, R., Vilter, H. High resolution XANES studies on vanadium containing haloperoxidase: pH-dependence and substrate binding. *FEBS Lett.*, 1993; 329: 5-8.
- Laugwitz, K.L., Offermans, S., Spicher, K., Schultz, G. μ and δ opioid receptors differentially couple to G protein subtypes in membranes of human neuroblastoma SH-SY 5Y cells. *Neuron*, 1993; 10: 233-242.
- Lennox, R.H., Watson, D.G. Lithium and the brain: A psychopharmacological strategy to a molecular basis for manic-depressive illness. *Clin. Chem.*, 1994; 40: 309-314.
- Lepock, J.R., Frey, H.E., Hallewell, D.A. Contribution of conformational stability and reversibility of unfolding to the increased thermostability of human and bovine superoxide dismutase mutated at free cysteines. *J. Biol. Chem.*, 1990; 265: 21612-21618.
- Liepkalns, V.A., Leli, U., Hauser, G. Alterations in the metabolism of choline-containing phospholipids by lithium and carbachol in SH-SY5Y neuroblastoma cells. *Biol. Psychiatry*, 1993; 34: 51-58.
- Liepkalns, V.A., Myher, J.J., Kuklis, A., Leli, U., Freysz, N., Hauser, G. Complementary chromatographic analysis of free diacylglycerols and potential glycerophospholipid precursors in human SH-SY5Y neuroblastoma cells following incubation with lithium chloride. *J. Chromatogr B.*, 1994; 658: 223-232.
- Liochev, S.I., Fridovich, I. Vanadate-stimulated oxidation of NAD(P)H in the presence of biological membranes and other sources of O_2^- . *Arch. Biochem. Biophys.*, 1990; 279: 1-7.
- Lippard, S.J., Burger, A.R., Ugurbil, K., Pantoliano, M.W., Valentine J.S. Nuclear magnetic resonance and chemical modification studies of bovine erythrocyte superoxide dismutase: Evidence for zinc-promoted organisation of the active site structure. *Biochemistry*, 1977; 16: 1136-1141.

- Lowry, O.H., Rosebrough, N.J., Farr, A.L., Randall, R. Protein measurement with the folin phenol reagent. J. Biol. Chem., 1951; 193: 265-275.
- Malinowski, D.P., Fridovich, I. Chemical modification of arginine at the active site of the bovine erythrocyte superoxide dismutase. Biochemistry, 1979; 18: 5909-5917.
- Mann, T., Klein, D. Hemocuprein, a Cu-protein compound of red blood corpuscles. Proc. Roy. Soc. (London), Series B, 1938; 126: 303-315.
- Marmochi, F., Mavelli, I., Rigo, A., Stevanato, R., Bossa, F., Rotilio G. Succinylated copper-zinc superoxide dismutase. A novel approach to the problem of active subunits. Biochemistry, 1982; 21: 2853-2856.
- McAdam, M., Fielden, E.M., Lavelle, F., Calabrese, L., Cocco, D., Rotilio G. The involvement of the bridging imidazolate in the catalytic mechanism of action of bovine superoxide dismutase. Biochem. J., 1977; 167: 271-274.
- McCord, J.M., Fridovich, I. Superoxide dismutase. An enzymic function for erythrocuprein. J. Biol. Chem., 1969; 244: 6049-6055.
- McCord, J.M., Keele Jr., B.B., Fridovich, I. An enzyme-based theory of obligate anaerobiosis: the physiological function of superoxide dismutase. Proc. Natl. Acad. Sci. USA, 1971; 68: 1024-1027.
- McDonald, R.L., Vaughn, P.F.T., Peers, C. Muscarinic (M_1) receptor-mediated inhibition of K^+ -evoked [3H]-noradrenaline release from human neuroblastoma (SH-SY5Y) cells via inhibition of L- and N-type Ca^{2+} channels. Br. J. Pharmacol., 1994; 113: 621-627.
- McRee, D.E., Redford, S.M., Getzoff, E.D., Lepock, J.R., Hallewell, R.A., Tainer, J.A. Changes in crystallographic structure and thermostability of a Cu,Zn superoxide dismutase mutant resulting from the removal of a buried cysteine. J. Biol. Chem., 1990; 265: 14234-14241.
- Meltzer, H.L. Is there a specific membrane defect in bipolar disorders? Biol. Psychiatry, 1991; 30: 1071-1074.
- Mendels, J., Frazer, A. Alterations in cell membrane activity in depression. Am. J. Psychiatry, 1974; 131: 1240-1246.
- Meneses, P., Glonek, T. High resolution ^{31}P NMR of extracted phospholipids. J. Lipid Res., 1988; 29: 679-689.
- Metzger, E., Dohener, R., Simon, W. Lithium/sodium ion concentration ratio measurements in blood serum with lithium and sodium ion-selective liquid membrane electrodes. Anal. Chem., 1987; 59: 1600-1603.

- Moody, C.S., Hasan, H.M. Mutagenicity of oxygen free radicals. Proc. Natl. Acad. Sci. USA, 1982; 79: 2855-2859.
- Mørk, A. Actions of lithium on second messenger activity in the brain. The adenylate cyclase and phosphoinositide systems. Lithium, 1990; 1: 131-147.
- Mota de Freitas, D. Alkali metal NMR. Methods Enzymol., 1993; 227: 78-106.
- Mota de Freitas, D., Abraha, A., Rong, Q., Silberberg, J., Whang, W., Borge, G.F., Elenz, E. Relationship between lithium ion transport and phospholipid composition in erythrocytes from bipolar patients receiving lithium carbonate. Lithium, 1994a; 5: 29-39.
- Mota de Freitas, D., Amari, L., Srinivasan, C., Rong, Q., Ramasamy, R., Abraha, A., Gerald, C.F.G.S., Boyd, M. Competition between Li^+ and Mg^{2+} for the phosphate groups in the human erythrocyte membrane and ATP: An NMR and fluorescence study. Biochemistry, 1994b; 33: 4101-4110.
- Mota de Freitas, D., Espanol, M.T., Dorus, E. Lithium Transport in Red Blood Cells of Bipolar Patients. In V.S. Gallicchio (ed) Lithium Therapy Monographs vol. 4. Switzerland: S. Karger, 1991, pp 96-120.
- Mota de Freitas, D., Espanol, M.T., Ramasamy, R., Labotka, R.J. Comparison of Li^+ transport and distribution in human red blood cells in the presence and absence of dysprosium (III) complexes of triphosphate and triethylenetetraminehexaacetate. Inorg. Chem., 1990a; 29: 3972-3979.
- Mota de Freitas, D., Luchinat, C., Banci, L., Bertini, I., Valentine, J.S. ^{31}P NMR study of the interaction of inorganic phosphate with bovine copper-zinc superoxide dismutase. Inorg. Chem., 1987; 26: 2788-2791.
- Mota de Freitas, D., Ming, L-J., Ramasamy, R., Valentine, J.S. ^{35}Cl and ^1H NMR study of anion binding to reduced bovine copper-zinc superoxide dismutase. Inorg. Chem., 1990b; 29: 3512-3518.
- Mota de Freitas, D., Silberberg, J., Espanol, M.T., Dorus, E., Abraha, A., Dorus, E., Elenz, E., Whang, W. Measurement of lithium transport in RBCs from patients receiving lithium carbonate and normal individuals by ^7Li NMR spectroscopy. Biol. Psychiatry, 1990c; 28: 415-424.
- Mota de Freitas, D., Valentine, J.S. Phosphate is an inhibitor of copper-zinc superoxide dismutase. Biochemistry, 1984; 23: 2079-2082.
- Nechay, B.R. Mechanisms of action of vanadium. Ann. Rev. Pharmacol. Toxicol., 1984; 24: 501-524.
- Nieves, J., Kim, L., Puett, D., Echegoyen, L. Electron spin resonance of calmodulin-vanadyl

- complexes. Biochemistry, 1987; 26: 4523-4527.
- Ostrow, D.G., Pandey, G.N., Davis, J.M., Hurt, S.W., Tosteson, D.C. A heritable disorder of lithium transport in erythrocytes of a subpopulation of manic-depressive patients. Am. J. Psychiatry, 1978; 135: 1070-1078.
- Pacey, G.E. Lithium crown ether complexes. In: Bach R.O., ed. Lithium: current applications in science, medicine and technology. New York: Wiley Interscience 1985: 35-45.
- Painter, G.R., Pressman, B.C. Cation complexes of the monovalent and polyvalent carboxylic ionophores: Lasalocid, Monensin, Calcimycin, and related antibiotics. In H. Sigel (ed.) Metal Ions in Biological Systems: Antibiotics and their Complexes. New York: Marcel Dekker, Inc., 1985, pp 173-206.
- Pandey, G.N., Ostrow, D.G., Haas, M., Dorus, E., Casper, R.C., Davis, J.M., Tosteson, D.C. Abnormal lithium and sodium transport in erythrocytes of a manic patient and some members of his family. Proc. Natl. Acad. Sci. USA, 1977; 74: 3607-3611.
- Patterson, M.K. Jr. Measurement of growth and viability of cells in culture. Methods. Enzymol., 1979; 58: 141-152.
- Pollack, S.J., Atack, J.R., Knowles, M.R., McAllister, G., Ragan, C.I., Baker, R., Fletcher, S.P., Iversen, L.I., Broughton, H.B. Mechanism of inositol monophosphatase, the putative target of lithium therapy. Proc. Natl. Acad. Sci. USA, 1994: 91: 5766-5770.
- Polticelli, F., Bottaro, G., Battistoni, A., Carri, M.T., Djinovic-Carugo, K., Bolognesi, M., O'Neill, P., Rotilio, G., Desideri, A. Modulation of the catalytic rate of Cu,Zn superoxide dismutase in single and double mutants of conserved positively and negatively charged residues. Biochemistry, 1995; 34: 6043-6049.
- Pressman, B.C. Biological applications of ionophores. Ann. Rev. Biochem., 1976; 45: 501-530.
- Rabizadeh, S., Gralla, E.D., Borchelt, D.R., Gwinn, R., Valentine, J.S., Sisodia, S., Wong, P., Lee, M., Hahn, H., Bredesen, D.E. Mutations associated with amyotrophic lateral sclerosis convert superoxide dismutase from an antiapoptotic gene to a proapoptotic gene; Studies in yeast and neural cells. Proc. Natl. Acad. Sci. USA, 1995; 92: 3024-3028.
- Ramasamy, R., Castro, M.M.C.A., Mota de Freitas, D., Geraldès, C.F.G.C. Lanthanide complexes of aminophosphonates as shift reagents for ^7Li and ^{23}Na NMR studies in biological systems. Biochimie, 1992; 74: 777-783.
- Ramasamy, R., Espanol, M.C., Long, K.M., Mota de Freitas, D., Geraldès, C.F.G.C. Aqueous shift reagents for $^7\text{Li}^+$ NMR transport studies in cell systems. Inorg. Chim. Acta, 1989; 163: 41-52.

- Ramasamy, R., Mota de Freitas, D. Competition between Li^+ and Mg^{2+} for ATP in erythrocytes. FEBS Lett., 1989, 244: 223-226.
- Ramasamy, R., Mota de Freitas, D., Jones, W., Wezeman, F., Labotka, R., Geraldès, C.F.G.C. Effects of negatively charged shift reagents on red blood cell morphology, Li^+ transport and membrane potential. Inorg. Chem., 1990; 29: 3979-3985.
- Rehder, D.: Inorganic considerations on the function of vanadium in biological systems. In H. Sigel and A. Sigel (eds.) *Metal Ions in Biological Systems*, Vol. 31. New York: Marcel Dekker, Inc., 1995, pp 2-43.
- Rehder, D., Holst, H., Pribsch, W., Vilter, H. Vanadate dependent bromo/iodoperoxidase from *Ascophyllum nodosum* also contains unspecific low-affinity binding sites for vanadate (V): A ^{51}V NMR investigation, including the model peptides Phe-Glu and Glu-Tyr. J. Inorg. Biochem., 1991; 41: 171-185.
- Reiser, G., Duhm, J. Transport pathways for lithium ions in neuroblastoma X glioma hybrid cells at "therapeutic" concentrations of Li^+ . Brain Res., 1982; 252: 247-258.
- Richelson, E. Lithium ion entry through the sodium channel of cultured mouse neuroblastoma cells: A biochemical study. Science, 1977; 196: 1001-1002.
- Rigo, A., Stevanato, R., Viglino, P., Rotilio, G. Competitive inhibition of Cu,Zn superoxide dismutase by monovalent anions. Biochem. Biophys. Res. Commun., 1977; 79: 776-783.
- Roe, J.A., Butler, A., Scholler, D.M., Valentine, J.S. Differential scanning calorimetry of Cu,Zn superoxide dismutase, the apoprotein and its zinc-substituted derivatives. Biochemistry, 1988; 27: 950-958.
- Rong, Q., Espanol, M., Mota de Freitas, D., Geraldès, C.F.G.C. ^7Li NMR relaxation study of Li^+ binding in human erythrocytes. Biochemistry, 1993; 32: 13490-13498.
- Rong, Q., Mota de Freitas, D., Geraldès, C.F.G.C. Competition between lithium and magnesium ions for guanosine di- and triphosphates in aqueous solution: a nuclear magnetic resonance study. Lithium, 1992; 3: 213-220.
- Rong, Q., Mota de Freitas, D., Geraldès, C.F.G.C. Competition between lithium and magnesium ions for the substrates of second messenger systems: a nuclear magnetic resonance study. Lithium, 1994; 5: 147-156.
- Rosen, D.R., Siddique, T., Patterson, D., Figlewicz, D.S., Sapp, P., Hentati, A., Donaldson, D., Goto, J., O'Regan, J.P., Deng, H.X., Rahmani, Z., Krizus, A., McKenna-Yasek, D., Cayabyab, A., Gaston, S.M., Berger, R., Tanzi, R.E., Halperin, J.J., Herzfeldt, B., Van den Bergh, R., Hung, W.Y., Bird, T., Deng, G., Mulder, D.W., Smyth, C., Laing, N.G., Soriano, E., Pericak-Vance, M.A., Haines, J., Rouleau, G.A., Gusella, J.S., Horvitz, H.R., Brown, Jr., R.H. Mutations in the Cu/Zn superoxide dismutase gene are associated with

familial amyotrophic lateral sclerosis. Nature, 1993; 362: 59-62.

Rotilio, G., Morpurgo, L., Giovagnoli, C., Calabrese, L., Mondovi, B. Studies of the metal sites of copper proteins. Symmetry of copper in bovine superoxide dismutase and its functional significance. Biochemistry, 1972; 11: 2187-2192.

Sakurai, H., Nishida, M., Kida, K., Koyama, M., Takada, J. Determination and characterization of vanadium ion in serum albumins. Inorg. Chim. Acta, 1987; 138: 149-153.

Scheller, K.H., Hofstetter, F., Mitchell, P.R., Prijs, B., Sigel, H. Macrochelate formation in monomeric metal ion complexes of nucleoside 5'-triphosphates and the promotion of stacking by metal ions. Comparison of the self-association of the purine and pyrimidine 5'-triphosphates using proton nuclear magnetic resonance. J. Am. Chem. Soc., 1981; 103: 247-260.

Schreiber, G., Avissar, S., Danon, A., Belmaker, R.H. Hyperfunctional G proteins in mononuclear leukocytes of patients with mania. Biol. Psychiatry, 1991; 29: 273-280.

Schwartz, R.S., Chiu, D.T.Y., Lubin, B. In Erythrocyte Membranes 3: Recent Clinical and Experimental Advances. Kruckeberg W.C., Eaton J.W., Aster J., Brewer G.J. (eds.) Alan R. Liss, Inc., New York, 1984, pp 89-122.

Seiler, H.G.: Analytical procedures for the determination of vanadium in biological Materials. In H. Sigel and A. Sigel (eds.) Metal Ions in Biological Systems, Vol. 31. New York: Marcel Dekker, Inc., 1995, pp 671-688.

Sette, M., Paci, M., Desideri, A., Rotilio, G. Formate as an NMR probe of anion binding to Cu,Zn and Cu,Co bovine erythrocyte superoxide dismutases. Biochemistry, 1992; 31: 12410-12415.

Shah, V.K., Brill, W.J. Isolation of an iron-molybdenum cofactor from nitrogenase. Proc. Natl. Acad. Sci. USA, 1977; 74: 3249-3253.

Shedd, S.F., Spicer, L.D. Characterization of a microcarrier cell culture system for ^{23}Na MR spectroscopy studies. NMR Biomed. 1991; 4: 246-253.

Shinar, H., Navon, G., Klaui, W. Novel organometallic ionophore with specificity toward Li^+ . J. Am. Chem. Soc., 1986; 108: 5005-5006.

Simonyan, M.A., Nalbandyan, R.M. Preparation of electrophoretically homogeneous erythrocyte protein and investigation of its thermodenaturation. Biokhimiya, 1975; 40: 726-732.

Spinedi, A., Pacini, L., Luly, P., Lombardi, U., Nistico, G. Rubidium shows effects different from lithium on phosphatidylinositol metabolism in a cell line of human neuroblastoma. Funct. Neurol., 1992; 7: 305-308.

- Steinman, H.M. Superoxide dismutases: Protein chemistry and structure-function relationships. In Oberley, L.W. (ed.) *Superoxide Dismutase* vol.1, CRC Press, Inc., Fl., 1982, pp 27-38.
- Steinman, H.M., Naik, V.R., Abernethy, J.L., Hill, R.L. Bovine erythrocyte superoxide dismutase: Complete amino acid sequence. J. Biol. Chem., 1974; 7326-7388.
- Stubbs, E.B., Jr., Agranoff, B.W. Lithium enhances muscarinic receptor-stimulated CDP-diacylglycerol formation in inositol-depleted SK-N-SH neuroblastoma cells. J. Neurochem., 1993; 60: 1292-1299.
- Stubbs, E.B., Jr., Carlson, R.O., Lee, C-H., Fisher, S.K., Hajra, A.K., Agranoff, B.W. Essential fatty acid deficiency in cultured SK-N-SH human neuroblastoma cells. Adv. Exp. Med. Biol., 1992; 318: 171-182.
- Swergold, B.S. NMR spectroscopy of cells. Annu. Rev. Physiol., 1992; 54: 775-798.
- Szentistvanyi, I., Janka, Z. Correlation between lithium ratio and Na-dependent Li transport in red blood cells during lithium prophylaxis. Biol. Psychiatry, 1979a; 973-977.
- Szentistvanyi, I., Janka, Z., Joo, F., Rimanoczy, A., Juhasz, A., Latzkovits, L. Na-dependent Li-transport in primary nerve cell cultures. Neurosci. Lett., 1979b; 13: 157-161.
- Tainer, J.A., Getzoff, E.D., Beem, K.M., Richardson, J.S. Richardson, D.C. Determination and analysis of the 2 Å structure of copper,zinc superoxide-dismutase. J. Mol. Biol., 1982; 160: 181-217.
- Tandon, R., Bradley, W.G. Amyolateral sclerosis: Part 1. Clinical features, pathology, and ethical issues in management. Annal. Neurol., 1985; 18: 271-280.
- Valentine, J.S., Pantoliano, M.W. Protein-metal ion interactions in cupro-zinc protein (superoxide dismutase). In "Copper Proteins", (Spiro, T.G., ed.), Wiley, New York, 1981; 291-358.
- Valentine, J.S., Mota de Freitas, D. Copper-zinc superoxide dismutase: a unique biological "ligand" for bioinorganic studies. J. Chem. Ed., 1985; 62: 990-997.
- VanEtten, R.L., Waymack, P.P., Rehkop, D.M. Transition metal ion inhibition of enzyme-catalyzed phosphate ester displacement reactions. J. Am. Chem. Soc., 1974; 96: 6782-6785.
- Viglino, P., Scarpa, M., Cocco, D., Rigo, A. Preparation of reduced bovine Cu,Zn superoxide dismutase. Biochem. J., 1985; 229: 87-90.
- Webb. D.A. Observations on the blood of certain ascidians, with special reference to the biochemistry of vanadium. J. Exp. Biol., 1939; 16: 499-523.

- Wever, R., Kustin, K. Vanadium: A biologically relevant element. Adv. Inorg. Chem., 1990; 35: 81-115.
- Wheeling, K., Christian, G.D. Spectrofluorimetric determination of serum lithium using 1,8-dihydroxyanthroquinone. Anal. Lett., 1984; 17: 217-227.
- Wittenkeller, L., Abraha, A., Ramasamy, R., Mota de Freitas, D., Theisen, L.A., Crans, D.C. Vanadate interactions with bovine Cu,Zn-superoxide dismutase as probed by ^{51}V NMR spectroscopy. J. Am. Chem. Soc., 1991; 113: 7872-7881.
- Wittenkeller, L., Mota de Freitas, D., Geraldles, C.F.G.C., Tomé, A.J.R. Physical basis for the resolution of intra- and extracellular ^{133}Cs NMR resonances in Cs^+ -loaded human erythrocyte suspensions in the presence and absence of shift reagents. Inorg. Chem., 1992; 31: 1135-1144.
- Young, L.T., Li, P.P., Kamble, A., Siu, K.P., Warsh, J.J. Mononuclear leukocyte levels of G proteins in depressed patients with bipolar disorder or major depressive disorder. Am. J. Psychiatry, 1994; 151: 594-596.
- Young, L.T., Li, P.P., Kish, S.J., Siu, K.P., Warsh, J.J. Postmortem cerebral cortex $G_{s\alpha}$ -subunit levels are elevated in bipolar affective disorder. Brain Res., 1991; 553: 323-326.

VITA

The author, Cherian Zachariah, was born February, 1962, in Bangalore, India. In 1981, he entered St. Joseph's College, Bangalore and received the Bachelor in Science degree in June 1983. He obtained a Master's degree in Biochemistry from the M.S. University of Baroda in 1986 and a M.Phil. degree in Neurophysiology from the National Institute of Mental Health and Neurosciences, Bangalore in 1989. He was supported by a NIMHANS fellowship from 1987-1989.

In August 1991, he joined Loyola University Chicago to pursue graduate studies in Chemistry. He was awarded a teaching assistantship from August 1991 to May 1992. Following this, he was supported by a research assistantship as part of the NIMH research grant awarded to Prof. Duarte Mota de Freitas. He was awarded the Loyola University Dissertation Fellowship by the Graduate School in August 1995.

PUBLICATIONS

A. Refereed Articles:

The use of microcarrier beads in ion transport NMR studies of perfused cells. C. Zachariah, D. Mota de Freitas, M.M.C.A. Castro, C.F.G.C. Geraldes, M.C.P. Lima, and C.R. Oliveira. *J. Magn. Res. B* **1995**; 108: 81-85.

Comparison of the use of agarose threads and microcarrier beads in Li⁺ transport studies of human neuroblastoma SH-SY5Y cells. Joyce Nikolakopoulos, Cherian Zachariah, and Duarte Mota de Freitas. *Inorg. Chim. Acta*, (in press).

B. Book Chapter and Abstracts:

⁷Li NMR study of lithium ion transport in perfused human neuroblastoma cells. Cherian Zachariah, Joyce Nikolakopoulos, Duarte Mota de Freitas, Evan B. Stubbs, Jr., M. Margarida C.A. Castro, Carlos F.G.C. Geraldes, Maria C.D. de Lima, Catarina R. Oliveira, Ravi Ramasamy. *Lithium: Biochemical and Clinical Advances* (in press).

Use of non-permeable microcarrier beads in alkali metal ion transport NMR studies of perfused neuroblastoma cells. C. Zachariah and D. Freitas. *Society for Neuroscience: Abstracts*, 1994; 20: 1775.

⁷Li NMR study of lithium ion transport in perfused human neuroblastoma cells. J. Nikolakopoulos, C. Zachariah, D. Mota de Freitas, E.B. Stubbs, Jr., M.M.C.A. Castro, C.F.G.C. Geraldes, M.C.P. Lima, C.R. Oliveira, and R. Ramasamy. *Journal of Trace and Microprobe Techniques*, 1995; 13 (4): 525.

⁷Li NMR study of lithium ion transport in human neuroblastoma cells. J. Nikolakopoulos, C. Zachariah and D. Mota de Freitas. *37th Experimental NMR Conference Abstracts*, 1996; 328.

Biochemical properties of lithium in human neuroblastoma SH-SY5Y cells by ⁷Li NMR spectroscopy. J. Nikolakopoulos, C. Zachariah and D. Mota de Freitas. *ISMRM : Proceedings*, 1996; 2: 1138.

APPROVAL SHEET

The dissertation submitted by Cherian Zachariah has been read and approved by the following committee:

Duarte E. Mota de Freitas, Ph.D., Director
Professor, Chemistry
Loyola University Chicago

David S. Crumrine, Ph.D.
Associate Professor, Chemistry
Loyola University Chicago

Kenneth E. Olsen, Ph.D.
Professor, Chemistry
Loyola University Chicago

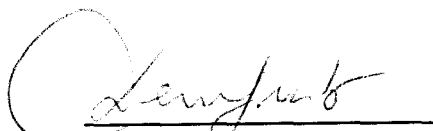
Mir Shamsuddin, Ph.D.
Associate Professor, Medicine
Northwestern University

The final copies have been examined by the director of the dissertation and the signature which appears below verifies the fact that any necessary changes have been incorporated and the dissertation is now given final approval by the committee with reference to content and form.

The dissertation is, therefore, accepted in partial fulfillment of the requirements for the degree of Doctor of Philosophy.

7/5/96

Date


Director's Signature